Surface structuring in xy- and z-direction on the examples of peptide array synthesis and molecular layer deposition.

Zur Erlangung des akademischen Grades eines

DOKTORS DER NATURWISSENSCHAFTEN

(Dr. rer. nat.)

der KIT-Fakultät für Chemie und Biowissenschaften

des Karlsruher Instituts für Technologie (KIT)

genehmigte

DISSERTATION

von

M.Sc. Barbara Ridder

aus

Paderborn

KIT-Dekan: Prof. Dr. Willem Klopper

Referent: Prof. Dr. Frank Breitling

Korreferent: Prof. Dr. Michael A.R. Meier

Tag der mündlichen Prüfung: 16.12.2016

„Eine Antwort ist immer ein Stück des Weges, der hinter dir liegt. Nur eine Frage kann uns weiterführen."

Jostein Gaarder, Hallo, ist da jemand?

Die vorliegende Arbeit wurde von September 2013 bis Oktober 2016 unter Anleitung von Prof. Dr. Frank Breitling und Prof. Dr. Michael A. R. Meier am Institut für Mikrostrukturtechnik (IMT) und am Institut für Organische Chemie (IOC) des Karlsruher Instituts für Technologie (KIT) angefertigt.

Erklärung:

Hiermit erkläre ich wahrheitsgemäß, dass ich die vorliegende Arbeit selbständig angefertigt und keine anderen als die angegebenen Quellen und Hilfsmittel benutzt sowie die wörtlich oder inhaltlich übernommenen Stellen als solche kenntlich gemacht und die Satzung des Karlsruher Instituts für Technologie (KIT) zur Sicherung guter wissenschaftlicher Praxis beachtet habe. Des Weiteren erkläre ich, dass ich mich derzeit in keinem laufenden Promotionsverfahren befinde, und auch keine vorausgegangenen Promotionsversuche unternommen habe. Die elektronische Version der Arbeit stimmt mit der schriftlichen Version überein und die Archivierung der Primärdaten gemäß Abs. A (6) der Regeln zur Sicherung guter wissenschaftlicher Praxis des KIT ist beim Institut für Mikrostrukturtechnik (IMT) am KIT gesichert.

Karlsruhe, 31.10.2016

Barbara Ridder

Abstract

Surfaces can be protected, stabilized or given extra functionality by covering them with a defined layer of material with suitable properties. Additionally, the properties of the surface can be tuned. These functional surfaces have applications in many different fields, such as automobiles, electronics or bio based applications. Additional information and functionality can be given to the surface by structuring it, e.g., with a lithographic mask or by transferring material only to select positions.

In this work, structuring of surfaces in the xy-direction on the example of peptide array synthesis and in the z-direction by molecular layer deposition was investigated.

The focus of the first part of this thesis lies on the structuring of a surface in xy-direction, specifically on the application of peptide array synthesis. Peptide arrays were produced with the 'solid' solvent approach and structured with combinatorial laser-induced forward transfer. Usually, a commercial styrene-acrylic copolymer resin is used as the matrix material in 'solid' solvent peptide array synthesis. The exact composition of the commercially available resin is not known. The synthesis and development of a new matrix material provides knowledge on its exact composition, but more importantly allows for adaptations of the material when the requirements of the application change in the future. In this work, the development of a new matrix material was investigated. Poly(dimethylacrylamide)s (p(DMAA)) were synthesized using Atom Transfer Radical Polymerization (ATRP) and their suitability as matrix materials was investigated. Additionally, model arrays were synthesized to prove that the polymer could serve as a reaction medium for peptide bond formation. Therefore, among other experiments, a small tripeptide was synthesized to show that not only one but multiple amino acids could be coupled to the synthesis film to form a peptide chain. Additionally, the penetration depth of the amino acid derivatives when using p(DMAA) as the matrix material was investigated by Time of Flight Secondary Ion Mass Spectrometry (ToF-SIMS). It could be shown that p(DMAA) is a suitable matrix material for peptide array synthesis with the 'solid' solvent approach structured by laser-induced forward transfer and that multiple layers of amino acids can be coupled.

Abstract

The second part of this thesis is again dedicated to the field of peptide array synthesis. The Ugi Four Component Reaction (U-4CR) was investigated as post-functionalization methodology for the side chains of a peptide directly on the array. Therefore, different combinations of isocyanides and aldehydes were investigated. The anchor to the surface was always provided by a free amine in the side chain of a lysine. It was shown that the U-4CR could successfully be performed with different combinations and therefore that the U-4CR is a suitable reaction for post-synthesis side chain modification of peptide arrays. Additionally, as a pre-study for the synthesis of peptidomimetics on arrays, it was shown that an U-4CR product can be integrated into the growing peptide chain.

The third part focuses on the structuring of a surface in z-direction by molecular layer deposition. First, a silicon wafer was functionalized *via* silanization to provide an anchor on the substrate for further functionalization. Different silanes were investigated to find the optimal transition between the inorganic substrate and the subsequent organic layers. Subsequently, layers were built by using alternating Thiol-Ene reactions of dithiols and dienes. Indeed, a bifunctional molecule couples to the silane and then serves as functionalization anchor for the next layer. The optimal reaction conditions for the first two layers were determined and a thorough characterization scheme with the combination of ToF-SIMS, X-ray Photoelectron Spectroscopy (XPS) and height determination of the layers by Atomic Force Microscopy (AFM) has been established, which is suitable for future investigations, when additional layers are added.

Kurzfassung

Oberflächen können durch Beschichtung mit einer zusätzlichen Lage von (funktionellem) Material geschützt oder stabilisiert werden. Diese Schicht kann die Materialeigenschaften der Oberfläche wie Hydrophilie oder elektrische Funktionen verändern. Solche funktionellen Materialen werden zum Beispiel in der Automobiltechnik, in der Elektronik aber auch für biologische Anwendungen verwendet. Im Normalfall wird die komplette Oberfläche mit demselben Material bedeckt. Durch Strukturierung dieser Schicht mit unterschiedlichen Materialien, zum Beispiel mit Hilfe einer lithografischen Maske oder selektivem Transfer zu vorgegebenen Positionen, erhält die Oberfläche zusätzliche Funktionalität.

In dieser Arbeit wurden Oberflächenstrukturierungen in der xy-Fläche am Beispiel der Peptidarraysynthese und in z-Richtung an Hand molekularer Lagenabscheidung durchgeführt.

Der erste Teil der Arbeit befasst sich mit Oberflächenstrukturierung in xy-Richtung am Beispiel der Synthese von Peptidarrays. Die Peptidarrays wurden mit einer Methode hergestellt, bei der ein „festes" Lösungsmittel zum Einsatz kommt. Die Strukturierung der Oberfläche wurde durch kombinatorischen laserinitiierten Vorwärtstransfer erreicht. Als „festes" Lösungsmittel wird normalerweise ein kommerziell erhältliches Styrol-co-Acrylharz verwendet. Ziel dieser Arbeit war es, ein neues Matrixmaterial zu entwickeln, weil für das kommerziell erhältliche Harz die genauen Herstellungsbedingungen und die exakte Zusammensetzung unbekannt sind. Bei eigener Synthese des Matrixmaterials wären diese Variablen dagegen bekannt und könnten an sich verändernde Anforderungen der Methode oder des Fabrikationsprozesses angepasst werden. Poly(dimethylacrylamid)polymere wurden mit Hilfe der Atomtransferradikalpolymerisation synthetisiert und auf ihre Eignung als Matrixmaterialien untersucht. Außerdem wurden Modellarrays synthetisiert, um die Eignung des Polymers als Medium für die Reaktion der aktivierten Aminosäurederivate mit den Peptiden am Synthesefilm zu untersuchen. Um zu zeigen, dass es auch möglich ist, eine Kette von Aminosäuren in mehreren Schritten aufzubauen, wurde ein Tripeptid synthetisiert. Zusätzlich wurde die Eindringtiefe der verwendeten Aminosäurederivate in den Synthesefilm untersucht, wenn Poly(dimethylacrylamid) als Matrixmaterial verwendet wurde. Dabei wurde die Sekundärionenmassenspektrometrie eingesetzt.

Im zweiten Kapitel dieser Arbeit wurden Peptidarrays mit der Ugi-Vier-Komponenten Reaktion funktionalisiert. Hierzu wurden post-synthetische Seitenkettenfunktionalisierungen der Peptide am Array durchgeführt. Dafür wurden

verschiedene Kombinationen von Isocyaniden und Aldehyden getestet. Die für die Ugi-Reaktion zusätzlich notwendigen Amine wurden durch seitenkettenentschützte Lysine an der Oberfläche bereitgestellt. Die Ugi-Reaktion wurde erfolgreich mit verschiedenen Aldehyd- und Isocyanidkombinationen durchgeführt und ist damit eine geeignete Möglichkeit für die postsynthetische Modifikation von Seitenketten eines Peptids am Array. Zusätzlich wurde als Vorstufe zu möglichen Peptidomimeticarrays gezeigt, dass ein Ugi-Produkt in die wachsende Peptidkette integriert werden kann.

Im dritten Teil der Arbeit wurde die Strukturierung von Oberflächen in z-Richtung an Hand molekularer Lagenabscheidung untersucht. Dabei sollte die Strukturierung durch unterschiedliche Eigenschaften der verschiedenen Lagen erreicht werden. Zuerst wurde ein Siliziumwafer mit verschiedenen Silanen funktionalisiert, um die optimale Verbindung zwischen anorganischem Substrat und organischer Strukturierung zu finden. Danach wurde eine zweite Lage kovalent mit Thiol-En-Chemie an die erste Lage gebunden. Die Reaktionsbedingungen und die nötigen analytischen Schritte wurden optimiert, um den zukünftigen Aufbau eines Multilagensystems zu ermöglichen.

Table of Contents

1. Introduction

The field of surface chemistry has been growing over the past years. Materials can be protected or stabilized by coating them with a functional layer. Extra functionality can also be introduced into the material by modifying its surfaces. Furthermore, surfaces can act as carriers for a synthesis film, which in turn carries the actual functionality. Additional information can be added to the surface by structuring it; this can be realized with various methods, *e.g.,* using a lithographic mask or transferring material only to selected positions.[1]

Functional surfaces find their use in many different applications such as automobiles, electronics or bio based applications.[2]

In the main part of this thesis, three different projects are described concerning the structuring of different surfaces in xy- or in z-direction. The structuring in xy-direction was investigated on the example of peptide arrays, where different peptides are placed in different positions in the xy-plane on the array. A matrix material was developed to serve as the 'solid' solvent in peptide array synthesis structured with a laser based method. Additionally, the Ugi four component reaction was investigated as a tool for peptide array functionalization The structuring in z-direction was investigated on the example of covalent molecular layer deposition of bifunctional molecules to set up a multilayer and multifunctional, hierarchical surface structure *via* Thiol-Ene chemistry.

The first two chapters are focused on one special application in the bio field, which is peptide arrays where structuring in xy-direction is necessary. Different peptides are placed on a functional surface, which can then be used, among others, for antibody binding studies. In this way, antibodies present in patients' sera after an illness can be detected or epitopes within a protein can be mapped.

For understanding the synthesis of peptide arrays, knowledge of the chemistry of peptide synthesis with its challenges and requirements is crucial.

1.1. Peptide synthesis

Peptides and proteins consist of a chain of amino acids, which are linked by peptide bonds. Such molecules with a molecular weight of underneath 10,000 Da are referred to as peptides; above, they are called proteins.[3] In nature, 20 common amino acids occur in addition to many specialized ones.[4] They all have the same basic structural motif in common: an amino group - the N-terminus - and a carboxylic acid - the C-terminus. Their

distinct characteristic is the chiral side chain, which is different for each amino acid. Nature uses almost exclusively L-amino acids.[3] When the C-terminal carboxylic acid group of an amino acid and the N-terminal amino group of a second amino acid react with each other in a condensation reaction, an amide bond is formed. In this special case the bond is called a peptide bond (see Figure 1).
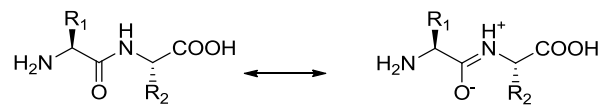

Figure 1: Schematic illustration of a peptide bond between two amino acids.

The peptide bond has two different resonance structures, conferring double bond character to the amide bond.

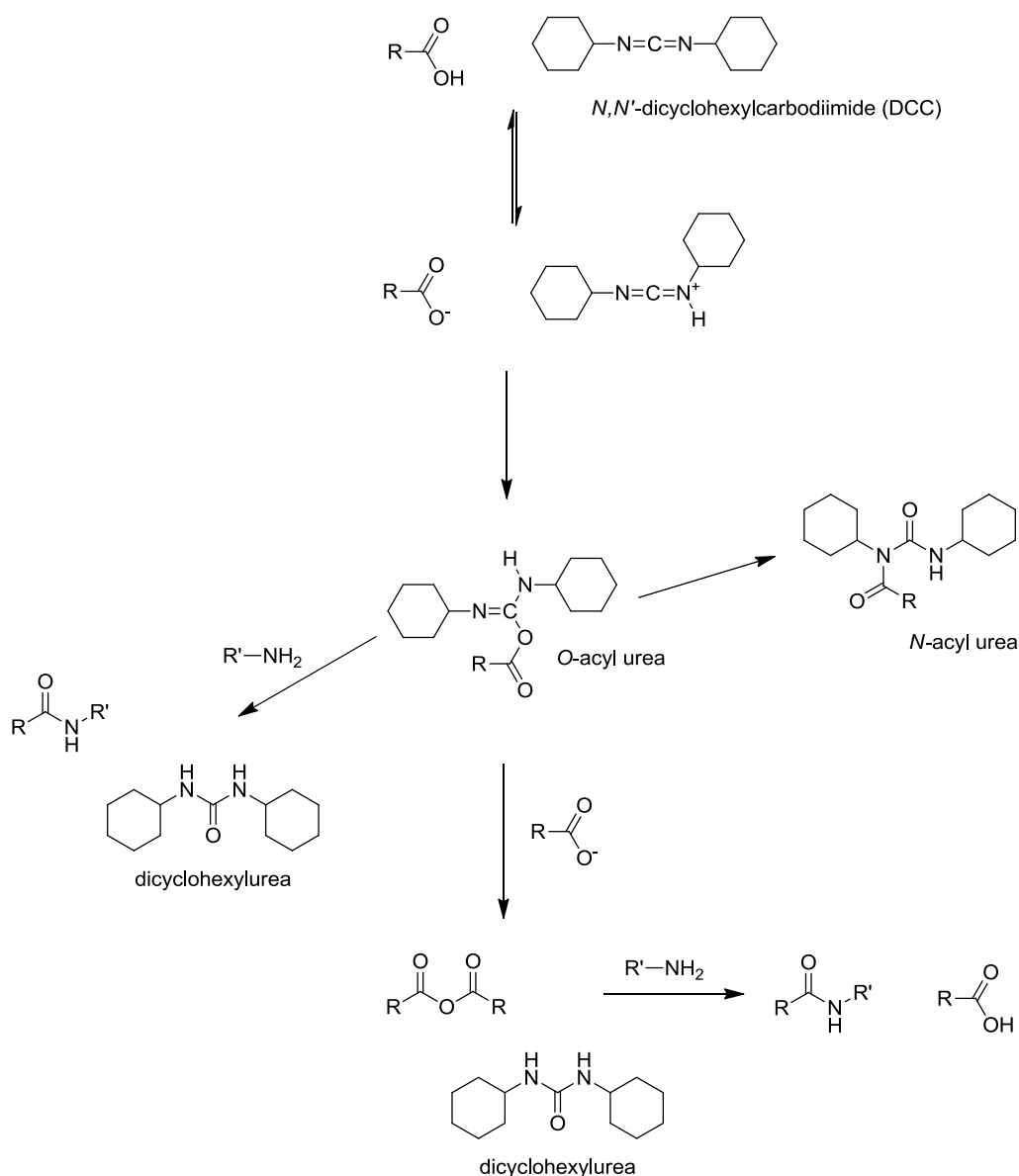## 1.1.1. Peptide bond formation

In nature, peptide bond formation takes place in the ribosome, where proteins are synthesized. Proteins are formed in a five step process: activation of the amino acid, initiation of protein synthesis, elongation, termination and finally release and peptide folding.[3] The peptide bond is formed in the third, the elongation step in a catalytic center called the peptidyl transferase center. The catalytic activity is driven by proximity and orientation (see Scheme 1).[5] The C-terminus of the growing peptide chain and of the amino acids is coupled to transfer ribonucleic acid (tRNA). The N-terminal amino group, of the amino acid to be coupled to the peptide chain, is positioned opposite to the ester group enabling peptide bond formation. Additionally, the peptidyl transferase center contains bases, which facilitate the presence of a NH_2-group and stabilize the tetrahedral transition state.
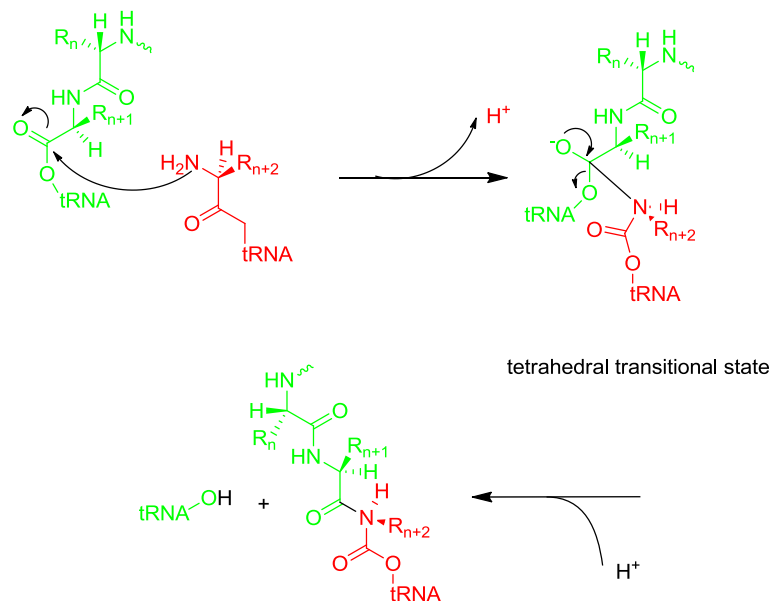
Scheme 1: Schematic representation of peptide bond formation in the ribosome.

Peptides can also be synthesized synthetically in the laboratory. On the contrary to the synthesis in nature, where whole proteins can be synthesized, the laboratory synthesis is limited. Peptides with a length of up to 50 amino acids can be synthesized by default,[6] whereas natural proteins easily range into the hundreds and thousands. For the artificial synthesis, where no facilitating ribozymes/ enzymes are present, it is also necessary to activate the amino acids to achieve peptide bond formation. Usually, the C-terminus is chosen to be the activated part of the amino acid.[7] Different strategies have been developed for the activation, such as anhydrides, carbodiimides, active esters, acyl halides, phosphonium reagents, immonium reagents and uronium reagents.[7–9]

The C-terminal activation with carbodiimides is a very commonly used pathway. Already in 1955, Sheehan *et al.* presented *N,N'*-dicyclohexylcarbodiimide (DCC) as a coupling agent in peptide chemistry.[10] In the first step, the DCC reacts with the C-terminus of the amino acid and an *O*-acyl urea intermediate is formed (see Scheme 2). Peptide bond formation can then take place via two different routes either the amine reacts directly with the *O*-acyl urea intermediate or first an anhydride intermediate is formed, which then reacts further with the N-terminus of the second amino acid to result in the desired peptide bond. A disadvantage of the DCC activation is the formation of the *N*-acyl urea byproduct and that the *O*-acyl urea intermediate is prone to undergo racemization.[11]

Scheme 2: Peptide bond formation using *N,N'*-dicyclohexylcarbodiimide (DCC) as the activation agent.

When using DCC, the dicyclohexylurea byproduct formed is insoluble in most solvents and can easily be removed by filtration.[8] This can be problematic if the synthesized peptide also precipitates from the reaction mixture: it is almost impossible to separate it from the solid urea byproduct. Therefore, activating agents such as diisopropylcarbodiimide (DIC) and *N*-isopropylcarbodiimide were developed, where the different side groups make the urea byproducts soluble in dichloromethane (DCM).

Another possibility for C-terminal activation are phosphonium reagents, which were discovered in the 1970's.[12,13] The disadvantage of these compounds was that high rates of racemization were observed and therefore the compounds were not suitable for peptide synthesis.[8] The problem was solved in 1975 when Castro *et al.* presented a

benzotriazol based phosphonium reagent, benzotriazol-1-yloxy-tris(dimethylamino)phosphonium hexafluorophosphate (BOP) (see Figure 2).[14]

A major disadvantage of the BOP reagent is the occurrence of the toxic byproduct hexamethylphosphoric triamide during peptide synthesis while there is still a considerably high risk of racemization.[7,9] Nowadays a broad range of BOP based coupling agents are known, which have non-toxic side products. One of the most used is benzotriazol-1-yloxy-tris-pyrrolidinophosphonium hexafluorophosphate (PyBOP) (see Figure 2).
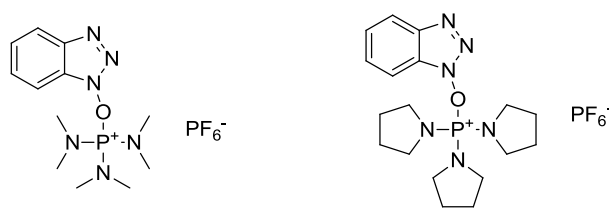

Figure 2: Benzotriazol-1-yloxy-tris(dimethylamino)phosphonium hexafluorophosphate (BOP, left) and benzotriazol-1-yloxy-tris-pyrrolidinophosphonium hexafluorophosphate (PyBOP, right).

All earlier described methods for the C-terminal activation are *in situ* methods, where two or more components have to come together for the activation. Active esters are an approach where the activation is already integrated into the amino acid. Under laboratory conditions the aminolysis rate of alkyl esters is too low, but phenyl esters have better properties.[9,15] Different phenyl esters are reported for the use in peptide synthesis such as thiophenol, *p*-nitrophenol, 2,4,5-trichlorophenol and pentafluorophenol.[7] Most commonly used is the pentafluorophenol activation, as the reaction with the N-terminus of the second amino acid is faster than for other esters. [15]

One major problem in laboratory peptide synthesis is the occurrence of side-reactions and racemization.[7,9] Racemic mixtures are undesirable, because the ubiquitous use of L-amino acids in nature means all biological processes are highly stereoselective.[3] Racemization can take place when an oxazolone intermediate is formed after the activation of the C-terminus of the growing peptide chain (see Scheme 3).[7] Under basic conditions, a proton is removed from the oxazolone and the steric information is lost, leading to a racemic mixture of products upon reaction with a nucleophile.
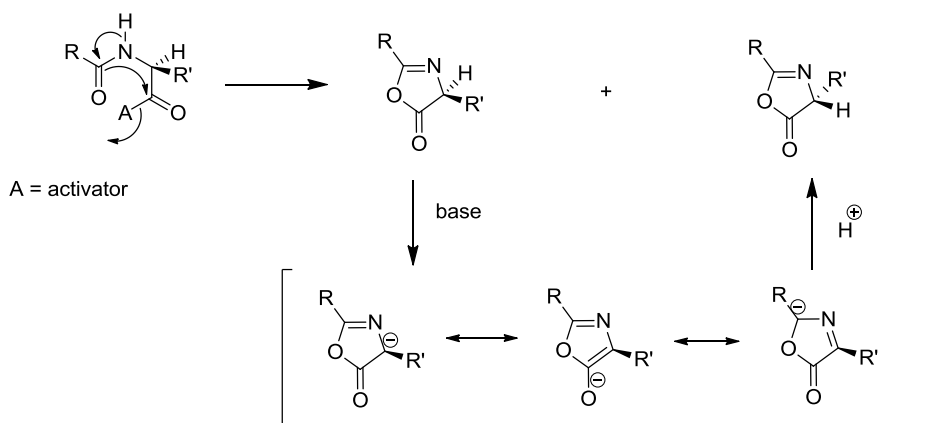
Scheme 3: Schematic illustration of the loss of sterical information under basic conditions after oxazolone formation.

By growing the peptide chain from the C- to the N-terminus, this can be reduced, additionally mild reaction conditions are necessary.[9]

Another option is the use of racemization suppressants to reduce racemization, *e.g.* hydroxybenzotriazole (HOBt), which is commonly used in combination with carbodiimide activation agents (see Scheme 4).[8]
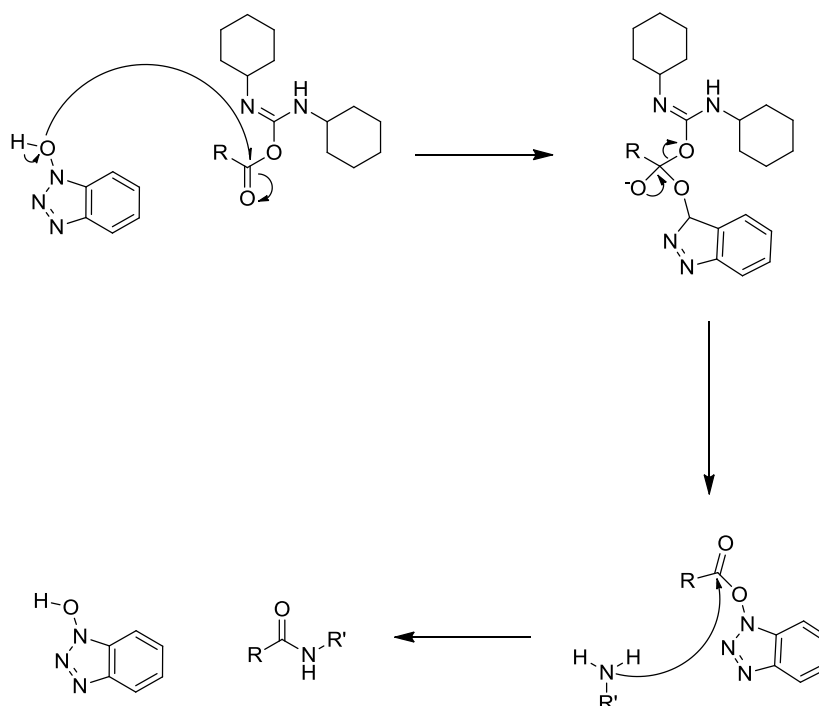
Scheme 4: Peptide bond formation using DCC in combination with HOBt as the activation agent

Side reactions usually take place during intermediate steps. Undesirable side products are the formation of *N*-carboxyanhydrides, diketopiperazine and guanidine.[8]

Another important factor to consider in the synthetic production of peptides is protecting groups. Amino acids are bifunctional, which could possibly lead to cyclization and uncontrolled polymerization. They also exhibit various side chains, which can interfere with the synthesis of the peptide backbone. In nature, bare amino acids without protecting groups are incorporated into the peptide chain correctly without undesirable side products. If one desires to artificially synthesize a peptide sequence, a protection group strategy is needed.

In peptide synthesis, as described earlier, it is a common approach to protect the N-terminal part of the amino acids and activate the C-terminal part.[9] Here it is important that the N-terminal protecting group is only temporary, whereas the side chain protecting groups should be semi-permanent and not be removed by the N-terminal deprotection steps.[7]

There are two major protection strategies for the N-terminus of an amino acid: *tert*-butyloxycarbonyl (Boc) and fluorenylmethyloxycarbonyl (Fmoc), each with its own side chain protection groups.

1.1.2. *Tert*-butyloxycarbonyl (Boc) protection strategy

The Boc protection strategy is based on the differences in acid liability between the N-terminal protecting group and the side chain protecting groups.[16] The N-terminus is deprotected by removal of the Boc protecting group in acidic conditions with trifluoroacetic acid (TFA) (see Scheme 5).
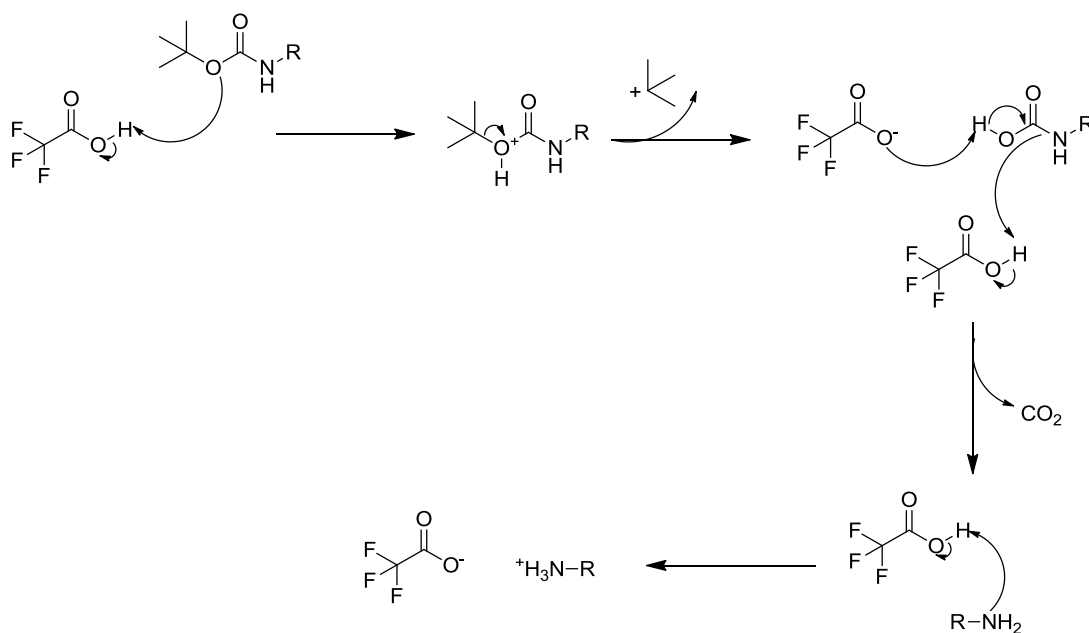
Scheme 5: Boc protecting group removal mechanism with TFA.

After completion of the peptide synthesis, the side chain protecting groups, *e.g.* tosyl, benzyl or benzyloxycarbonyl, are cleaved with hydrofluoric acid.[7] This is one of the major drawbacks of this approach, as the hydrofluoric acid is highly toxic and special equipment coated with polytetrafluoroethylene is required.[17] As this strategy is not truly orthogonal, there is a small risk that during the N-terminal deprotection small quantities of the side chains are accidentally also deprotected.

For the synthesis of difficult sequences, the Boc strategy is especially suited because the N-terminal deprotection with TFA also destroys aggregates that may have formed, leading to higher yields.[6]

1.1.3. Fluorenylmethyloxycarbonyl (Fmoc) protection strategy

The Fmoc group as potential N-terminal protecting group for peptide synthesis in solution, was introduced by Carpino and Han.[18]

In contrast to the Boc protection strategy, which uses a gradient-based cleaving strategy, the Fmoc approach is truly orthogonal. Here examples of side chain protecting groups are *tert*-butyl ester, trityl or Boc.[7] Side chain deprotection is performed under acidic conditions usually with TFA which is much milder than the hydrofluoric acid of the Boc-approach.[17,19] The N-terminal protecting Fmoc-group is cleaved under relatively mild basic conditions, usually with a mixture of piperidine and *N,N*-dimethylformamide (DMF) (20:80 vol-%).[7] The advantage of piperidine as the base is the dibenzofulvene molecule, which is formed during deprotection (see Scheme 6). It can be detected with a UV spectrometer at a wavelength of 301 nm, enabling monitoring of the deprotection process.
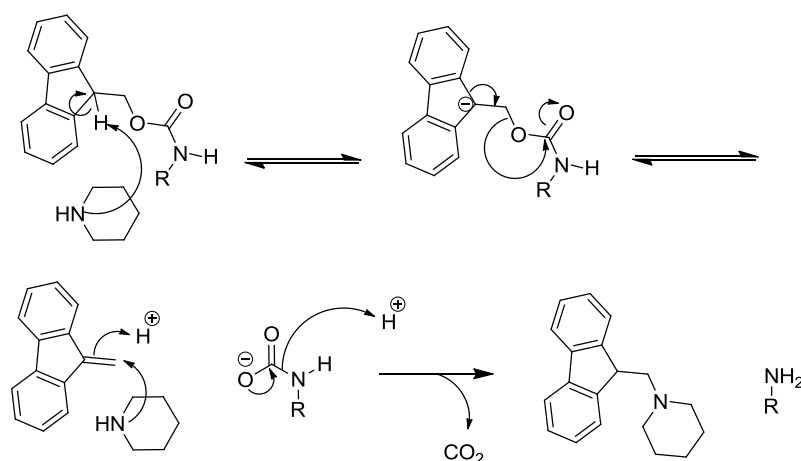
Scheme 6: Fmoc-deprotection mechanism with piperidine as the base and subsequent formation of dibenzofulvene.

However, the Fmoc protecting group proved to be difficult for peptide synthesis in solution, as the formed deprotection products are difficult to remove from the reaction mixture.[20]

For peptide synthesis in solution both the Fmoc and the Boc strategy have advantages and disadvantages. To determine the appropriate strategy, the properties of the peptide that is going to be synthesized and the laboratory equipment that is available need to be taken into account.

1.2. Solid phase peptide synthesis

The peptide synthesis in solution requires challenging purification steps to remove uncoupled sequences and remaining uncoupled amino acids after the addition of each amino acid. This is necessary to avoid false peptide sequences in the final product. In 1986, Merrifield invented the solid phase peptide synthesis (SPPS).[21] In this approach, the C-terminal end of the first amino acid is coupled to a polymeric bead *via* a linker molecule. The beads simplify the purification steps, as they can be easily held back by a sieve or membrane, allowing washing of the beads by pressing through different solvents. After each coupling step, unreacted N-terminal ends are capped, to prevent the synthesis of false sequences.

Initially, Merrifield used a Boc-protecting group strategy for SPPS, which has the disadvantage that the protecting groups are not truly orthogonal. In 1978 Shepard and coworkers introduced the orthogonal Fmoc chemistry to SPPS.[22] The side products, which were difficult to separate from the peptides in solution, could simply be washed away, while the growing peptides on the beads were held back by a membrane. The Fmoc approach proved to be superior to the Boc approach, as the mild deprotection conditions allowed for automatization of the process using synthesis machines. Therefore, the Fmoc protection strategy is used as the standard approach nowadays and Boc chemistry is applied only for 'specialist applications'.[20]

With the successful automatization of peptide synthesis using SPPS, large amounts of peptides with a huge variety of different sequences became available, but for some applications, *e.g.* investigations of protein-protein interactions and search for pharmaceutically active sequences, it is preferable when the peptides are bound to a surface, where a lot of peptides can be synthesized and screened at the same time.

1.3. Peptide arrays: synthesis on solid planar supports

Peptide arrays were invented to enable high-throughput screening of many different peptides at the same time.[23] Peptide arrays can be used to investigate binding events

between linear epitopes, the peptide chains, and components of an analyte (*e.g.* antibodies, drugs, proteins or DNA/RNA).[24] Applications are found in the fields of diagnostics, immunoassays, biomarkers, biosensors and pathogen detection. Especially screenings of a subject's immune response antibodies are of great interest. Mapping of immunosignatures detects if the subject was exposed to certain epitopes, which can aid diagnoses, check a vaccine's effectiveness, or even support research to improve the vaccines effectiveness.[25]

To create a peptide array, the peptides need to be immobilized on a surface in a known area.[23,26] Each peptide is placed in a designated area on the surface; usually this is referred to as a spot. For the final readout, it is very important to know in which position/ spot, which peptide sequence is localized. Typically, an array carries peptides between 8-20 mers.[27] To analyze a complete protein sequence, it is cut into overlapping sequence pieces that cover together the complete sequence of the protein.

The array is incubated with the analyte, *e.g.* blood serum or a solution containing antibodies. By employing fluorescent labeling techniques, interactions between antibodies and the immobilized peptides can be studied and analyzed. A disadvantage is that the peptide strands are linear.[28] Binding sequences, which are present in a rigid conformation in the protein due to the secondary or tertiary structure (*e.g.* loops or surfaces) might not be found, though there are approaches to synthesize arrays with circular peptides *e.g.* by the company PEPperPRINT.[29] Nevertheless, the large amount of different peptides that can be analyzed at the same time, on a small area, with a small amount of analyte is the great advantage of the peptide array strategy.

Functionalization of the surfaces with peptides can be achieved by two different approaches:[30] either immobilization of a completely pre-synthesized peptide or by synthesis, *i.e.* amino acid to amino acid, directly on the surface. In the first approach, the complete peptide is pipetted onto the surface, where an end group functionalization binds or interacts with the surface to immobilize the peptide. In the second approach, direct peptide synthesis on the surface takes place; the first amino acid is bound covalently to the substrate. Then, the amino acid is deprotected and the next one is coupled to the growing peptide chain. An advantage of the immobilization of complete peptides is that these can be purified before being positioned on the surface. Therefore, no false or aborted sequences are present. Additionally, defined concentrations of peptide can be deposited. Disadvantages of this method are solubility issues, which could prevent the peptide from binding to the surface and the expensive pre-synthesizing. By contrast, building up of the peptides directly on the surface is less expensive and more flexible, but has the disadvantage that false or interrupted

sequences cannot be separated from the correct sequences and the concentration depends heavily on the specific sequence.

1.3.1. Peptide macroarrays: SPOT technique

In 1992, Ronald Frank pioneered the *in situ* build-up of arrays with the SPOT synthesis technique.[31] The SPOT technique is a three step process:[32] first a cellulose membrane has to be pre-functionalized in a way that amino acid derivatives can be coupled to it. Typically, Fmoc-β-Ala-OH serves as an anchor molecule between the growing peptide chain and the substrate. The synthesis of the peptides is then carried out on the anchor by using the Fmoc protection strategy. The amino acids used need to be activated to form a peptide bond. Either pre-activated derivatives (e.g. ortho-pentafluorophenol (OPfp) activated amino acids) are used or DIC and HOBt are added to the solution to activate the amino acids *in situ*. The solution is then pipetted onto the substrate in small drops to localize the peptide bond formation, each drop defining a single eponymous spot. In a third and final step, the side chain protecting groups are removed from the completed peptide. The array is now ready and can be used for screening studies.

Peptide arrays produced by the SPOT technology have been used to study a wide range of applications, such as B-cell epitope and paratope mapping, protein-protein interactions, enzyme-substrate recognition and T-cell epitope mapping.[28] This broad range of applications was achieved by wide accessibility of the arrays through commercialization and automation of the method. Companies selling peptide arrays produced by the SPOT technique are for example INTA-VIS and JPT.[30]

One of the major drawbacks of the SPOT method is the limited spot density as the spot size is determined by the size of the droplet applied.[33] Arrays produced with this technique are usually macroarrays with spot densities of about 14 per cm^2,[32] as macroarrays usually have a spot density of about 20 spots per cm^2.[34] To screen more peptides with the same amount of analyte, higher spot densities are desirable, which leads to the field of microarray synthesis with typical spot densities of about 200+ spots per cm^2.

1.3.2. Peptide microarrays: lithographic approach

In 1991, Stephen Fodor, the second pioneer of peptide arrays, presented the lithographic approach to peptide array synthesis.[35] For this approach, the glass substrate is functionalized with amino acids carrying a nitroveratryloxycarbonyl (NVOC) group. Glass is an ideal substrate for microarrays.[30] It is planar, rigid, transparent, impermeable and

does not contain pores.[36] Especially, the last property is advantageous for binding assays, as diffusion into the pores prolongs the binding time.

Upon irradiation with light, the photolabile NVOC group is removed and an amino acid can be coupled to the free N-terminus of the growing peptide chain. The array is structured by the use of masks, which allows illuminating selected areas and shielding the other parts of the array. Only the illuminated areas are deprotected. The coupling can be performed in solution, since amino acid building blocks can only couple to those parts of the array that have been illuminated. For each different amino acid in each layer an individual masking, illumination and coupling step has to take place. This is also one of the major disadvantages of this technique: it is very time consuming.[23] If for example 20 different amino acids are used in each layer, an array carrying 10-mer peptides requires $20 \times 10 = 200$ masking, illumination and coupling steps.

The disadvantage of physical masks, which are time intensive and expensive to produce, was eliminated with the invention of virtual masks. Here, a digital micro mirror is used instead of the physical masks.[37–39] With this technique, spot densities of to up to 1,000,000 spots per cm^2 can be achieved.[40]

The photolithographic approach to peptide array synthesis has been commercialized by the company LC Sciences.[41]

1.3.3. Peptide microarrays: 'solid' solvent approach with laser structuring

Peptide arrays can also be synthesized by a 'solid' solvent approach.[42–45] This method is based on the SPOT technique, but the role of the liquid solvent in this case is fulfilled by a polymeric matrix material, which is solid at room temperature and softens upon heating, serves as a solvent-like coupling medium for the peptide bond formation (see Figure 3).[23]
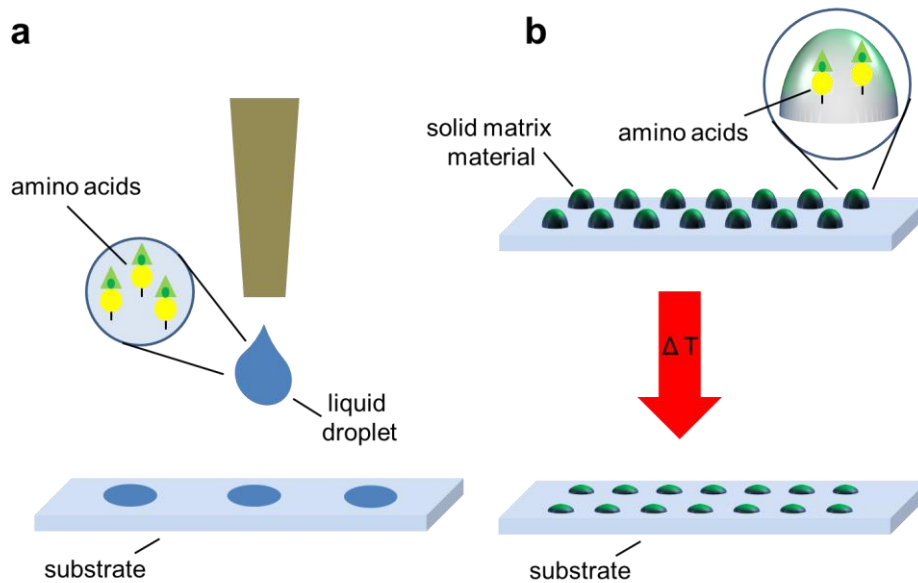
Figure 3: Peptide array synthesis: (a) the SPOT technology is liquid solution based, the amino acids are dissolved in and then coupled from a liquid; (b) the solid matrix material approach, the amino acids are embedded in a solid matrix material, upon heating the matrix softens; this leads to diffusion of the amino acids and enables peptide bond formation

For the 'solid' solvent approach, the arrays are synthesized on a glass slide, which is covered with a polymeric synthesis film.[42–49] The polymeric synthesis film is anchored to the glass substrate via a silane. The synthesis film consists either of pure poly(ethylene glycol) methacrylate (PEGMA) or of poly(ethylene glycol) methacrylate-co-methyl methacrylate (PEGMA-co-MMA). The peptides are bound to the synthesis film *via* a β-alanine (β-Ala) that is coupled via an ester bond to the hydroxyl end groups of the PEGMA. Peptides are synthesized using chemical steps analogous to Fmoc-SPPS. OPfp activated amino acid derivatives are used. By pre-activating the derivative it is not necessary to add additional activation components to the reaction mixture, thereby simplifying the reaction. Peptide synthesis proceeds *via* a cycle consisting of four major synthesis steps (see Figure 4).
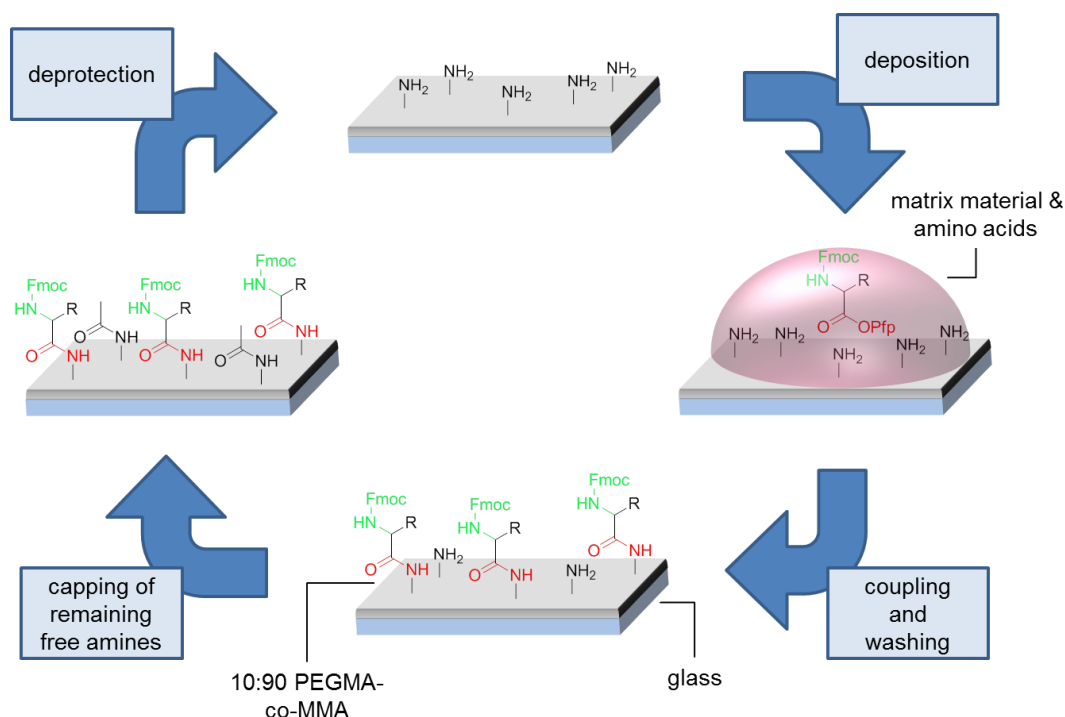
Figure 4: Synthesis cycle of peptide arrays in the 'solid' solvent approach: deprotection, deposition, coupling and washing, capping of remaining free amines.

First, the Fmoc protection group on the growing peptide chain is removed using a mixture of piperidine/DMF (20:80 vol-%).[7] In the next step, a mixture of solid matrix material and amino acid derivative is deposited on the surface. Subsequently, the coupling is induced by heating in the oven. The matrix material softens at temperatures above its glass transition temperature (T_g). This enables diffusion of the amino acid derivatives through the matrix material and also coupling, as the matrix materials serves as a solvent-like reaction medium at elevated temperatures. After the coupling, remaining matrix material and unreacted amino acid derivatives are washed away. To prevent the synthesis of false sequences, unreacted amines on the surfaces are capped with a solution of acetic anhydride, *N,N*-diisopropylethylamine (DIPEA) and DMF (10:20:70 vol-%).[44,45,47,48] After washing the elongated peptide, it can be Fmoc-deprotected again and the cycle repeats.

To create an array, it is necessary to structure the surface and have information about the exact position and sequence of the peptide spots on the array. The deposition of the amino acid and matrix material mixture needs to be precise with a high spatial resolution

and high repeatability over several cycles. This can be achieved by different laser based methods.[*]

1.3.3.1. Xerographic approach

One approach is the xerographic method, where particles consisting of matrix material and amino acid derivatives are deposited on the surface by a laser printer.[42,43]

Figure 5: View inside the laser printer used to produce peptide arrays by the xerographic method showing the different cartridges. Image © PEPperPRINT, reproduced with permission.[50]

The laser printer (see Figure 5 for illustration) contains 20 different cartridges.[42] By adding extra cartridges to the setup, it is also possible to integrate a limited number of special building blocks into the array. A prerequisite is that the special building blocks are compatible with the Fmoc-protection strategy for peptide synthesis and that they can be OPfp-activated. The amino acid derivatives are embedded into a polymeric matrix material. This mixture is then used for particle production. This can be done by two different strategies: the milling process and the spray drying process.[42,47] The resulting particles are filled into the printer cartridges.

The positioning of the amino acids from the reservoir within the cartridge onto the target position on the synthesis surface is achieved with an organic photoconducting (OPC)

---

[*] Where not noted otherwise, figures in this section have previously been published in Ridder, B.; Foertsch, T. C.; Welle, A.; Mattes, D. S.; von Bojnicic-Kninski, C. M.; Loeffler, F. F.; Nesterov-Mueller, A.; Meier, M. A. R.; Breitling, F. *Appl. Surf. Sci.* 2016, *389*, 942-951, reprinted with permission from Elsevier.

drum.[42] The printing procedure starts with a uniformly electrically charged OPC drum. Light emitting diodes (LEDs) pattern the drum. Irradiated areas on the drum are discharged, the others remain charged. The drum then passes a cartridge containing the amino acid derivative loaded polymeric particles, which have been charged triboelectrically *via* friction beforehand. The charged particles stick to the neutralized positions on the OPC drum. Subsequently, the loaded drum rolls over the synthesis surface where the particles are deposited.

This approach is limited by the amount of cartridges, thus limiting the number of different amino acid derivatives that can be incorporated into a single array. For very expensive special building blocks, this method is not suitable, since for the particle production process, a large minimum amount of material is required (> 10 g of activated amino acid building block). Finally, the resolution depends on the amount of pixels that can be achieved by the LED irradiation. Currently, with this technique, spot densities of up to 775 per cm^2 can be reached.[48]

An advantage of the xerographic method is its enormous throughput as deposition of all amino acids all over the array takes place in a very short time in one printing step and no processing is required in between structuring steps with different amino acids. Afterwards, the entire layer of amino acids can be coupled, washed, capped and Fmoc-deprotected in one step.

The method to produce peptide arrays xerographically has been commercialized by the company PEPperPRINT.[50]

1.3.3.2. Laser fusing

The laser fusing approach to peptide array synthesis was presented by Maerkle *et al.* in 2014.[44] Here, the synthesis slide was covered homogenously with a layer of particles consisting of a polymeric matrix material, in which OPfp activated amino acids were embedded. A pulsed laser is used to melt the particles at each position on the array, where the amino acid, currently embedded into the matrix material, must be added to the growing peptide chain. By melting the matrix material, it is fixated on the surface. In a next step, the unfixated particles are removed from the surface. Then the surface is coated again with particles carrying a different amino acid derivative. Subsequently another laser based fixating step is carried out. The procedure is repeated until all positions are filled with fixated particles of the target amino acid derivative. Only after the completion of all the structuring steps, a coupling step in the oven is performed, followed by the synthesis cycle described above in Figure 4. With this method, spot densities of up to 40,000 spots per cm^2 are possible. A major disadvantage is the time consumption,

as the particle deposition and subsequent laser based fixating step have to be done separately for each amino acid with required cleaning in between. This method has been patented but has not been commercialized.[51]

1.3.3.3. Combinatorial laser-induced forward transfer

The latest laser based method to synthesize peptide arrays was presented by Loeffler and Foertsch *et al.* in 2016.[45] Here, a donor-acceptor based method is used; where a material transfer between the two takes place to create an array. The donor consists of a glass slide covered with polyimide foil, onto which a mixture of a polymeric matrix material and amino acid derivative is spin-coated. The acceptor is a glass slide functionalized with a PEGMA-co-MMA synthesis film functionalized with at least one β-Ala. The two slides are placed on top of each other, the donor facing down and the acceptor facing up. At the target position, a laser beam impulse transfers matrix material with embedded amino acid derivatives from the donor to the acceptor slide (for illustration see Figure 6).
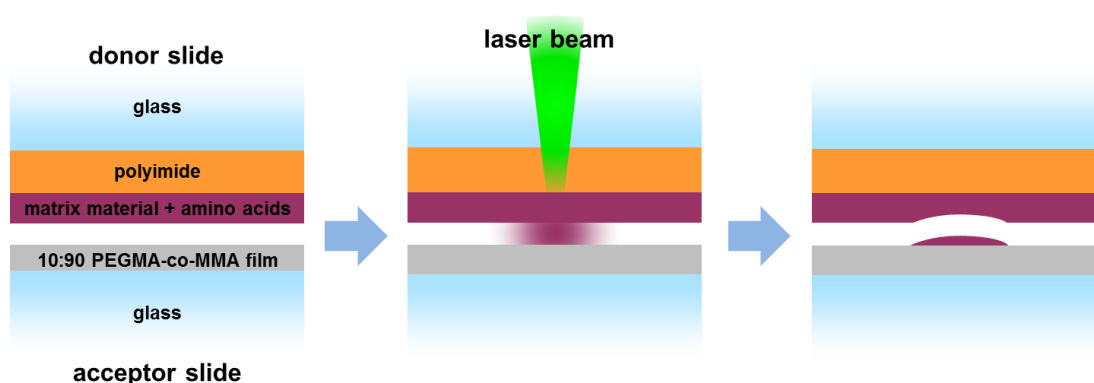
Figure 6: Schematic illustration of the combinatorial laser-induced forward transfer.

One amino acid derivative can be used per donor slide, but the donors can be reused up to 20 times. Donor slides can be exchanged easily by an automated system using a slide loader (see Figure 7). The slide sandwich is positioned under the laser beam by a moveable x-y stage. The pulse duration and the laser intensity can be regulated by an acoustic optic modulator (AOM). In this way the transfer parameters can be adjusted to application needs (*e.g.* varying pitch sizes and adjusting for different materials). For the structuring it is also necessary to move the laser beam between target positions; this is done by a scan head. With this approach, spot densities of up to 17,777 spots per cm^2 can be achieved.
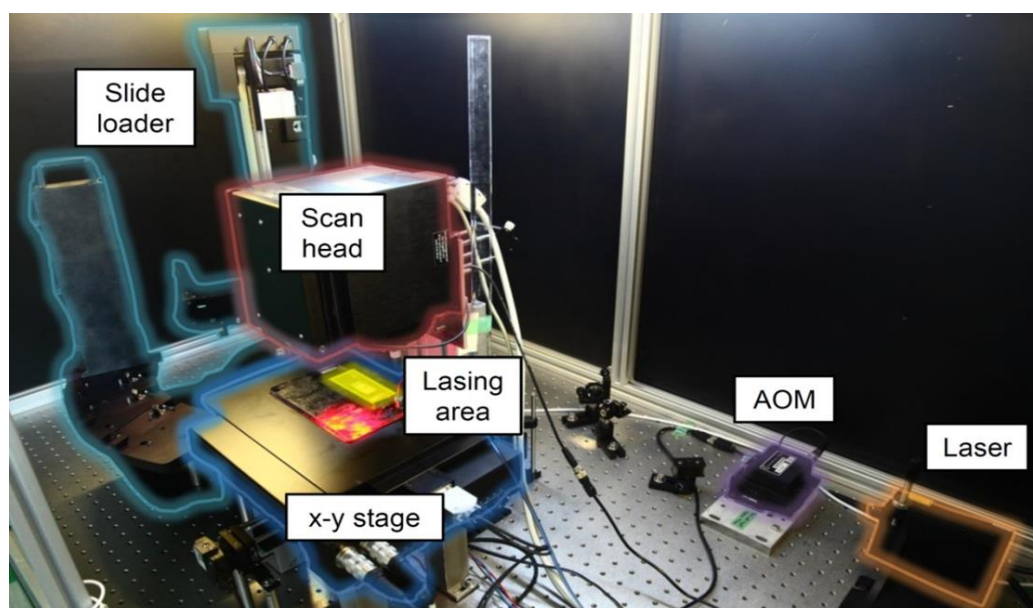
Figure 7: Combinatorial laser-induced forward transfer machine setup. An acousto-optic modulator (AOM) regulates the laser beam, which then passes through a scan head system. The laser transfer takes place on an x-y microscope stage (see highlighted in yellow the lasing area). Slides are manipulated and placed by a robotic slide loader. Reproduced under CC-BY, Loeffler and Foertsch *et al.*[45]

The advantages of the laser-induced forward transfer system are its flexibility and versatility. Special building blocks can be easily incorporated into the array by producing a donor slide covered with the desired building block. Also reactions with multiple starting materials are possible. To achieve this, first a transfer from the first donor onto the acceptor slide is performed. In a second step material from another donor is placed directly on top of the first deposited spot. This can be repeated. Finally, during the coupling step in the oven, the components from the top layer(s) diffuse into the lower layer(s), where *e.g.*, an *in situ* activation can take place. Then they diffuse further and can couple to the synthesis film.

The high flexibility also comes at a price. For each component in each layer the donor slide has to be exchanged. The mechanical impact during this exchange disturbs the alignment of the acceptor slide, which then needs to be repositioned with respect to the laser's position to align the new layer precisely with the previous. Even though the exchange and re-alignment can be automated with a slide loader it is still time consuming. On the other hand, the method is suited very well when using expensive starting materials, as only small amounts of material are needed to produce a donor slide, which can then even be reused and recycled.

## 1.4. Multicomponent reactions as tools for library synthesis for screening

Until now, only peptides were presented as objects of interest for high throughput screenings in biomedical or in other bio applications, either synthesized with the SPPS approach on beads or on surfaces in the peptide array approach. Libraries of small organic molecules for screening purposes are also of great interest for screening and drug development for pharmaceutical applications.[52,53]

One possibility to achieve such libraries is to use multicomponent reactions. Multicomponent reactions (MCRs) are defined as: 'One-pot reactions that form products from three or more different starting compounds…'.[53] Characteristic for MCRs is their high atom economy; all or almost all atoms of the educts are also present in the product.[54] Furthermore, they are highly selective and the number of steps in synthesis and purification is minimized compared to classic synthesis procedures.[54,55] Examples of MCRs are the Hantzsch, the Biginelli, the Mannich, the Passerini and the Ugi multicomponent reactions.[53,55]

The rationes behind using MCRs for library synthesis are manifold. First and foremost, the possibility to obtain many different products relatively easy by varying the starting components and thereby the properties of the products of the MCRs.[53] As each starting material can carry a different side chain with functional groups, MCRs offer versatility and can broaden the complexity of a library consisting of many different molecules. In the literature, this was shown exemplarily on the Ugi four component reaction (U-4CR), which is a MCR. It was reported that if 40 different molecules of each of the four components necessary for the U-4CR were combined combinatorically, would lead to a library of 2,560,000 possible products.[56] Secondly, the commercial availability of many starting materials is an advantage. Thirdly, many of the products are biologically active also when they appear in racemic mixtures.[55] Fourthly, the one pot approach and a minimum of purification steps lead to high yields and save time and waste.[57] Fifth, the library built-up process can be automated to create giant libraries within few hours.[54] Disadvantages of MCRs are the requirement of often toxic solvents, the sometimes harsh reaction conditions that need to be applied and the long reaction times.[55]

One MCR that is especially suited for library synthesis is the U-4CR, because it offers high versatility with the four educts, each possibly carrying a different side chain, and its products have a 'peptide-like' structure.[54] The Ugi reaction belongs to the class of isocyanide based multicomponent reactions. In the four component variant of the Ugi

reaction, an amine, a ketone or aldehyde, an isocyanide and a carboxylic acid react to an α-aminoacylamide derivative under elimination of a water molecule (see Scheme 7).
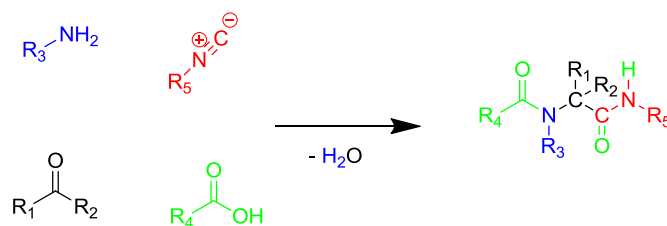
Scheme 7: The Ugi four component reaction: an amine, a ketone or aldehyde, an isocyanide and a carboxylic acid react to form an α-aminoacylamide derivative under elimination of a water molecule.

Armstrong and coworkers took inspiration from the 'peptide-like' structure of the U-4CR products and used a solid support, in a technique analogous to SPPS, to parallelly synthesize a combinatorial library of U-4CR products.[52,58] The library synthesis was performed on a Rink-Fmoc-amide resin, which is also used in peptide synthesis,[58] therefore well-established SPPS protocols such as Fmoc-deprotection with piperidine could be applied. The amine, which is present on the surface of the beads after Fmoc-deprotection, serves as the amine component of the U-4CR and thus anchors the reaction product to the bead.

For peptide libraries, the next step after SPPS was the synthesis of libraries on a surface to produce peptide arrays. The advantage of arrays is that the molecules are immobilized and many different structures can be screened at the same time. This step was also taken for the synthesis of small molecule libraries *via* the U-4CR.

Well-known and well-characterized substrates for peptide array synthesis are cellulose membranes, which are used for the SPOT synthesis. Cellulose as a substrate has various advantages: it is inexpensive, widely available and robust towards many different solvents and harsh reaction conditions such as microwave procedures and oven treatments.[59]

To be able to perform reactions on cellulose it has to be pre-activated first and functionalized with linker molecules so that free amines are present on the surface, which can then be used as the anchor to the surface in subsequent reactions.[59–61] Then, analogous to the SPOT technique, droplets containing the other components of the U-4CR are placed on the activated cellulose substrate. For higher yields, the subsequent reaction is performed with microwave assisted techniques.

Applications in biological context have already been reported, *e.g.* screening for diketopiperazines as activators as well as inhibitors for quorum sensing in Gram-negative bacteria.[60]

1.5. Polymers

An obvious requirement for 'solid' solvent approaches is the solid matrix material. Polymers are excellent candidates, because their properties such as softening points can be easily controlled.

Polymers are macromolecules, which are built up from smaller molecules, called monomers, which are linked together and form repeating units. Polymers occur in nature, for example proteins, DNA or cellulose. Polymers can also be synthesized *via* different pathways such as step-growth polymerization and chain-growth polymerization.[62,63]

Classic step-growth polymerization is based on polyaddition or condensation reactions such as ester formations between alcohols and acids or acid chlorides as well as amide links formed by reactions between amines and acids. To be able to form a polymer, it is necessary to use at least bifunctional monomers. In the step-growth mechanism, first two monomers react with each other to a dimer and later to a trimer, when the bifunctional monomer reacts with a monomer on each side. This leads to a rapid monomer conversion as most of it is consumed during this dimer formation. In the proceeding of the reaction, dimers and trimers can react with each other to form oligomers, which in turn react with each other to larger polymers.

One of the most commonly techniques to synthesize polymers is chain-growth polymerization. Here, one monomer at the time is added to an initiator molecule resulting in a growing polymer. The addition of the monomer into the growing polymer takes place at the active center. In this way the polymer only grows into one direction and when the active center is deactivated, the chain growth is terminated. For instance, ionic polymerization methods and free radical polymerization belong to the category of chain-growth polymerization techniques.

1.5.1. Free Radical Polymerization

Free radical polymerization is one of the most widely used polymerization methods on large scale in industry, where many different products are available.[64] It is very versatile, suitable for many different monomers, whose functional groups must not necessarily be protected, and it is relatively easy to perform with inexpensive reagents.[65]

Free radical polymerization proceeds *via* a three step mechanism: initiation, propagation and termination (see Scheme 8).[62,63,66]

Initiation

1.

$$I \xrightarrow{k_d} 2\,R\bullet$$

2.

$$R\bullet + M \xrightarrow{k_i} RM\bullet$$

Propagation

$$RM_n\bullet + M \xrightarrow{k_p} RM_{n+1}\bullet$$

Termination

$$2\,RM_n\bullet \xrightarrow{k_{tc}} RM_nM_nR$$

$$2\,RM_n\bullet \xrightarrow{k_{td}} RM_nH + RM_{n-1}$$

$$k_t = k_{tc} + k_{td}$$
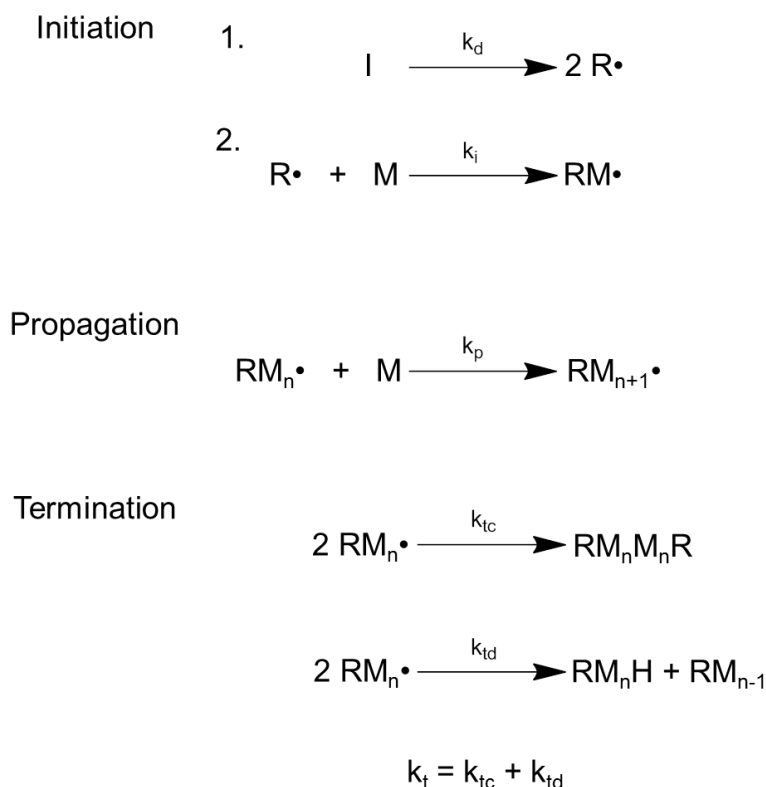
Scheme 8: Schematic representation of the three steps of the radical polymerization mechanism: initiation, propagation and termination. (I = initiator, R = radical, M =monomer, k_d = dissociation rate constant, k_i = initiation rate constant, k_p = polymerization rate constant, k_{tc} = combination rate constant, k_{td} = disproportionation rate constant, k_t = termination rate constant)

The first step is the initiation. Commonly peroxides, hydroperoxides, azo compounds or photoinitiators are used as initiator molecules. The initiator molecule decomposes into two radicals, which can in principle both react with a monomer. Not all of the produced radicals react with a monomer; some for instance react with each other and recombine. A polymeric chain is started by reaction of the initiating radical with the first monomer. Compared to the decomposition of the initiator, the reaction of a radical with a monomer is very fast, making radical production the rate limiting step and thus the decay of initiator molecules into radicals determines the rate constant of the initiation step (see Equation 1)

$$\left(\frac{+d[R\bullet]}{dt}\right) = 2fk_i[I]$$

Equation 1: Kinetic equation of the initiation step (R= radical, I= initiator, k_i= initiation rate constant, f= initiator efficiency)

After the initiation step, the propagation step follows. Here, the polymeric chain starts to grow as monomers are incorporated into the polymeric backbone. The reactivity of the radical determines the growth speed of the polymeric chain. From a kinetic point of view, the addition of monomers is a very fast step and is effectively of first order in radical concentration, as the monomer concentration is much larger than the radical concentration. The simplest form of propagation kinetics is described by Equation 2.

$$\left(\frac{-d[M]}{dt}\right) = k_p[RM_n\bullet][M]$$

Equation 2: Kinetic equation of the propagation step (RM$_n$= growing polymeric chain carrying a radical, M= monomer, k$_p$= propagation rate constant)

The last and final step, the termination step, ends the process of polymerization and the growth of the polymeric chain. Termination can take place *via* two ways, either combination or disproportionation. Combination takes place, when two radicals react with each other and the two growing chains are combined. The second possibility of a termination is the disproportionation. Disproportionation takes place when a radical chain abstracts a hydrogen atom from a second polymeric chain. This is energetically more demanding than recombination. The rate constants of recombination and disproportionation are added together to give the total rate constant of termination (see Scheme 8). The termination process is a second order process as two radicals have to recombine (see Equation 3)

$$\left(\frac{-d[RM_n\bullet]}{dt}\right) = 2k_t[RM_n\bullet]^2$$

Equation 3: Kinetic equation of the termination step (RM$_n$= growing polymeric chain carrying a radical, k$_t$= rate constant termination)

1.5.2. Controlled Radical Polymerization (CRP)

For many applications, it is necessary to have access to polymers with a narrow dispersity and a defined molecular weight. This control is not possible with classical free radical polymerization due to the short life-time of the growing polymeric chains.

One way to reach the goal of well-defined high molecular weight polymers is *via* Controlled Radical Polymerization (CRP) methods.

A polymerization method has to fulfill certain requirements to be classified as CRP:[62] the degree of polymerization has to grow in a linear fashion to the conversion, the dispersity of the product should be low (under 1.3), it should be possible to synthesize block copolymers, each polymer chain should carry a functional end group, to allow, *e.g.,* polymerization of a second monomer in a second polymerization step or post-modification. Additionally, if possible the method should be robust, *e.g.,* tolerate impurities and water.

CRP methodology enables reduction of the dispersity of polymers, but also control over the architecture and the possibility to synthesize block copolymers in contrast to free radical polymerization.[64] The composition can be varied when two different monomers are combined in various ways and different architectures can be achieved, for instance, with multifunctional initiators (see Figure 8).
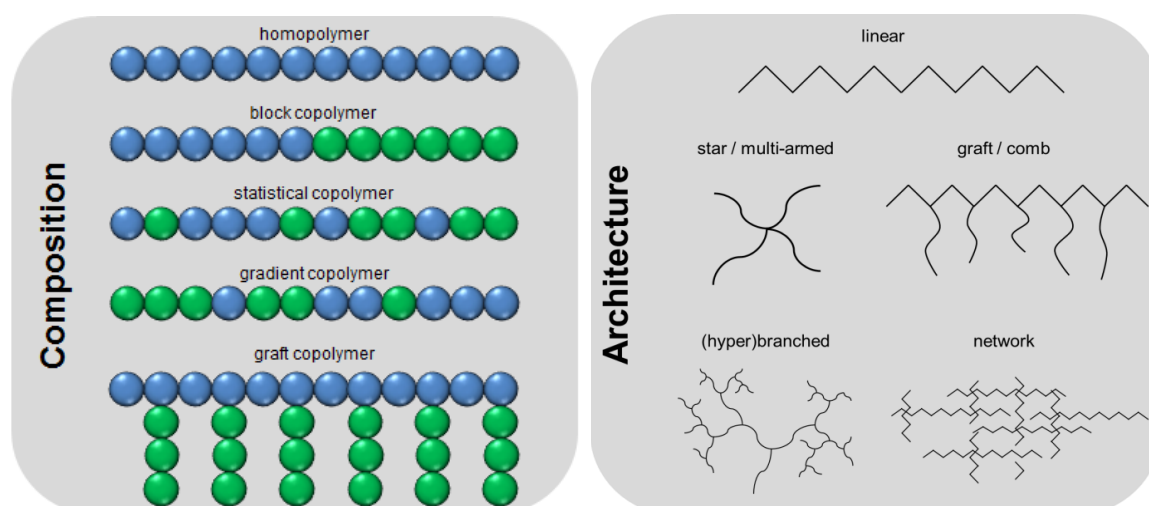
Figure 8: Illustration of different polymer compositions and architectures.

Control over a radical polymerization can be gained when a system of dormant and active chains is in an equilibrium which lies on the side of the dormant chains.[67,68] A dormant chain is a polymeric chain that is temporarily deactivated and therefore, no monomers are incorporated into the molecule at this stage. The deactivation in the case of a dormant chain is reversible and the chain can return to actively incorporating monomers. The dormant chains lower the concentration of radicals present in the reaction, thereby prolonging incorporation time of large numbers of monomer into the polymer. Here it is very important that the deactivation of the growing chains is reversible and fast. A fast initiation ensures that the initiation of all polymeric chains is started at the

same time. Under these conditions the monomers can be distributed evenly over a large amount of chains, which grow slowly but at about the same rate.

CRP processes are mainly achieved by three different routes:[64,69] stable free-radicals, degenerative transfer or metal mediated.

Nitroxide Mediated Polymerization (NMP), which is a stable free-radical polymerization, is one of the first CRP processes to be reported. It was invented in the 1980s in the CSIRO labs.[65] In this approach, the growing polymeric chain carries a radical but also a second radical is present, which by itself is not able to initiate chain growth (see Scheme 9). This second radical can reversibly combine with a growing chain, bringing it to the dormant state. Upon dissociation the polymeric chain regains its radical character and is able to grow again. The stable radicals that are used as counter radicals are often nitroxides, such as 2,2,6,6-tetramethylpiperidin-1-oxyl (TEMPO), 1,1,3,3-tetraethylisoindolin-N-oxyl or di-t-butyl nitroxide.

Scheme 9: Schematic illustration of the NMP mechanism.

A wide range of different monomers can be polymerized via NMP. It is especially suited for styrene and its derivatives, but also polymerization of acrylates, acrylamides, acrylic acids and acrylonitriles is possible.[70] The polymerization of methacrylates via NMP is difficult due to the side reaction of proton abstraction from the methyl group.[67] High temperatures of about 80 to 120 °C are necessary for the polymerization to proceed, even then, it remains quite slow.[62]

An example of degenerative transfer polymerization is the Reversible Addition Fragmentation Transfer polymerization (RAFT). Here, the polymerization is initiated by generation of a radical usually by thermal decomposition.[69] The generated radicals react with a monomer unit to a starting polymeric chain, but propagation is inhibited by the reaction of the starting chains with the carbon-sulfur double bond of the RAFT agent. Propagation now only takes place when the two dissociate again or when the R group, which was originally attached to the RAFT agent dissociates from the molecule (see Scheme 10). In this case it can start a second polymeric chain. The dissociation takes place fast, but the recombination is evenly fast, so that the chains exchange between active and dormant state rapidly.
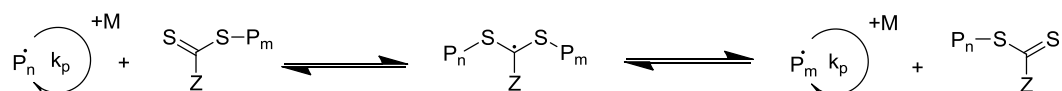
Scheme 10: Schematic illustration of the RAFT mechanism

One of the advantages of the RAFT method is that many different monomers can be polymerized under relatively mild conditions.[62] In this variety lies also one of the drawbacks: the initiator has to be chosen to fit the reaction and be adapted for each new monomer, for each new combination of monomers and for each new reaction conditions.[71]

The initiator can also be problematic with respect to the resulting polymeric products, as thiols are often smelly compounds which are undesirable in a product. Other problems with the dithioester end groups are instability at high temperatures and under influence of light and difficulties, when functionalizing these end groups with post-polymerization end group functionalization.[62] Despite these difficulties, end group functionalization is possible and has been strongly investigated.[69]

One example of metal mediated controlled polymerization is Atom Transfer Radical Polymerization (ATRP). Only halogenated compounds are usable as ATRP initiators, including halogenated alkanes, benzylic halides, α-haloesters, α-haloketones, α-halonitriles and sulfonyl halides.[72] When the halogen is attached to the polymer, the chain is dormant (see Scheme 11). Upon dissociation of the halogen, the chain becomes activated and starts to add monomers. The dissociated halogen attaches to the metal complex, usually consisting of Cu(I)X and a ligand. The copper gets oxidized by the addition of the halide. This is a reversible process, but the equilibrium lies on the side of the dormant chains.
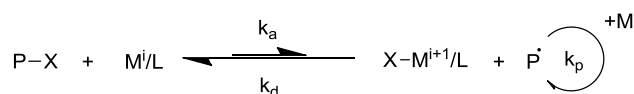
Scheme 11: Schematic illustration of the ATRP mechanism.

A major disadvantage of ATRP is the use of the copper catalyst: it is oxygen sensitive and degradation through oxidation can influence the effectiveness of the polymerization protocol.[67] Additionally, the copper catalyst needs to be removed after completion of the reaction because it is toxic towards many organisms, limiting the use for biomedical or other bio applications.[62] The removal remains a challenging task, therefore approaches are being investigated to limit the required amount of the copper catalyst.[64]

The halide end group is still present after completion of the polymerization and can then be used as an easy access point for end group functionalization, giving an extra point of versatility to the ATRP synthesis. A broad variety of monomers can be polymerized with ATRP in different topologies and copolymer compositions.[64]

1.6. Polymer characterization

After polymer synthesis, the next step is to characterize and investigate the mechanical properties, as well as the stereochemistry, crystallinity, thermal transitions, viscosity, end groups, polydispersity and mass averages.[63] Here Differential Scanning Calorimetry (DSC) and Size Exclusion Chromatography (SEC) will be briefly introduced, as they were also used in this thesis. SEC can be used to investigate the dispersity of a polymer and its mass averages, while DSC can be used to investigate thermal properties of polymers such as the glass transition temperature (T_g).

1.6.1. Glass transition temperature (T_g)

The glass transition temperature (T_g) is an important physical property of a polymeric material, as it determines if the material is stiff and brittle (below) or viscous and rubbery (above).[63] If the T_g of a material is above room temperature, it is referred to as a plastic, whereas materials with T_g's below room temperature are called rubbers. Above the T_g the chains of the polymers are more flexible and can move more freely, giving the material soft, rubbery properties, whereas below the T_g there is not enough energy for the chains to move, so they are in a sort of frozen state, giving the material brittle and hard properties.

Unlike the melting point, which is a phase transition according to thermodynamic definitions, the T_g is defined as a second-order phase change.[66] The mechanism of the transition is not yet completely understood, but as the cooling/heating rate of the sample influences its T_g, it is not a classical thermodynamical phase transition.[63]

The T_g of a polymer is influenced by various parameters, such as steric hindrance, side group effects, symmetry, polarity and copolymerization.[63]

1.6.2. Differential Scanning Calorimetry (DSC)

DSC measurements are used to determine the change in amount of heat during a chemical or physical transformation, such as a reaction between two educts, melting or crystallization of a substance.[62] To measure these differences in heat, two different approaches are described as DSC measurements:[73]

The power compensating DSC method has two ovens. The sample pan is placed in one oven and a reference pan in the other. When both ovens have the same temperature, the instrument heats both equally. If a thermic event takes place in the sample oven, this oven will be heated correspondingly more or less to keep matching the temperature of the reference oven. The heat flux can be derived from the difference in heating power between both ovens. This method is especially suitable to measure very fast reactions.

For the heat flux DSC approach, both samples are placed in one oven and are heated simultaneously and constantly. The reference pan and the sample pan each stand on a sensor, which measures their temperature. During heating, when no endo- or exothermic event takes place, the heat flow, calculated from the temperature difference between the two pans, is zero because both pans have the same temperature. If an endothermic event (*e.g.* melting) takes place in the sample pan, the temperature of that pan stays constant at the melting temperature until the sample is completely melted. The temperature of the reference pan continues to rise. From the difference in temperature between the two pans, the heat flow can be calculated. Conversely, an exothermic process in the sample pan will lead to a higher temperature than in the reference pan, again allowing the heat flux to be calculated from the temperature difference. Advantages of the heat-flux method are that it is an easy to handle and robust apparatus, which can also handle samples that produce gas during measurement. A stable baseline of the measured curves allows good determination of T_g.

1.6.3. Size Exclusion Chromatography (SEC)

SEC is a method to determine the molar mass distribution within a polymer sample as well as the mean of the molecular mass.[62,74,75] In SEC, the components of a sample are separated by their hydrodynamic radius. The sample is run over one or more columns containing a porous material with varying pore sizes. Molecules with a smaller hydrodynamic volume diffuse into the pores, whereas larger ones do not fit and elute directly. The small molecules have to diffuse out of the pores before being eluted and therefore their path through the column is longer. Thus, the elution of the components of the sample is from high to low hydrodynamic volume. An elution time can be matched to a molecular weight by inserting a sample of known molecular mass. When doing so with various samples of known molecular masses, a calibration curve is obtained, which can then be used to determine the molecular masses of new samples. A calibration can only be used for polymers of the same kind, as the hydrodynamic radius also depends on the molecular composition and architecture of the polymers not just the molecular weight. The obtained molecular mass of a polymer is then relative to the sample which was used for calibration.

Drawbacks of the method are that only soluble polymers can be characterized, the separation is limited by the of porosity of the column (too porous and it would collapse) and a risk of coelution of distinct components, since the hydrodynamic radius is determined not only by the molecular mass of the polymer but also by its architecture and composition.[74]

The method also has major advantages: it can be used for abroad range of applications from characterization of block copolymers *via* biopolymers to micelles.[75] Also it is a robust technique, which gives results with a high reproducibility and is relatively easy to use.[74]

1.7. Functional surfaces

In general, material properties can be tuned by functionalizing or covering their surface. This is of great interest both in the field of materials science as well as in the field of biomaterials.[76] By covering the surface of a material, it can be protected against corrosion or erosion; biocompatibility or electrical properties can be tuned. Extra properties, such as anti-fouling, hydrophobicity or promoting cell adhesion, can be added.[77–80]

One sort of functional surfaces has already been introduced with peptide arrays. In order to be able to synthesize a peptide on a surface with the 'solid' solvent approach, the surface has to be pre-functionalized with a polymeric film.

1.7.1. Surfaces covered with polymers

Surfaces can easily be coated with polymers by dip coating or spin coating. These physisorption processes are a very easy and fast way to coat materials with good control of the layer thickness. The major disadvantage of these techniques is that there is no covalent bond between the surface and the polymer and the films will detach from the surface over time.[81] For more durable materials, it is necessary to covalently attach the polymer to the surface. The two major approaches to achieve this are 'grafting onto' and 'grafting from' (see Figure 9).[81,82]

Grafting onto

polymer chains

Grafting from

monomer

substrate with anchor

substrate with initiator
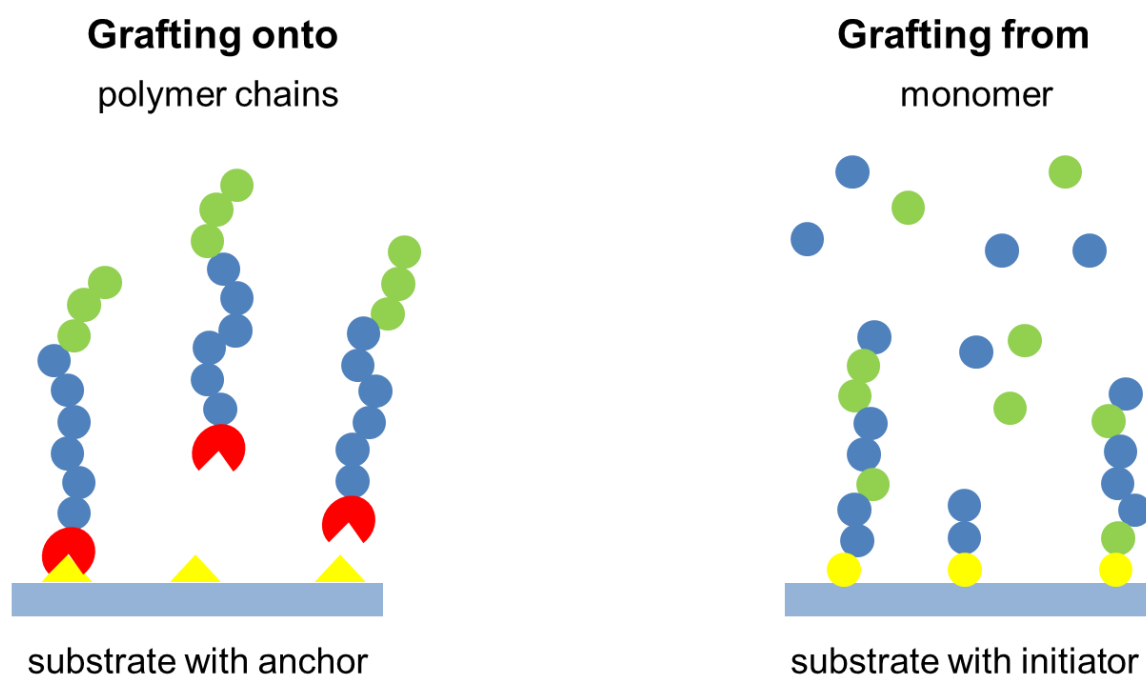
Figure 9: Schematic illustration of surface functionalization with polymers using the grafting onto and the grafting from method.

For the grafting onto approach, the surface is functionalized with anchor molecules. Pre-synthesized polymer chains, which are functionalized with the counter molecule to the anchor, can then bind to the surface. An advantage of this method is that the polymeric chains on the surface are of defined length and composition. The grafting density of this method is usually very low, as the polymers collapse onto the surface and block the anchor molecules, meaning only thin films can be synthesized.

In the grafting from approach, initiator molecules are immobilized on the surface. The surface is then immersed in a monomer solution and the polymeric chains are grown monomer by monomer directly on the surface. In this way, higher grafting densities are possible, as the parallel growing chains hold each other up, preventing chain collapse and allowing the synthesis of thicker polymeric layers. Another advantage of the method is its flexibility: because different monomers can be used, even ones carrying functional groups as there is no anchor binding chemistry involved. Also gradients can be achieved. Disadvantages are that not all polymeric chains will have the same length and composition, as the polymerization is not always fully controlled. Additionally, the analysis of the polymers is challenging as they have to be cleaved of the surface to perform *e.g.* SEC to gain information about the size distribution and the molecular weights. Polymerization rates can be influenced by surface effects, such as the substrate geometry. The polymeric film thickness that can be achieved with the grafting from

method is limited to about 500 nm.[83] This is thicker than with the 'grafting onto' method, but still quite thin if thick layers in the μm range are required. The limiting factors are still not completely understood; probably the monomer concentration near the surface drops due to crowding of the growing chains, but also the termination of the growing chains seems to play a role. The covalent connection to the substrate makes grafted surfaces very interesting materials.

1.7.2. Molecular layer deposition (MLD)

Instead of growing statistical polymers on the surface or binding pre-synthesized macromolecules, it is also possible to functionalize the surface with discrete layers of small molecules, thereby introducing structuring in z-direction. When each layer is covalently bound to the previous, this is called molecular layer deposition (MLD).[84] Here, the advantage of the high grafting density of the 'grafting from' approach can be combined with the information about the exact order of the different monomers from the 'grafting to' approach. An example of MLD deposition are porphyrines, which are for instance of interest for electronical applications.[85]

Bifunctional molecules are especially useful for this approach, as they can first react with the functional groups on the surface, after which they still offer a handle for the next layer.[84,86] The use of bifunctional molecules represents a risk: both sides of the molecules can react with the surface, leading finally to termination of the layer growth.

Condensation reactions are very suitable for MLD when aiming at polymers on the surface. Here polyamides, polyimides, polyureas and polyurethanes are reported.[84] Click reactions are also a very interesting option for the MLD as no byproducts or additional reactants are necessary, which have to be removed from the surface after the layer addition. One example of a click reaction is the Thiol-Ene reaction, which can be performed on surfaces under mild reaction conditions and be initiated simply by illuminating with UV-light.[87] For aliphatic dienes in combination with either aliphatic or aromatic dithiols, it has been reported that a linear growth of the layer system is possible for up to nine layers, but special care has to be taken when using molecules with alkyl chains of ten carbons or longer. These longer molecules tend to bend over, leading to a loss of functionality and non-linear growth.[86] Thiol-Ene based MDL functionalization has also been reported for potential electrical applications with redox-active allyl ferrocene derivatives.[77]

1.8. Surface Analysis

An important and difficult part of surface functionalization is the analysis. A thorough characterization requires multiple complementary techniques.[2] For example: layer thickness can be studied with ellipsometry, whereas hydrophilicity/hydrophobicity is determined by contact angle measurements and protein adsorption or repelling is examined with microscopic techniques. The surface properties (*i.e.* layer composition, topology, evenness, adsorption and clustering) can be investigated on an atomic level with different forms of microscopy, such as electron based, scanning probe or atomic force. Information can also be obtained from infrared reflection-absorption and Raman spectroscopy. Other important techniques are secondary ion mass spectrometry and electron spectroscopy.

Three surface analysis techniques, which were commented on in this thesis, will be discussed in further detail below.

1.8.1. Time of Flight Secondary Ion Mass Spectrometry (ToF-SIMS)

Time of Flight Secondary Ion Mass Spectrometry (ToF-SIMS) is a very powerful analysis technique to investigate the chemical structure and composition of a surface.[88] It is only possible to analyze solid and vacuum stable samples as the spectrometer is operated under ultra-high vacuum.

The name Secondary Ion Mass Spectrometry (SIMS) refers to the way in which the measured fragments are generated:[2,88–90] The surface is bombarded with a primary ion beam. The kinetic energy of these primary ions (25 keV) is high enough to break covalent bonds on impact on the surface and within the topmost atomic layers of the sample. Monoatomic ions and molecular fragments, which have gained enough energy to overcome the surface binding energy, are extracted by an electric field, accelerated to a constant kinetic energy and mass separated in a Time-of-Flight (ToF) mass analyzer. However, only the charged fragments can be analyzed, the also generated neutral fragments cannot be measured. In the ToF analyzer, in principle, all generated ions of the chosen polarity are measured and separated by their flight time.[88] The detection limit of the ToF analyzer lies in the range of parts per million (ppm)/parts per billion (ppb).[91] This generates large data sets, where all the detected information is stored. Data reconstruction for specific fragments is possible. Therefore, new arising questions during data analysis can be addressed without a new measurement. As the amount of generated data is very high, the operator needs to be familiar with the analysis and able to condense the high amount of data to the essential information.[88] In general, ToF-SIMS is not able to give fully quantitative information on elements or molecules.[2,88] This relies

on the so called matrix effect of samples. The sputter rate and ionization probability of individual secondary ions is different, depending on the sample composition. An option to achieve condensed information is the usage of mathematical or statistical methods like Principal Component Analysis.[88]

The SIMS can be operated in static and in dynamic mode. For the static SIMS mode, the primary ion dose is kept below a fluence of 1×10^{11} ions per cm^2. With this ion dose, the analyzed area of the surface layer is kept generally around 0.1% of the total area which results in a mostly undamaged surface.[89]

To investigate deeper regions of the sample, it is possible to operate the instrument in the dynamic mode. Here, a second ion gun (usually O_2, Cs, C_{60}, Ar-cluster) is used to remove material from the sample.[90] The primary gun continuously scans the sample layer by layer generating three dimensional information, which can be used to obtain depth profiles.

For depth profiling, it must be considered that different materials are eroded at different speeds and yield, so the sputter ion fluence cannot be directly converted into a depth scale.[92] The depth can be gained from profiling instruments and then be applied to the measurement.

Advantages of ToF-SIMS for surface analysis are the high mass range, the possibility to measure large areas, the high sensitivity and the two operational modes: depth profiling as well as investigations of the top monolayer are possible.[89]

1.8.2. X-ray photoelectron spectroscopy (XPS)

X-ray Photoelectron Spectroscopy (XPS) is one of the key spectroscopic techniques to gain quantitative information on chemical binding states of topmost surfaces, in many cases even in a non-destructive manner. It can be used for a wide range of applications in the fields of material science, metallurgy, thin films, catalysis, semiconductors, polymers and biomaterials.[93]

XPS is based on photoemission: the sample surface is irradiated using AlKα or MgKα X-rays, to emit photoelectrons of topmost surfaces.[94] The kinetic energy of these photoelectrons is measured and - since the energy of the X-rays is known - the binding energy of the photoelectron can be calculated using Equation 4. The XPS sampling depth is about 10 nm, depending on the inelastic mean free path of the photoelectrons in different materials.[95]

$$E_k = hv - E_B - \phi$$

Equation 4: E_K measured kinetic energy of the electron, *hv* photon energy, E_B binding energy of the electron, ϕ work function of the spectrometer.

The elementary composition of the near-surface is then given in an XPS spectrum. XPS is able to give quantitative information about the elemental concentration on the surface, which is a great advantage of the XPS technique. Moreover, XPS can differentiate between the binding states of atoms based on photoelectron binding energy shifts due to their different binding situation in different compounds. This capability can also be used to follow chemical reactions on the surface monitoring the change of chemical bonds. Therefore, it is possible to distinguish between chemical surface modification and *e.g.* simple physisorption.

With the exception of hydrogen and helium, XPS can detect all elements of the periodic table.[94] The detection limit of XPS is quite high and depending on different elements about 0.1 to 1 atomic percent.

Similar to complementary ToF-SIMS, it is only possible to analyze solid and vacuum stable samples, as the spectrometer is operated under ultra-high vacuum conditions mainly to avoid contaminations by gas adsorption and secondly to reduce scattering of the photoelectrons on their way to the analyzer.

Advances in today's XPS spectrometers allow for quantitative chemical imaging at a spatial resolution of around 3 μm.[93] Long measuring times are required depending on the selected elements up to hours or days. The possibility to easily obtain quantitative chemical-state information makes XPS a valuable surface analysis technique and gives it a unique analytical power.[2,93]

1.8.3. Atomic Force Microscopy (AFM)

Atomic Force Microscopy (AFM) is especially useful as a surface analysis technique when investigating the structure or topology of a surface. It measures surface properties such as structure in the nano regime, morphology, topology but also mechanical properties.[2] The AFM technique was invented in 1986 by Binning and coworkers.[96]

The surface is scanned with a cantilever, which at the front is equipped with a molecular sized tip.[97] The attractive and repulsive interactions on the molecular level between the tip and the surface are transmitted into the cantilever. Only very small forces are at work between the tip and the surface about 10^{-11} to 10^{-6} N.[98] Any movement of the cantilever is registered by a laser beam which is pointed onto the tip of the cantilever. These movements can then be converted into a profile of the topology of the surface. It is also

possible to measure the height of very thin layers by AFM. To do so, it is necessary to create a sharp edge between the layer and the substrate this can be achieved *e.g.* by scratching with a sharp item.[99] The height of the edge then correlates with the thickness of the layer.

AFM has the advantage that the sample, which is measured, does not need to be conductive.[100] Therefore it is an especially interesting technique to analyze surface that have been functionalized with organic molecules or polymers.

2. Motivation

The functionalization of surfaces can be performed in different ways, but achieving control over the structuring of surfaces is especially interesting for applications such as microelectronics or bio applications *e.g.* peptide arrays. In this thesis, structuring in the xy-direction as well as in the z-direction was investigated.

Three different projects are described. They all have in common that they are focused on surface functionalization, but different aspects of this very broad field are investigated.

For the first part, structuring in xy-direction in the form of peptide arrays synthesis employing laser based transfer methods and solid matrix materials are investigated. Until now, in the particle or laser based approaches to produce peptide arrays, a commercially available matrix material, S-LEC-P LT 7552 (Sekisui) has been used.[42,44,45,47] The material is a resin consisting of a styrene-acrylic copolymer, but the exact composition is unknown. This is a major disadvantage, if further development, of these kind of applications, demands adaptations of the matrix material. Moreover, if the company would decide to stop production of this resin, it would not be possible to recreate it with the exact same composition. One aim of this thesis was thus to synthesize a matrix material, which is suitable for peptide array synthesis with the combinatorial laser-induced forward transfer method and solid matrix materials. In this method, a laser impulse transfers a mixture of amino acid derivative and solid matrix material from a donor slide onto the acceptor synthesis film. Thereby, a surface is structured by simply targeting the laser only at specific coordinates and inducing material transfer. Matrix material candidates have to meet several requirements to be suitable for the application. The goal was to find a suitable matrix material of which the exact composition is known, it should also be defined and allow for application adaptations (for a short graphical abstract, see Figure 10).
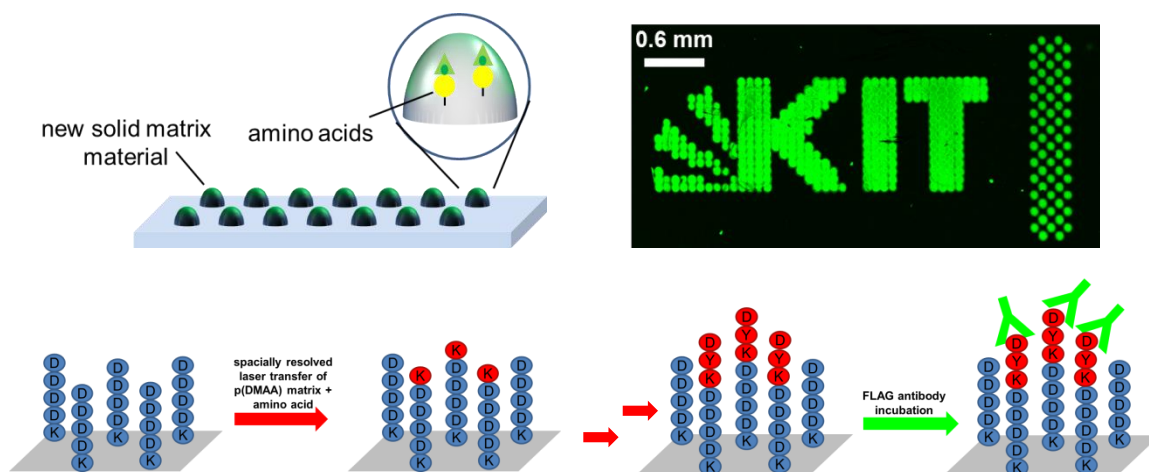
Figure 10: Graphical abstract matrix material development part, amino acids, embedded in the newly developed solid matrix material, can be coupled to a synthesis surface as evidenced by FLAG epitope staining.

The second part of the thesis also focuses on peptide arrays. Here, the U-4CR was tested for side chain modification of peptides on arrays. Post-synthesis modification of side chains of peptides on arrays *e.g.* with sugars is of great interest for investigation of glycoconjugates. Additionally, the possibility to integrate an Ugi product with its peptide like structure into a growing peptide chain as a proof of concept for a possible synthesis of peptidomimetics in array format was investigated (for a short graphical abstract, see Figure 11).
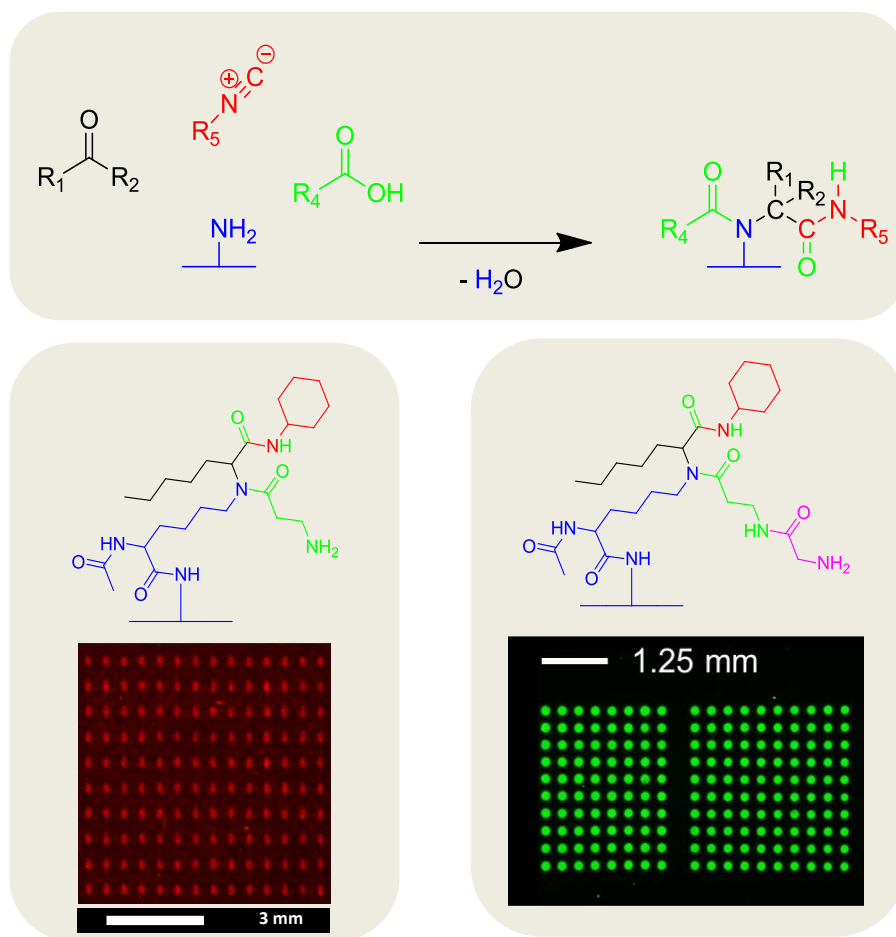
Figure 11: Graphical abstract for Ugi four component reactions on peptide arrays, side chain functionalization and integration into the peptide chain.

The first and the second part are focused on peptide arrays and structuring in xy-direction. The third part investigates control over the z-direction. As surfaces are three dimensional, gaining control over all three dimensions would open many possibilities to control the properties of a surface. It is imaginable to build in molecular barriers by control over the hydrophobic/hydrophilic properties. To achieve this goal, a layer system with a controlled structure in the z-direction is required. Thiol-Ene reactions are candidates for this layer systems, as they are click reactions and therefore very efficient and specific and no side products are formed, which would need to the removed after the synthesis. Therefore, the functionalization of the inorganic silicon wafer substrate with a silane to create the transition to the organic functional layers had to be optimized. The first functionalization with a Thiol-Ene reaction was investigated and the reaction

conditions and the surface analyses were optimized (for a short graphical abstract, see Figure 12).[†]
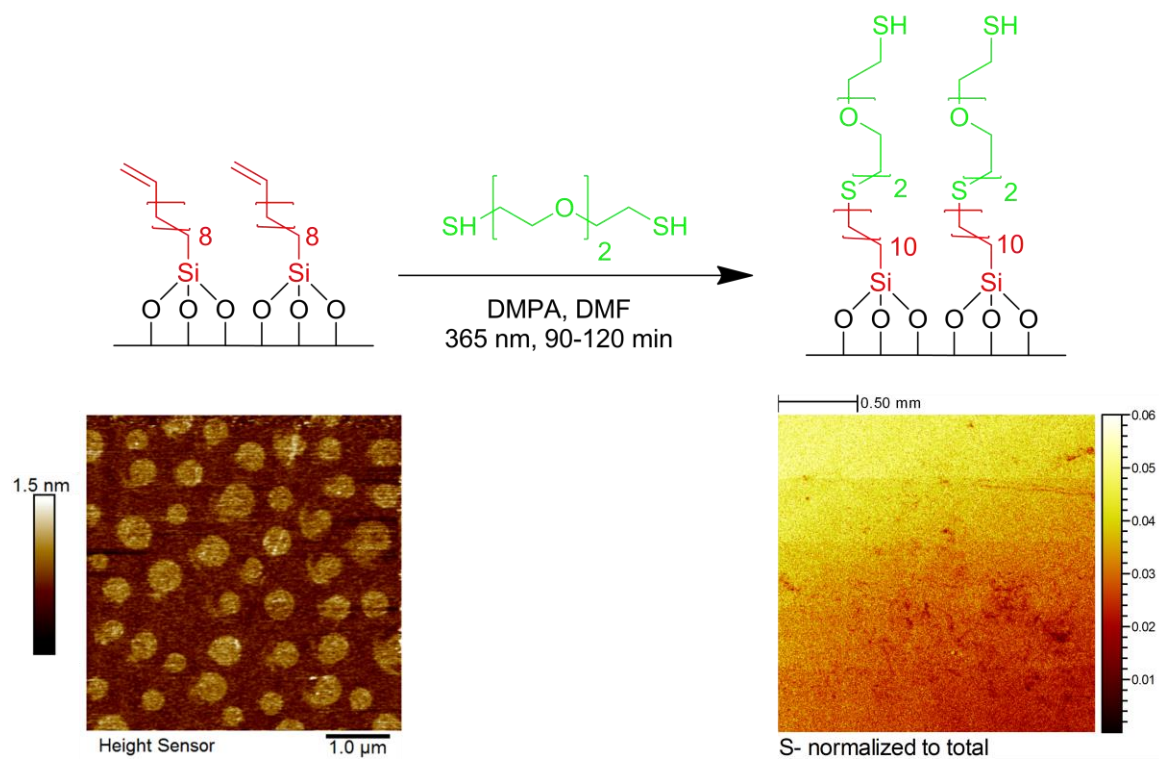
Figure 12: Graphical abstract for structuring in z-direction *via* molecular layer deposition. Layers were covalently attached by Thiol-Ene chemistry as proven by AFM and ToF-SIMS measurements.

[†] The graphical abstract for the matrix material development has previously been published in Ridder, B.; Foertsch, T. C.; Welle, A.; Mattes, D. S.; von Bojnicic-Kninski, C. M.; Loeffler, F. F.; Nesterov-Mueller, A.; Meier, M. A. R.; Breitling, F. *Appl. Surf. Sci.* 2016, *389*, 942-951, reprinted with permission from Elsevier.

3. A matrix material for 'solid' solvent synthesis of high density peptide arrays

An important research area when doing surface functionalization is the field of biomaterials. One example of these bio functional surfaces are peptide arrays. Since the invention of peptide macroarrays on cellulose substrates by Ronald Frank in 1992,[31] major steps have been taken to miniaturize peptide arrays from macro to micro. Arrays with higher spot density per cm^2 accommodate more peptides of different sequences, which can be analyzed at the same time with only a small amount of sometimes very precious analyte.[30,34] Usually, glass is used as the substrate for microarrays, which are synthesized *via* two major pathways: the lithographic method and the 'solid' solvent approach. The latter is usually combined with laser based structuring methods.

The matrix material used in the 'solid' solvent approach to peptide array synthesis by different methods (laser printing, laser fusing and combinatorial laser-induced forward transfer) is the same commercially available styrene-acrylic copolymer resin.[42–45,47] As the manufacturer does not supply the exact composition of the resin, it is not possible to modify or optimize it towards new requirements or application needs. Therefore, it was aimed to synthesize a polymer, which could be used as a matrix material for peptide array synthesis by the 'solid' solvent approach employing laser-induced forward transfer for structuring of the array.

Several requirements have to be met by a possible matrix material candidate in order to be suitable for the peptide array synthesis application. First, it is highly important that no reactive groups are present in the matrix material, which could potentially bind to the surface or react with the OPfp-activated amino acid derivatives and form side products. The mechanistics, demands and challenges of peptide synthesis, especially on microarrays are discussed in the introduction part. This is a necessary requirement to prevent loss of the desired product and formation of side products, which could possibly also bind to the synthesis film. Secondly, the matrix material has to penetrate into the synthesis film and have good wettability properties with the synthesis film to make contact with the synthesis film and facilitate peptide bond formation. Thirdly, the matrix material has to be solid at room temperature, thus the T_g of the material should be higher than room temperature. At temperatures above the T_g of the polymeric matrix material, the resulting viscous liquid needs to be miscible with the amino acid derivatives that are used for the peptide array synthesis. In this state, the matrix material also needs to serve as a solvent allowing peptide bond formation between an amino acid derivative and the

reactive groups, free amines, on the surface. Additionally, the T_g of the matrix material cannot be too high, because otherwise racemization and side reactions could cause problems during peptide synthesis, which needs to take place at temperatures above T_g.[101] The synthesis film is only suitable for reactions at temperatures not higher than 110 °C. Therefore, the T_g of the matrix material needs to be below this temperature. Nevertheless it should still be possible to optimize, change and modify the polymer to be able to adapt to potential special requirements or method adaptations. Therefore, it is necessary to synthesize a well-defined polymer carrying functional groups for post-synthetic modification. As many demands have to be fulfilled by the matrix material, it was decided to take the solubility of the amino acid derivatives in the matrix material at temperatures above T_g as the most important property and examine possible matrix material candidates for this first. After finding a possible matrix material candidate, it will be tested on the other requirements.[‡,§]

3.1. Six-arm star poly(dimethylacrylamide) polymers as possible matrix material candidates

A branched poly(dimethylacrylamide) (p(DMAA)) was chosen as matrix material candidate because the structure of its side chains resembles the structure of an amino acid, but also the structure of DMF, which is a commonly used solvent in peptide synthesis (see Figure 13). These structural similarities should ensure good miscibility with the amino acid derivatives.
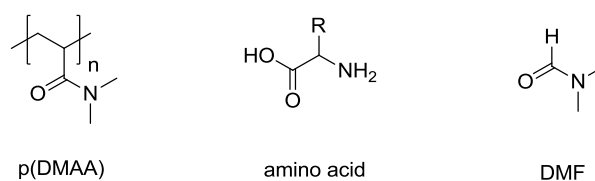
Figure 13: Structure of p(DMAA) backbone, global structure of an amino acid and structure of DMF to show the structural similarity between the three.

The side chains of p(DMAA) do not contain any functional groups that could possibly interfere with the peptide synthesis. P(DMAA) contains polar side chains, which usually

raise the T_g of a material.[63] Therefore, a six-arm star polymer was synthesized, where the branching should lower the thermal transitions and therefore also have a lower T_g than the linear equivalent.[62] To obtain well-defined polymers ATRP or RAFT are two possible controlled polymerization methods that could be used to synthesize p(DMAA).

RAFT was not suitable in this case, as the initiator for this polymerization method necessarily contains sulfur atoms. Indeed, as ToF-SIMS was intended to be used as a surface analysis technique and *N*-(9-Fluorenylmethyloxycarbonyl)-trityl-cysteine pentafluorophenyl ester (Fmoc-Cys(Trt)-OPfp) as a model amino acid at a later stage for coupling test experiments, RAFT had to be excluded. The coupling of the amino acid into the polymeric synthesis film of the array will be investigated. The thiol side chain of the cysteine will be used as marker for analysis with ToF-SIMS. If sulfur-containing polymeric matrix material, *i.e.* synthesized with RAFT polymerization, remains in the synthesis film it might not have been distinguishable from the cysteine. Therefore, ATRP was selected as the polymerization method as no sulfur is involved in the polymerization process.

The principles of ATRP of dimethylacrylamide (DMAA) are described in literature,[102–105] but p(DMAA) has not been used as a matrix material before. In contrast to methacrylates and styrene, ATRP of DMAA is challenging. Teodorescu *et al.* give possible examples of problems that might occur in ATRP of DMAA, such as the growing polymer chains could complex with the copper and therefore deactivate the catalyst or the bond between the terminally incorporated acrylamide and the halogen could be too strong, preventing the halogen from dissociating and therefore shifting the equilibrium too heavily to the side of the dormant chains.[105]

Still, when using the right conditions, ATRP of DMAA is possible but the synthesis of p(DMAA) polymers with high molecular weights remains problematic.[106] However, as a T_g between 50 and 110 °C is desirable for a polymer to be used in the application of peptide array synthesis from 'solid' solvents, polymers with low molecular weights are suitable here. To lower T_g even further branching was introduced by synthesizing a six-arm star p(DMAA). The synthesis of six-arm star polymers of this kind in combination with ATRP has already been described in literature.[107]

For the ATRP of DMAA, copper(I)chloride (Cu(I)Cl) was selected as the catalyst and tris[2-(dimethylamino)ethyl]amine (Me$_6$Tren) as the ligand (see Scheme 12). This combination has a high catalytic activity, while still allowing sufficiently fast deactivation to have control over the ATRP process.[103] Additionally, polymerization at room temperature is possible with this catalyst and ligand combination. In literature, a chlorine

based-initiator is preferred to the bromine equivalent, as a pure chlorine based system should give better polymerization results.[105] As no commercial six-arm star initiator with a chlorine based initiation is available, instead the commercially available dipentaerithritol hexakis (2-bromoisobutyrate), which carries a bromine end group, was used. Attempts to synthesize a chlorine based-initiator were tried as well, but proved to be very challenging in synthesis and purification; therefore, it was decided to resort to commercially available products.

As the aim was to synthesize polymers with low molecular weights, termination and loss of catalyst activity due to complexation with the growing chain should be less likely to be a problem.

Scheme 12: ATRP of DMAA using the six-arm star shaped initiator dipentaerithritol hexakis (2-bromoisobutyrate)

ATRP was carried out in toluene under argon atmosphere. To ensure a stable complex between the copper catalyst and the ligand, the two were premixed for about 10 min before addition of the monomer, which could possibly interfere with the complexation. Obtained polymers were purified by dialysis.

Different batches of p(DMAA) six-arm star polymers were synthesized. The different polymer batches with variable size and reaction conditions are referred to as **P1**-**P6**. **P1** and **P3** were synthesized with quadrupled amounts of reactants, for **P4** 0.20 mmol of initiator was used instead of 0.15 mmol and for **P5** and **P6** reactants were doubled compared to the reaction conditions of **P2**. The obtained polymers were analyzed by proton nuclear magnetic resonance spectroscopy (^{1}H-NMR), SEC and DSC (see Table 1).

A matrix material for 'solid' solvent synthesis of high density peptide arrays

Table 1: Properties of the different p(DMAA) star polymer batches and their respective synthesis yields; Đ and Mn (per arm) were determined by SEC using a linear poly(methyl methacrylate) standard as well as by 1H-NMR. The Tg was determined by DSC.

Polymer batch	M_n[a]	Đ[b]	DP[c]	DP[d]	DP[e]	T_g (°C)[f]	yield[g]
P1	6300	1.5	8	7	8	107.3	62%
P2	6100	1.3	8	7	8	107.5	50%
P3	3250	1.2	4	3	8	81.1	33%
P4	3850	1.2	5	5	6	98.8	42%
P5	6450	1.3	8	6	8	104.2	19%
P6	4250	1.3	3	5	8	88.5	23%

(a) determined by SEC, (b) determined by SEC, (c) per arm, determined by SEC, (d) per arm, determined by ^{1}H-NMR, (e) per arm, theoretically, (f) determined by DSC, (g) after purification with dialysis

The degree of polymerization (DP) per arm of the polymers was calculated from SEC and ^{1}H-NMR. For the arm length calculated from ^{1}H-NMR, the protons belonging to the methyl groups of the amide were compared to the protons of the ether at the core of the original initiator molecule. The arm lengths calculated from the SEC and the NMR data only differ by a few units (see Table 1). For the SEC measurements, a linear poly(methyl methacrylate) standard was used, as p(DMAA) or six-arm p(DMAA) standards were not available. Therefore, the measured values for molecular weight are just an indication and not an absolute value. These indications still give valuable information about the dispersity of the polymers and an approximation of the average molecular weight. For all batches except **P1**, polymers with a relatively narrow molecular weight distribution were obtained, indicating well-defined polymers. For **P1** a quadrupled reaction mixture was used, which probably led to higher dispersity when high molecular weights were reached. For **P3** and **P6** the arm length is shorter than expected, which was probably due to aging of the catalyst as the different batches were synthesized at different points of time. For **P3** also quadrupled amount of reaction mixture was used, but the less active catalyst compared to the one used for **P1** probably still gave good control because the arms were growing more slowly.

The yields are overall low. An explanation might be that the polymer sticks to the cellulose dialysis membrane and that this causes product loss. Precipitation as an alternative purification method was not possible because the solubility and insolubility of the polymer in different solvents was too similar compared to the monomers. For **P3** and **P6** the low yields can be explained by the low DP's per arm; here not all the monomers

were incorporated into the polymer, which leads to a low conversion and thus a low yield. For **P5** maybe the dialysis bag leaked, this is not always visible by eyesight, but could explain the low yield.

The DSC data confirmed that a shorter arm length leads to a lower T_g. This offers the possibility to tune the T_g, which is one of the key requirements to a matrix material candidate. For further test experiments, all synthesized polymers were used, as all of their glass transition temperatures were below the maximum coupling temperature of 110 °C and above room temperature.

3.2. Miscibility of various amino acid derivatives with p(DMAA) at temperatures above T_g

One requirement for a possible matrix material candidate is the miscibility of the activated amino acid derivatives that are used for the peptide synthesis with the polymeric matrix material at temperatures above T_g. Therefore it was investigated if the synthesized six-arm star-shaped p(DMAA) fulfilled this requirement.

Fmoc-protected and OPfp-activated amino acid derivatives were mixed with p(DMAA) (10:90 wt-%). The OPfp activated amino acid derivatives are normally used when producing peptide arrays by the 'solid' matrix material approach.[42–45] Activated esters are especially suited for this method as they have a relatively low risk of racemization even at elevated temperatures.[101] The T_g of the mixtures was determined with DSC measurements. The DSC program used to characterize the mixtures of six-arm star p(DMAA) and the Fmoc-OPfp amino acid derivatives was the same as the one used to characterize amino acid derivative-containing particles made with the commercially available styrene-co-acrylamide resin.[108] To ensure the same thermal history for all samples, only the second heating run was analyzed to determine the T_g.

The amino acid derivative can act as a plasticizer for the polymeric material if it is properly dispersed in the polymer and therefore the T_g of the mixture should be lower compared to the pure material. Thus, the drop in T_g in comparison to a sample only containing the pure p(DMAA) polymer indicates that the amino acid derivative was soluble in the matrix material at temperatures above T_g. Therefore, different amino acids were tested (see Table 2) as the side chain of the amino acid can be quite large with its attached protecting group and thus can have a dramatic influence on the miscibility.

Table 2: T_g's determined with DSC measurements of different activated amino acid derivatives mixed with six-arm star p(DMAA) (P1)

Material (wt-%)	T_g (°C)
p(DMAA) **P1** (100)	107.3
Fmoc-Gly-OPfp (10) + p(DMAA) **P1** (90)	96.4
Fmoc-Cys(Trt)-OPfp (10) + p(DMAA) **P1** (90)	97.6
Fmoc-Tyr(tBu)-OPfp (10) + p(DMAA) **P1** (90)	91.3
Fmoc-Asp(OtBu)-OPfp (10) + p(DMAA) **P1** (90)	86.8
Fmoc-Pro-OPfp (10) + p(DMAA) **P1** (90)	97.7
Fmoc-Phe-OPfp (10) + p(DMAA) **P1** (90)	93.2
Fmoc-Gln(Trt)-OPfp (10) + p(DMAA) **P1** (90)	97.9
Fmoc-Lys(Boc)-OPfp (10) + p(DMAA) **P1** (90)	94.6

In addition to determining the T_g of the mixture, the curve was also analyzed to see if any thermal events other than the glass transition took place, indicating possible demixing events.

For all tested amino acids, a significant drop in T_g could be detected compared to the pure material. The range of the drop in T_g is quite broad, between 10 and 20 °C. The differences in the T_g drop are probably caused by the different properties of the amino acid derivatives, some have very bulky side chain protection groups whereas others do not have side chain protecting groups or these are very small. Also they differ in their polarity. These differences influence their properties as plasticizers, which influences the mobility of the polymeric chains and therefore the T_g. No additional thermal transitions to the glass transition temperature were detected in any of the analyzed heating cycles for any of the tested amino acids, indicating that the derivatives are miscible with six-arm star p(DMAA).

3.3. Wettability of the synthesis film by the matrix material

The polymeric matrix material also needs to be compatible with the PEGMA-co-MMA synthesis film on a glass slide, which is used as the substrate for the peptide array. The matrix material carrying the amino acids needs to have a large contact area with the synthesis film to ensure a good yield of formed peptide bonds. A good wettability ensures the diffusion of the matrix material into the synthesis film, dragging the embedded amino acid derivatives into the film.

For the investigation of the surface wettability of the p(DMAA) with the PEGMA-co-MMA synthesis film, contact angles were measured. A small amount of the polymeric material was placed on a copper heating plate equipped with a control element and a power supply in the form of a constant current box. The temperature was constantly increased and the softening process was followed with a camera system (see Figure 14, for illustration of set-up).
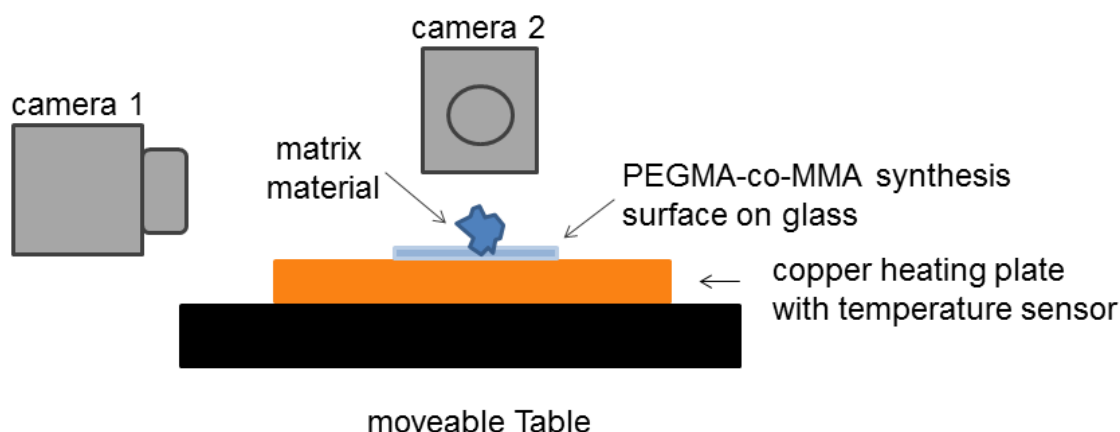
Figure 14: Set-up for the contact angle measurements, cameras follow the melting process, heat is generated by a copper heating plate onto which the PEGMA-co-MMA glass slide is placed with on top of it a small amount of the matrix material.

As the T_g is not the melting temperature, contact angle measurement is not a completely accurate approach, but it gives an indication if the polymer is capable of wetting the synthesis surface when it is in a rubbery state. The temperatures at which the contact angle was determined were above 110 °C, where the stability of the synthesis film is not guaranteed due to decomposition. It was assumed that the synthesis film was still intact, as the heating was done very quickly and complete decomposition of the synthesis film in this short time period is very unlikely. The contact angles were determined at the visual onset of the melting process and after the visually complete melting of the matrix material (see Table 3).

Table 3: Contact angles of the different matrix materials, contact angle 1 at the visual onset of the melting process and contact angle 2 at the end of the melting process as visually determined.

Material	Contact angle 1 (onset)	Contact angle 2 (melting complete)
p(DMAA) (**P4**)	42°	31°
styrene acrylic copolymer resin	94°	41°

The measured contact angle completion of melting is quite low, about 31°. This indicates a very good wettability of the surface, which is even improved comparing to the styrene acrylic copolymer resin. The difference in contact angle 1 is even larger, but this measurement is less reliable as it is measured at the onset of the melting process where the contact angle is difficult to determine.

3.4. P(DMAA) as matrix material for 'solid' solvent peptide array synthesis

The miscibility tests of p(DMAA) with activated amino acid derivatives and the wettability tests were very promising. The T_g of the p(DMAA) polymer dropped when mixing in amino acid derivatives and no demixing effects could be observed. Furthermore, the contact angle measurements indicated a good wettability of the synthesis surface. With these two requirements fulfilled, first coupling tests using p(DMAA) as the matrix material were performed. As a surface structuring technique, combinatorial laser-induced forward transfer was used. This method is based on a donor and acceptor system. As the acceptor for all coupling tests microscopy glass slides functionalized with a PEGMA-co-MMA synthesis film carrying one Fmoc-ß-Ala were used unless stated otherwise. The slides were Fmoc-deprotected by rocking them in a solution of piperidine/ DMF (20:80 vol-%).[7,45,47]

For the donor slide preparation, a mixture of an Fmoc-protected and an OPfp-activated amino acid derivative and six-arm star p(DMAA) (10:90 wt-%) was dissolved in dichloromethane (DCM) and spin-coated onto a microscopy glass slide covered with polyimide foil. For the laser-induced forward transfer, the acceptor slide was placed in a holder facing upwards. The donor was placed on top of the acceptor facing downwards. Then the transfer was carried out by laser-induced forward transfer. Afterwards, the acceptor slide was placed in an oven at 110 °C (unless stated otherwise) for 1.5 h under argon atmosphere. After each coupling step, the acceptor slide was capped in a mixture of acetic anhydride/ DIPEA/ DMF (10:20:70 vol-%).[42,45,47] The capping step ensures that

no more free amines are present on the surface. Formation of false sequences by unreacted intermediate chains of the previous cycle should thus be prevented.

As the optimal parameters for the laser transfer were not known, pulse duration and relative laser power were varied. For these experiments, Fmoc-Cys(Trt)-OPfp was chosen as the model amino acid with p(DMAA) from batch **P2** as the matrix material (10:90 wt-%). After lasing, coupling, washing, and capping, the trityl side chain protecting group was removed with a solution of DCM/ TFA/ triisobutylsilane (TIBS)/ ultrapure water (44:51:3:2 vol-%).[19,42,45] For the fluorescent staining of the now free thiol side chain, the slides were rocked in a solution of 5-(6)-carboxytetramethylrhodamine maleimide (0.4 µg.mL^{-1}) (TAMRA maleimide) in phosphate buffer saline with Tween 20 (500 µL.L^{-1}) (PBS-T) for 2 h (see Scheme 13 for complete preparation from deprotection to staining).
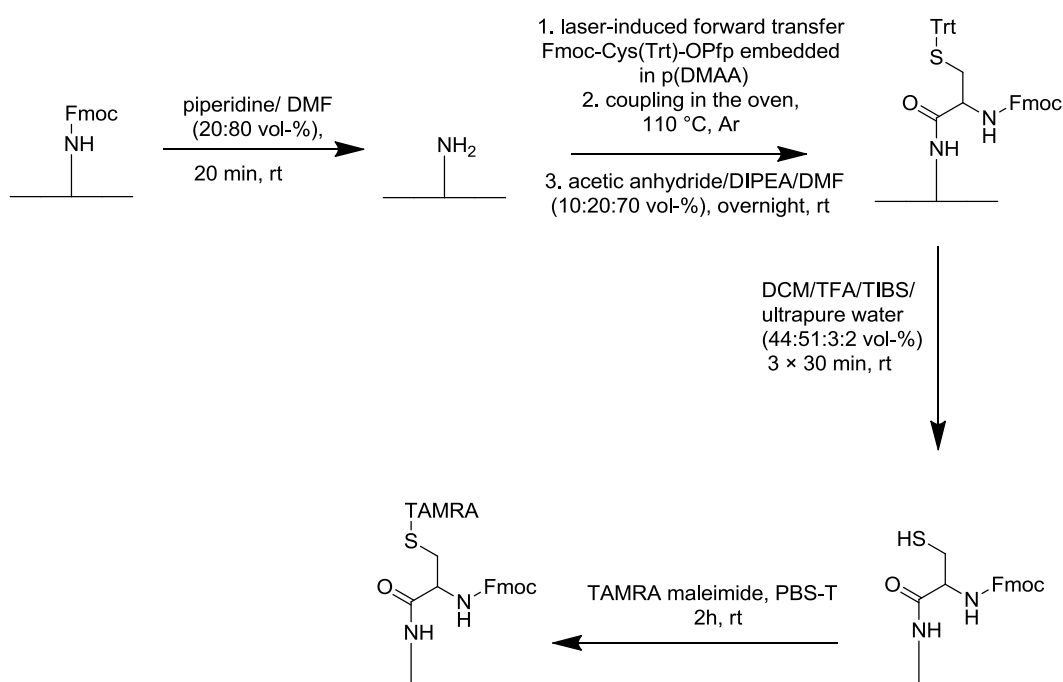
Scheme 13: Schematic illustration of the slide functionalization steps, from Fmoc-deprotection, over lasing step and side chain deprotection to staining with a fluorescent dye.

For a first trial experiment, a pitch of 250 µm was chosen and the laser parameters were varied. The parameter variation was necessary to investigate the impact of the pulse duration and the relative laser power on the transfer. After staining, the slide was scanned in a fluorescence scanner (see Figure 15).
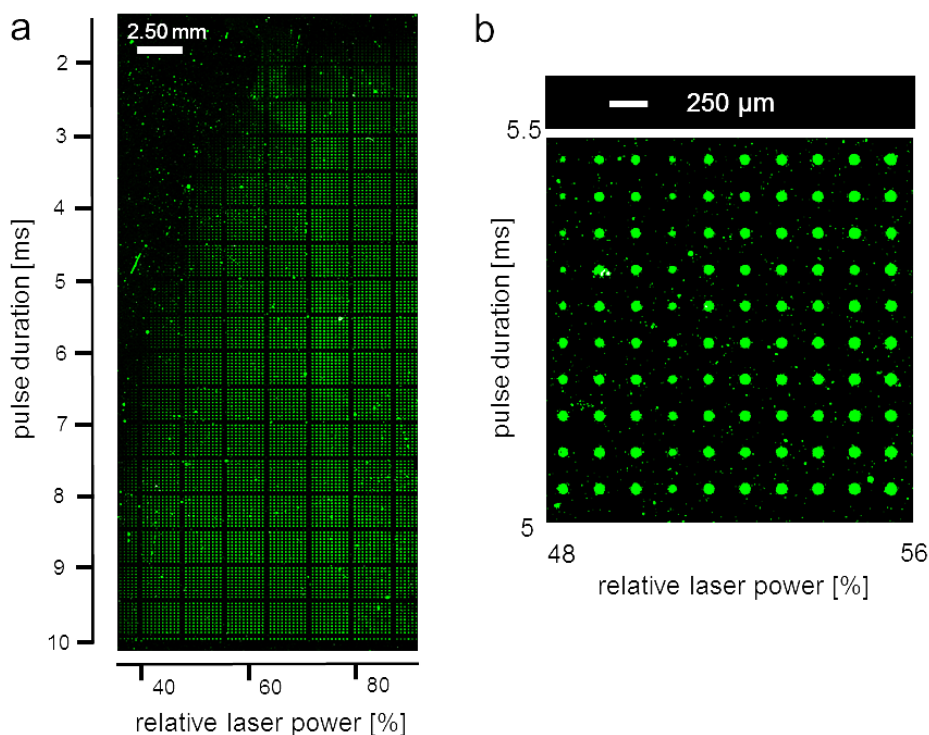
Figure 15: Fluorescence scan of spots at laser parameter variation. Fmoc-Cys(Trt)-OPfp was transferred, coupled at 110°C. The trityl protection group was removed and the thiol was stained with TAMRA maleimide. (a) Full scan of the complete slide; laser parameters: pulse duration from 1 to 10 ms with a step size of 0.05 and relative laser power from 30% to 100% with a step size of 0.8. The cut-off of the scan on the left and the right hand side is due to scanner limitations, where the slide was masked by the scanners sample holder. (b) Zoomed in area of the slide. The slide was scanned in the GenePix scanner, contrast and brightness were adjusted.

The variation of the laser parameters showed that for most of the parameters a transfer and subsequent peptide bond formation took place. The fluorescent signal becomes undetectable only when a very short pulse duration, about 5 ms or less, is combined with low laser power percentages (see Figure 15 a). To confirm that a transfer takes place, higher laser powers and pulse durations can be chosen, as evidenced by the defined spots in those regions. The resulting spots also have a larger diameter (for exemplarily illustration see Figure 15 b) but are still defined and separated from each other. To ensure that the spots are still defined and not bleed into each other, it is therefore not advisable to take the maximal parameters for experiments with a lower pitch.

As the coupling temperature of 110 °C is relatively high, the possibility of coupling at 90 °C was investigated (see Figure 16). Again, Fmoc-Cys(Trt)-OPfp was chosen as the model amino acid and this time batch **P1** as the matrix material (see Figure 16). Steps were larger in this case, to minimize the cut-off on the side by the scanner limitations.
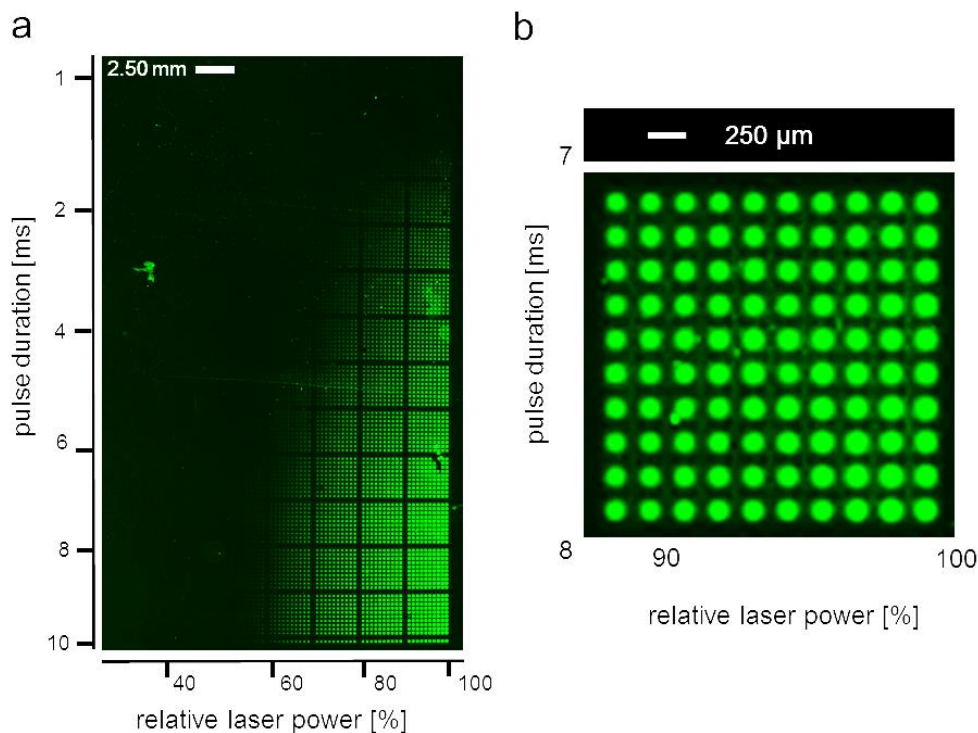
Figure 16: Fluorescence scan of spots at laser parameter variation. Fmoc-Cys(Trt)-OPfp was transferred, coupled at 90 °C, the trityl protection group was removed and the thiol was stained with TAMRA maleimide. (a) Full scan of the complete slide. The pitch was set at 250 µm. The pulse duration was varied from 1 to 10 ms, with a step size of 0.075 ms, and the laser power was varied from 30% to 100%, with a step size of one. (b) Zoomed in area of the slide. The slide was scanned in the GenePix scanner, contrast and brightness were adjusted.

The scan shows, that coupling is possible at 90 °C, but that higher laser powers and longer pulse durations are necessary to get signals when compared to 110 °C. Again, spots get larger with higher laser power and longer pulse durations. It is a promising result that the coupling temperature can be lowered to 90 °C, which is the standard coupling temperature for peptide array synthesis with the classic 'solid' solvent approach used in literature.[42,44,45]

With these experiments it was shown that p(DMAA) is a suitable matrix material candidate to couple one amino acid derivative to the synthesis film. To produce a peptide array, it is necessary to synthesize sequences of amino acids.

Therefore in the next step, the possibility to synthesize a short sequence of amino acids using p(DMAA) (**P2**, **P4**) as the matrix material was investigated. As a model peptide, the FLAG epitope was chosen. The FLAG epitope has a sequence of Asp-Tyr-Lys-Asp-Asp-Asp-Asp-Lys, following the standard amino acid codes for Aspartic acid (Asp, K), Tyrosine (Tyr, Y) and Lysine (Lys, K). It is known from literature that the Asp-Tyr-Lys part

of the FLAG-sequence is necessary to be present and in the correct order for the anti-body to be able to bind to the peptide.[109] This essential trimer was chosen as the proof-of-concept sequence for the short peptide synthesis from p(DMAA) as the matrix material (see Figure 17 for illustration).
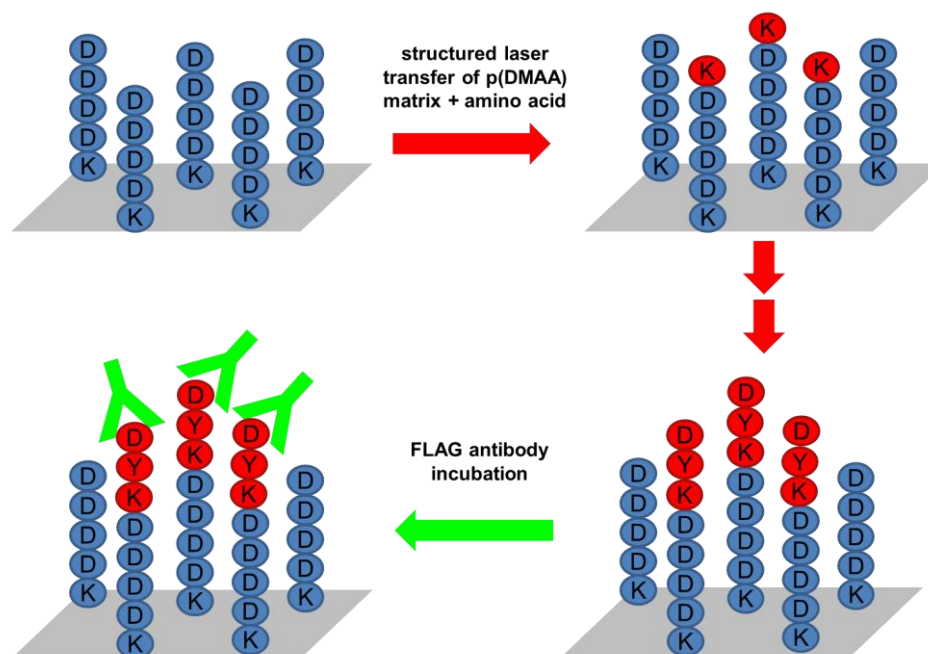
Figure 17: A synthesis surface carrying a pentamer pre-synthesized from solution is structured by laser-induced forward transfer with Lys(K). Subsequently a trimer is built up by adding Tyr(Y) and Asp(D). After complete deprotection the peptide is incubated with a monoclonal FLAG antibody

In a first step, a PEGMA-co-MMA synthesis surface and a pure PEGMA surface were functionalized with two additional β-alanines from a solution in DMF to serve as a spacer between the surface and the peptide chain. It should be possible to functionalize both sorts of surfaces in the same way. In the next step, the pentapeptide Asp (tBu)-Asp(tBu)-Asp(tBu)-Asp(tBu)-Lys(Boc) was synthesized from solution, where tBu is the standard *tert*-butyl ester protective group and Boc is *tert*-butyloxycarbonyl. In this step the synthesis slides were incubated with a solution of the respective Fmoc-protected and OPfp-activated amino acid derivative in DMF. A capping step followed coupling of each layer and an Fmoc-deprotection step prior to coupling of the next amino acid was performed. In accordance with convention, peptide sequences are noted from N- to C-terminus in this thesis, but synthesis was done in the opposite direction from C- to N-terminal, where the C-terminal end of the peptide is always anchored to the synthesis surface. Onto this pentapeptide synthesized from solution, the protected Asp-Tyr-Lys tripeptide was synthesized, again from the C-terminus to the N-terminus, using p(DMAA) (**P2**, **P4**) as the matrix material and laser-induced forward transfer as the structuring

method. The pitch and the lasing parameters, pulse duration and laser power, were varied over different parts of the array. After transfer of each amino acid, a coupling step, a washing step, a capping step and an Fmoc deprotection step were executed. To be able to exactly position the amino acids on top of each other in the lasing steps, an alignment system was used as described elsewhere.[45] After completion of the peptide synthesis, a final Fmoc-deprotection was performed, followed by deprotection of the side chains. For anti-body staining the slides were incubated with monoclonal mouse anti-FLAG M2-DyLight 800 antibodies. The slides were analysed in a fluorescent scanner (see Figure 18).
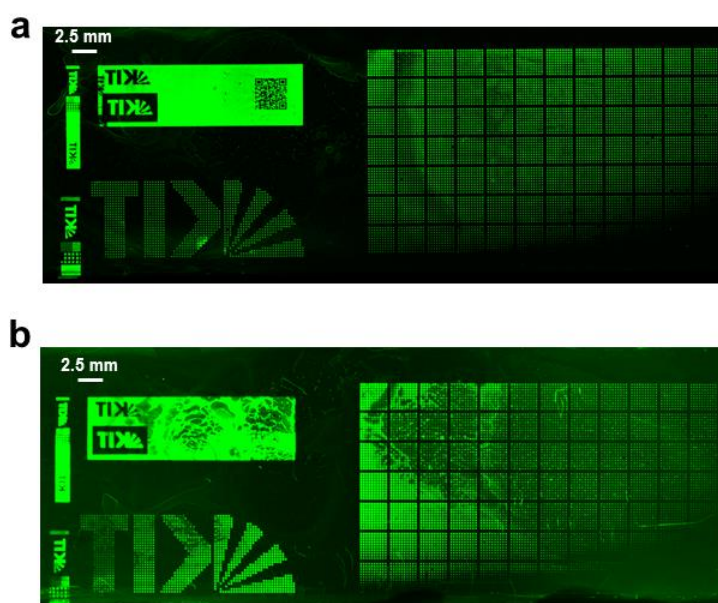
Figure 18: Full size fluorescence scan of the FLAG epitope array in the Odyssey scanner at intensity 7 at a resolution of 21 µm. The FLAG epitope was stained with monoclonal mouse anti-FLAG M2-DyLight 800: (a) PEGMA-co-MMA synthesis surface (b) pure PEGMA synthesis surface. For both the contrast and brightness were adjusted.

The pure PEGMA slide shows more background than the PEGMA-co-MMA slide. This is probably caused by decomposition of the PEGMA synthesis film due to hydrolysis. This can also be seen by the circular spots and large lower-intensity stains. The decomposition by hydrolysis is probably due to aging of the synthesis film during storage. The pure PEGMA films suffer a lot more and faster from this problem compared to the PEGMA-co-MMA synthesis films. However, the scans proved that p(DMAA) as a matrix material worked on both synthesis surfaces. As the PEGMA-co-MMA synthesis film remained completely intact in these experiments, it was used for further analysis.

Detail shots of different parts of the array were taken, as different laser parameters and different pitch sizes were used (see Figure 19)
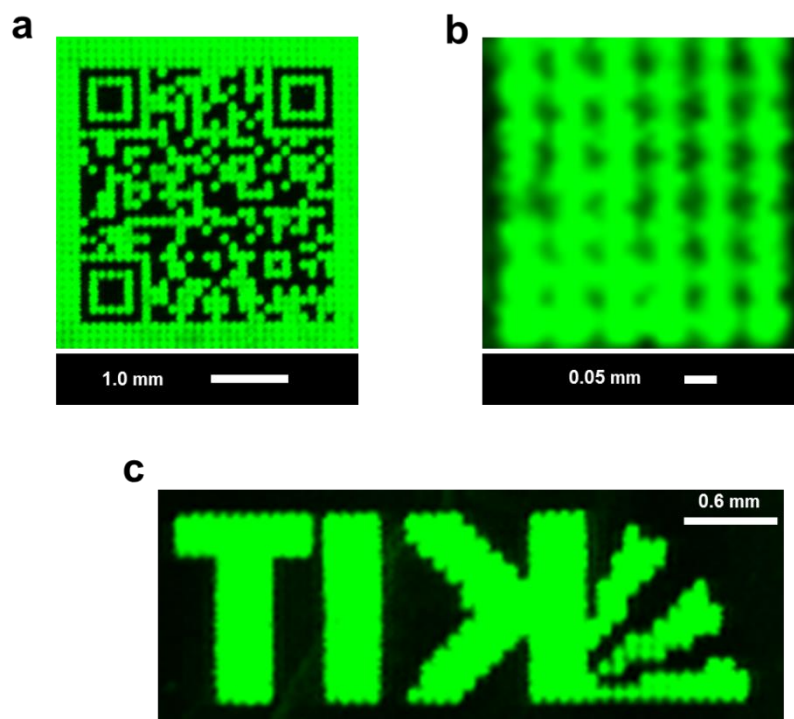
Figure 19: Detail images of FLAG synthesis on the PEGMA-co-MMA synthesis slide (a) QR code, pitch 100 µm, laser power 100%, pulse duration 3 ms (b) grid pattern, pitch 50 µm, laser power 100%, pulse duration 2 ms (c) KIT logo, pitch 75 µm, laser power 100%, pulse duration 2 ms. The FLAG epitope was stained with monoclonal mouse anti-FLAG M2-DyLight 800 and scanned in the Odyssey scanner. Contrast and brightness were adjusted.

Especially for the smaller pitches the spots are blurry. Either, at these pitch sizes it is not possible to get defined spots anymore as the diameter is getting too large and spots bleed into each other and the production of defined spots is not possible or the limited resolution of the Odyssey scanner, which is 21 µm, was the problem: it might be not good enough to resolve the outlines of the spots exactly.

To investigate this, a GenePix scanner with a much better maximum resolution of 5 µm was used to scan the PEGMA-co-MMA slide again. The pure PEGMA slide was not rescanned as the synthesis film was already degrading. First, the antibodies, from the initial staining experiment, had to be removed from the surface, as their 800 nm excitation wavelength was not suitable for the GenePix scanner, which can only excite at wavelengths of 532 and 635 nm.[110]

The antibodies were removed by sonificating the slide in chloroform ($CHCl_3$). Then the slide was incubated with monoclonal mouse anti-FLAG M2-Cy3 antibodies. Finally, the slide was scanned in the GenePix scanner with a resolution of 5 µm (see Figure 20).
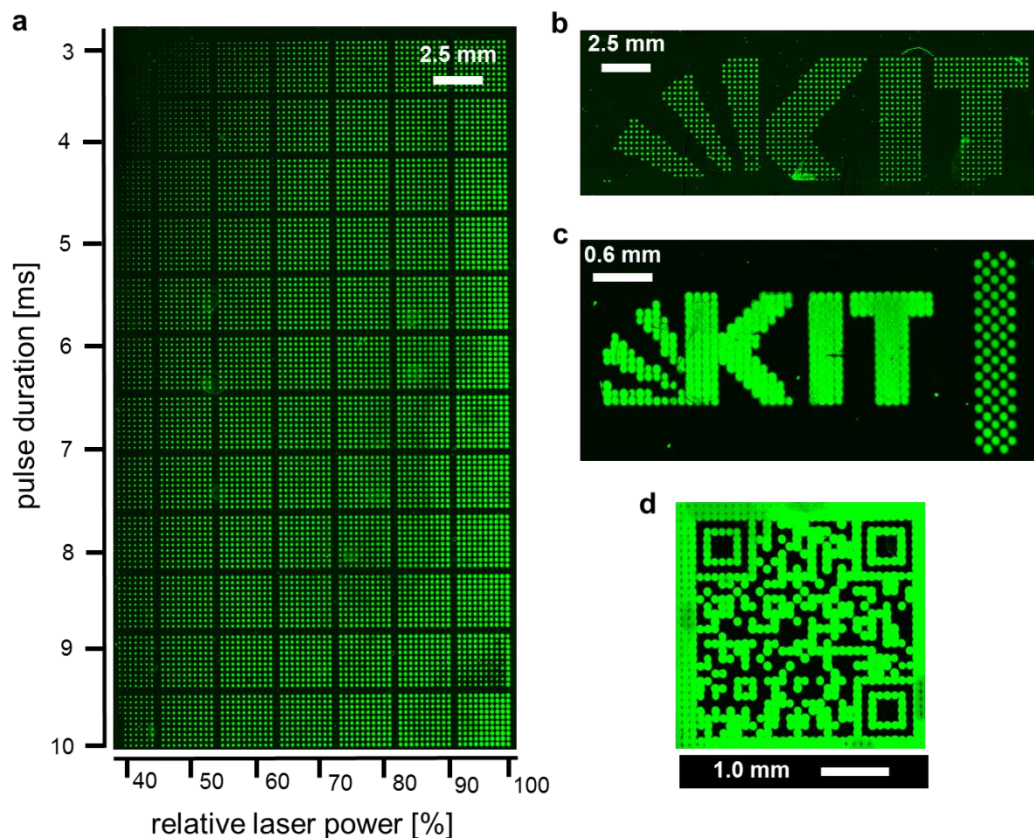
Figure 20: (a) Parameter variation at pitch 250 µm; laser power from 37% to 100% (step size 0.9%), pulse duration from 2.86 to 10 ms (step size 0.06 ms). Edge clipping due to scanner limitations (b) KIT logo, pitch 250 µm, laser power 60%, pulse duration 6 ms (clipping due to scanner limitations) (c) KIT logo, pitch 75 µm, laser power 100%, pulse duration 2 ms (d) QR code, pitch 100 µm, laser power 100%, pulse duration 3 ms. The FLAG epitope was stained with monoclonal mouse anti-FLAG M2-Cy3. The slide was scanned with the GenePix scanner, contrast and brightness were adjusted for each image individually.

In these higher resolution scans, the spots appear to be much more defined and less blurry, an improvement that was observed even for pitch sizes of 100 µm. The array was stained evenly, indicating that the antibodies, from previous experiments, could be removed and a second staining of the regenerated array indeed is possible. As the antibody specifically recognizes the three N-terminal amino acids that were synthesized with the laser based structuring and p(DMAA) as the matrix material, the synthesis of the trimer peptide is proven to be successful and in the correct order, as anti-FLAG M2

monoclonal antibodies recognize the peptide **Asp-Tyr-Lys**-Asp-Asp-**Asp**-Asp-Lys (amino acid positions that are mandatory for binding are **highlighted**).[109]

For a grid pattern, which was barely recognizable with the Odyssey scanner (cf. Figure 19 b), the GenePix displays defined spots (see Figure 21 a). If the holes between the spots were to be filled up with extra spots, spot densities of up to 20.000 per cm^2 would be possible (see Figure 21 b). This is an increase compared to the 17.777 spots per cm^2, which has been reported for the commercially available matrix material.[45]
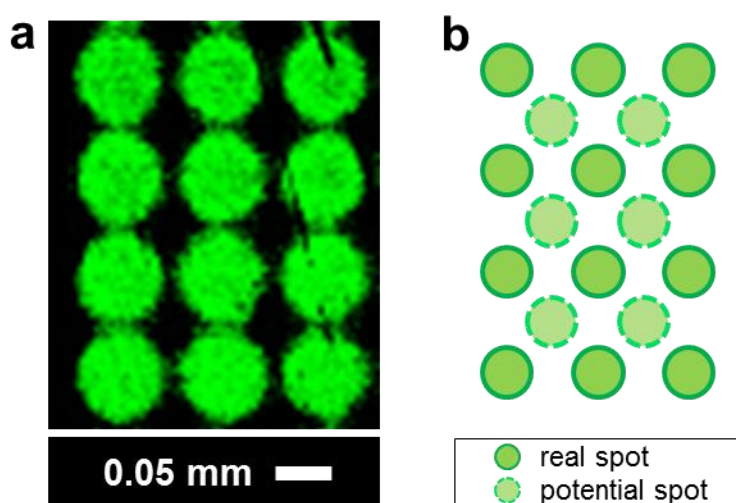
Figure 21: (a) grid pattern, pitch 50 µm, laser power 100%, pulse duration 2 ms, FLAG epitope stained with monoclonal mouse anti-FLAG M2-Cy3 and scanned in the GenePix scanner. Contrast and brightness were adjusted (b) possible pattern to fill up empty spaces and increase the spot density to 20.000 per cm^2.

3.5. Lowering T_g of the p(DMAA) six-arm star polymers

For the array synthesis from solid matrix materials lower T_g of the polymeric matrix material could be beneficial, so that either diffusion of the reaction partners within the softened material could be facilitated, or the coupling temperature for the peptide bond formation between the amino acid derivatives and the free amines on the synthesis film could be lowered. Thereby, possible side reactions and racemization could be avoided. Therefore, three different routes were tested. One approach was to mix in additives, which should act as plasticizers and lower the T_g of the matrix material. The other two approaches were to change the composition of the matrix material to lower the T_g of the polymers directly: On the one hand, the end group functionalization of the synthesized polymers was investigated and on the other hand copolymerization of two different monomers.

3.5.1. Mixing in additives

One way to lower the T_g could be to mix in additives with the polymer. The additives get in between the chains of the polymer giving them more freedom of movement thereby lowering the T_g of the mixture.[62,63] As a first trial molecule, *p*-tolyl sulfoxide was chosen, as it carries no functional groups which could possibly interfere with the peptide synthesis and should be well miscible with the p(DMAA) and the amino acid derivatives. For miscibility tests DSC measurements were performed on different mixtures of linear p(DMAA) as matrix material model, *p*-tolyl sulfoxide itself and Fmoc-Cys(Trt)-OPfp as a model amino acid (see Table 4).

Table 4: T_gs of p(DMAA) mixed with *p*-tolyl sulfoxide and/or Fmoc-Cys(Trt)-OPfp

Material (wt-%)	T_g (°C)
p(DMAA)(linear) (100)	118.4
p(DMAA)(linear) (85) + *p*-tolyl sulfoxide (15)	102.2
p(DMAA)(linear) (91) + *p*-tolyl sulfoxide (9)	93.6
p(DMAA)(linear) (90) + Fmoc-Cys(Trt)-OPfp (10)	100.4
p(DMAA)(linear) (79) + *p*-tolyl sulfoxide (10) + Fmoc Cys(Trt)-OPfp (11)	78.8

The T_g of p(DMAA) could successfully be lowered by mixing in *p*-tolyl sulfoxide. The DSC curves also did not show any transitions indicating demixing effects. Subsequently, lasing experiments were done to investigate the transfer behavior of a mixture with p(DMAA), Fmoc-Cys(Trt)-OPfp and *p*-tolyl sulfoxide when compared to just p(DMAA) and the amino acid derivative. For the donor slide preparation Fmoc-Cys(Trt)-OPfp and linear p(DMAA) (10:90 wt-%, control) or Fmoc-Cys(Trt)-OPfp, *p*-tolyl sulfoxide and linear p(DMAA) (10:10:80 wt-%, experiment) were dissolved in DCM and spin-coated onto separate polyimide covered glass slides. After coupling, washing, capping, side chain deprotection and staining with TAMRA maleimide, the slides were scanned (see Figure 22).
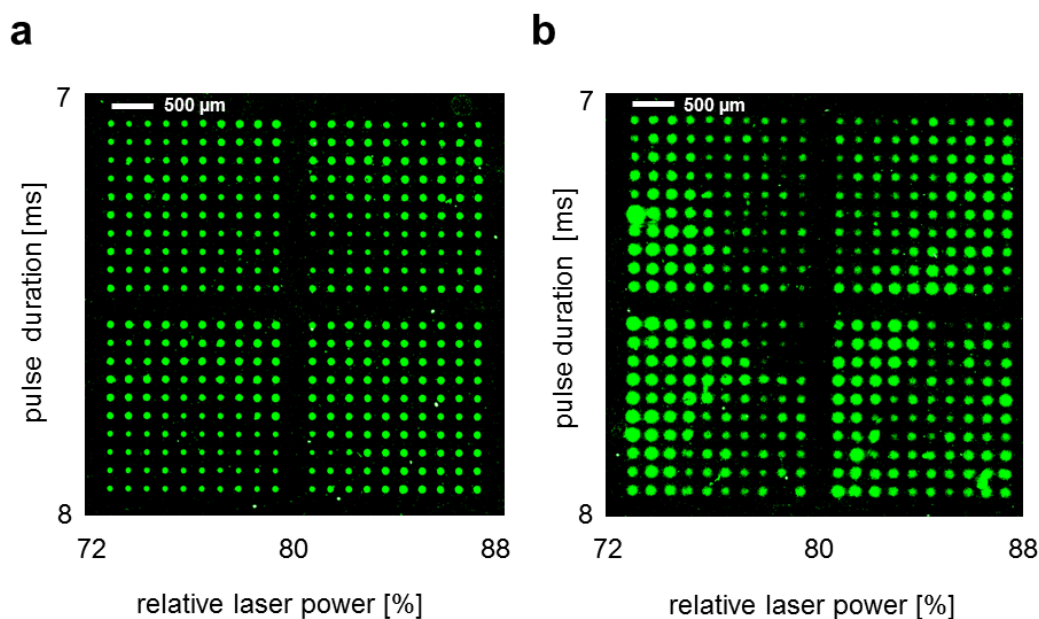
Figure 22: (a) mixture laser transfer: Fmoc-Cys(Trt)-OPfp/p(DMAA) (10:90 wt-%), (b) mixture laser transfer: Fmoc-Cys(Trt)-OPfp/ *p*-tolyl sulfoxide/ p(DMAA) (10:10:80 wt-%), both stained with TAMRA maleimide and scanned in the GenePix scanner. Contrast and brightness were enhanced.

The spots that are produced when *p*-tolyl sulfoxide is added to the matrix material are irregular (see Figure 22 b). Very broad spots are occurring as well as very small spots and in some cases no transfer occurs. Spot sizes seem to vary more irregularly compared to the transfer where no *p*-tolyl sulfoxide was used (cf. Figure 22 a). The spots where only p(DMAA) is used as the matrix material are smaller, more evenly sized and the shapes are less blurry. Broad spots in a transfer will cause problems at lower pitches and possibly even lead to a loss of spatial information. As the produced spots were very irregular and blurry when *p*-tolyl sulfoxide was added to the matrix material, it was decided not to continue with the approach to lower the T_g by mixing in additives.

3.5.2. End group functionalization

In a second approach to lower the T_g of the matrix material and thus the coupling temperature, the functionalization of the polymer end group with a non-polar group was investigated. Polar side chains in polymers usually lead to higher T_g's, whereas non-polar side chains result in lower T_g's.[63] Another advantage is that the end group functionalization approach is compatible with the polymerization method of ATRP, which was used to synthesize the six-arm star p(DMAA) polymers. The terminal group of the polymers after the ATRP is a halogen atom, either bromine or chlorine. This halogen group can be used to do a substitution reaction. Here, two different thiols, 2-methyl-2-popanethiol and 3-methyl-1-butanethiol, were tested. Their apolar and

branched chains were intended to act as plasticizers, to break the stacking of the polar side chains of the p(DMAA). The six arm star polymer (**P5**) was end group functionalized with the two thiols *via* a nucleophilic substitution reaction (see Scheme 14).
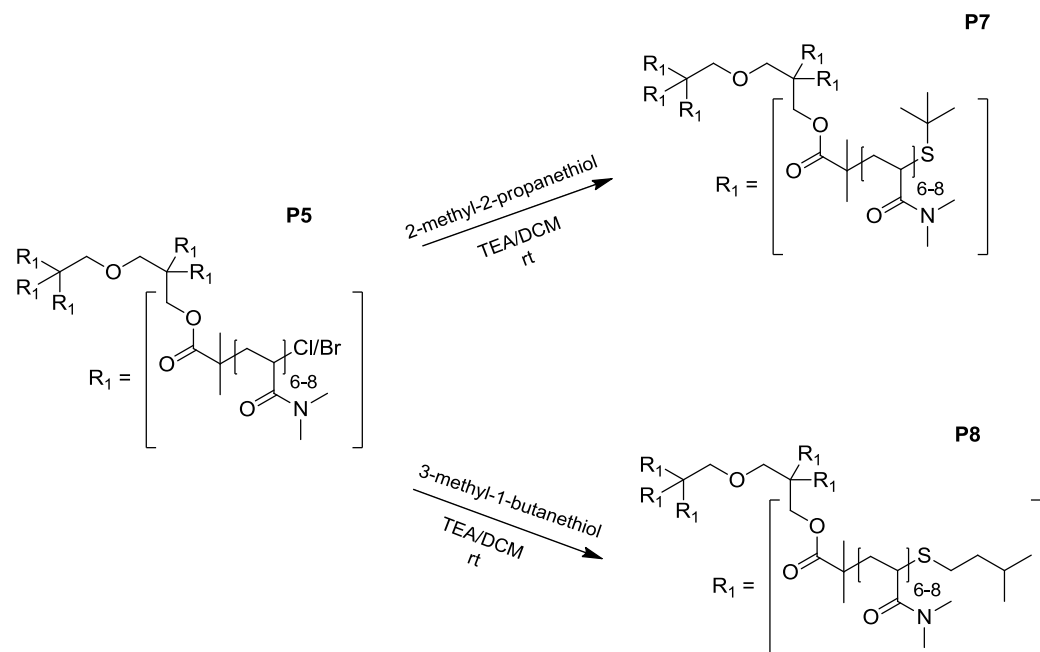
Scheme 14: Reaction scheme for the end group functionalization of p(DMAA) (P5) with 2-methyl-2-propanethiol or 3-methyl-1-butanethiol.

The reactions were performed in DCM with triethylamine (TEA) as a base at room temperature. The resulting products were purified by dialysis against ultrapure water. The products, after purification, were obtained in a yield of 78% for the 2-methyl-2-propanethiol functionalized polymer (**P7**) and 81% for the 3-methyl-1-butanethiol functionalized polymer (**P8**).

The functionalization of the purified product was analyzed by ^{1}H-NMR and the effect on the T_g was analyzed with DSC measurements. For both thiols, new peaks appeared in the NMR spectra after functionalization compared to the spectrum of the original material. The peaks appear in the region of 0.89 to 0.77 ppm for the 3-methyl-1-butanethiol functionalized polymer (**P8**) and at 0.99 to 0.91 for the 2-methyl-2-propanethiol functionalized polymer (**P7**). This region is characteristic of the methyl groups of the thiol molecules, indicating a successful functionalization of the p(DMAA). This showed that an end group functionalization is possible also for later arising necessities to tune the properties of the matrix material.

Surprisingly, the DSC measurements showed an increase of the T_g instead of the expected decrease. For the 2-methyl-2-propanethiol functionalized p(DMAA) (**P7**) the T_g increased from 104 °C to 108 °C and for the 3-methyl-1-butanethiol functionalized p(DMAA) (**P8**) to 111 °C. The increase might be explained by the large difference in polarity between the side chains of the p(DMAA), which are very polar, and the alkyl groups of the thiols, which are very apolar. Probably, the apolar end groups stick together instead of mixing in between the polar chains. The polymer chains probably loose freedom of movements because of these hydrophobic interactions and therefore the T_g increases. The pathway of the end group functionalization was not pursued further, as it was not possible to lower the T_g by introduction of apolar end groups, the T_g was even raised.

3.5.3. Copolymerization of different monomers

The synthesized p(DMAA) six-arm star polymers have quite high glass transition temperatures, at ~100 °C, for the intended application. By synthesizing branched polymers, the T_g (107.3 °C for a polymer with a M_n 6300 g.mol^{-1}) could already be lowered compared to linear p(DMAA) (117.8 °C for a polymer with a M_n of 2100 g.mol^{-1}, M_n provided by the manufacturer). In this section the lowering of the T_g by copolymerization of different monomers was examined.

Monomers with apolar side chains were tested in order to lower the T_g of the polymer, as the T_g is also partly dependent on the polarity of the side chains of the monomers used.[63]

Additionally, acrylamide monomers were chosen in order to introduce extra branching points and larger side chains.

2-ethylhexylacrylate was copolymerized with DMAA (2:98 mol-%) to yield a p(DMAA-co-2-ethylhexylacrylate) (**P9**) polymer. DMAA was also copolymerized with diethylacrylamide (DEAA) (50:50 mol-%) to give a p(DMAA-co-DEAA) (**P10**) polymer. Finally, [N-(3dimethylamino)propyl] methacrylamide was homopolymerized (**P11**) (see Scheme 15) and copolymerized with DEAA (**P12**). For all polymerizations, dipentaerithritol hexakis (2-bromoisobutyrate) was used as the ATRP initiator in combination with the catalyst/ ligand system Cu(I)Cl/ Me$_6$Tren. All products were purified by dialysis against ultrapure water. Subsequently, the yield was determined and the products were analyzed by ^{1}H-NMR, SEC and DSC.
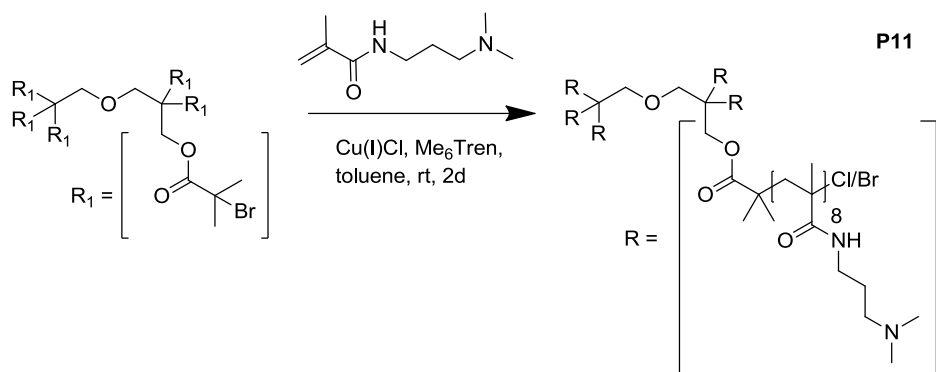
Scheme 15: ATRP of p([N-(3dimethylamino)propyl] methacrylamide) using the six-arm star shaped initiator dipentaerithritol hexakis (2-bromoisobutyrate)

In general, the yields of all of these approaches were very low, below 30%, except for the p(DMAA-co-DEAA) (**P10**) which had a yield of 71%. The low yields of **P11** and **P12** were probably partly caused by the low molecular mass of the polymers or oligomers, which were probably partly removed during dialysis. The SEC analysis of the remaining polymer showed an undefined signal almost at the lower detection limit of the SEC (see Figure 23 b, c). Probably only oligomers were formed and the irregular shape of the SEC-curves indicates a non-uniform polymerization. The irregular polymerization and termination at low molecular weight might be caused by the side chain of the monomer. It is long and flexible and thus the dimethylamine can probably easily complex with the copper catalyst causing the chains to die as reported in literature.[105] The side chain of the DEAA and DMAA monomers is quite short and probably the polymer needs to grow first before being able to bend back and complex with the copper catalyst at the growing end of the chain. The copolymerization showed better control than the homopolymer, when one compares the SEC-curves but both polymers elute at the lower detection limit of the machine.
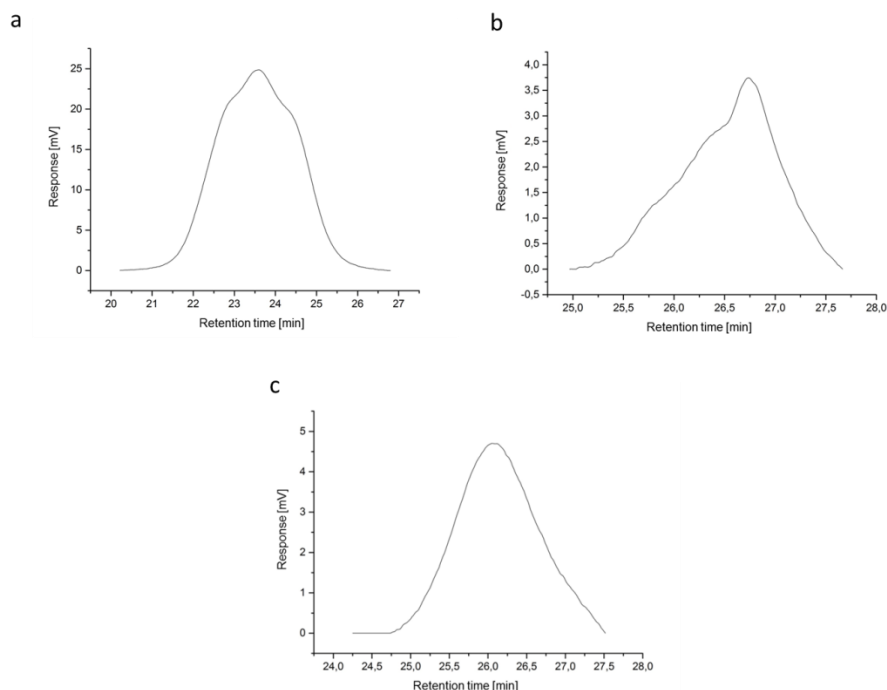
Figure 23: SEC traces of (a) poly(DMAA-co-2-ethylhexylacrylate) (P9), (b) p([N-(3dimethylamino)propyl] methacrylamide) homopolymer (P11) and (c) p([N-(3dimethylamino)propyl] methacrylamide-co-DEAA) copolymer (P12).

The SEC measurement of the p(DMAA-co-2-ethylhexylacrylate) (**P9**) also showed a broad size distribution of 1.6. Additionally, the SEC trace is not unimodal but carries shoulders on the high and on the low molecular weight side, indicating a non-uniform polymerization (see Figure 23 a). The SEC measurement of the p(DMAA-co-DEAA) (**P10**) yielded a reasonable M_n of 8650 g.mol^{-1} and combined with a relative low dispersity of 1.3.

The ^{1}H-NMR measurements showed for all copolymerization products that both monomers were integrated into the polymer, but due to overlapping peaks it was not possible to determine the ratio of the different monomers in the polymeric chain in any of the cases. Therefore, for the calculations of the theoretical DP, the initial ratios of the monomers in the polymerization mixture were used.

In general the NMR showed a lower DP per arm than the SEC measurements, where the SEC measurements sometimes even showed a higher DP than theoretically possible. Trials to determine the molecular mass with matrix-assisted laser desorption/ionization time of flight (MALDI-ToF) mass spectrometry failed.

Compared to the pure p(DMAA), the T_g the p(DMAA-co-2-ethylhexylacrylate) (**P9**) (93.9 °C) and of the p(DMAA-co DEAA) (**P10**) (90.7 °C) polymers decreased but not

significantly enough for the targeted application. Therefore, these two approaches were not investigated further.

Only for the p([N-(3dimethylamino)propyl] methacrylamide) homopolymer (**P11**) (33.1 °C) and the respective copolymer with DEAA (**P12**) (35.9 °C) low T_g's could be achieved. This was probably caused by the very low molecular weight of the synthesized products.

The copolymer (**P12**) was investigated as matrix material for peptide array synthesis with laser-induced forward transfer.

For the donor preparation, Fmoc-Cys(Trt)-OPfp was mixed with the copolymer (**P12**) (10:90 wt-%) and dissolved in DCM. A microscopy slide covered with polyimide foil was then spin-coated with the solution. As acceptor slide, an Fmoc-deprotected PEGMA-co-MMA slide with one ß-Ala was used. After the transfer, the slide was baked in the oven, washed, capped, side chain deprotected, stained with TAMRA maleimide and scanned (see Figure 24).
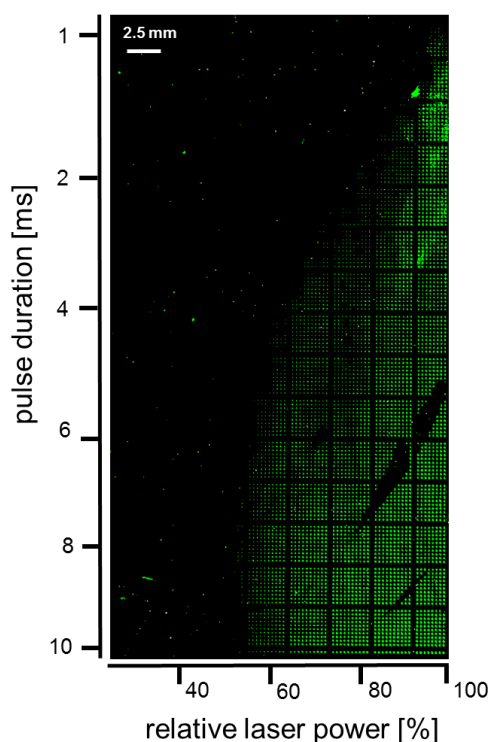
Figure 24: Fluorescence scan of a laser parameter variation. Fmoc-Cys(Trt)-OPfp was transferred with the p([N-(3dimethylamino)propyl] methacrylamide-co-DEAA) (P12) copolymer as matrix material. The laser based transfer was executed with pulse durations from 1 to 10 ms (step size 0.05) and laser power from 30% to 100% (step size 0.8). Coupling was performed at 90 °C, the Trityl protection group was removed and the thiol was stained with TAMRA maleimide. The diagonal defects were caused by incomplete coverage of the slide during the spin-coating process. Scanned in the GenePix scanner. Contrast and brightness were adjusted.

It is possible to use the p([N-(3dimethylamino)propyl] methacrylamide-co-DEAA) copolymer (**P12**) as matrix material at 90 °C. A coupling experiment at 60 °C was also performed and proved possible, but the pulse duration and the relative laser power need to be longer and stronger at this lower temperature for the first spots to become visible.

Even though the p([N-(3dimethylamino)propyl] methacrylamide-co-DEAA) copolymer (**P12**) can be used as matrix material, it is not a good candidate. The initial polymerization is wasteful as the monomer must be present in excess for the reaction to proceed but only a small fraction is incorporated. Additionally, the requirement of a well-defined polymer is not fulfilled as evidenced by the broad SEC trace.

3.6. ToF-SIMS experiments

To get further insight into the coupling of the amino acid derivatives to the synthesis film and the effectiveness of the washing protocols, ToF-SIMS experiments were executed using Fmoc-Cys(Trt)-OPfp as the model amino acid (see Figure 25 for illustration of the various components).

Fmoc-Cys(Trt)-OPfp

p(DMAA) matrix material

pure PEGMA synthesis film on acceptor slide

PEGMA-co-MMA synthesis film on acceptor slide
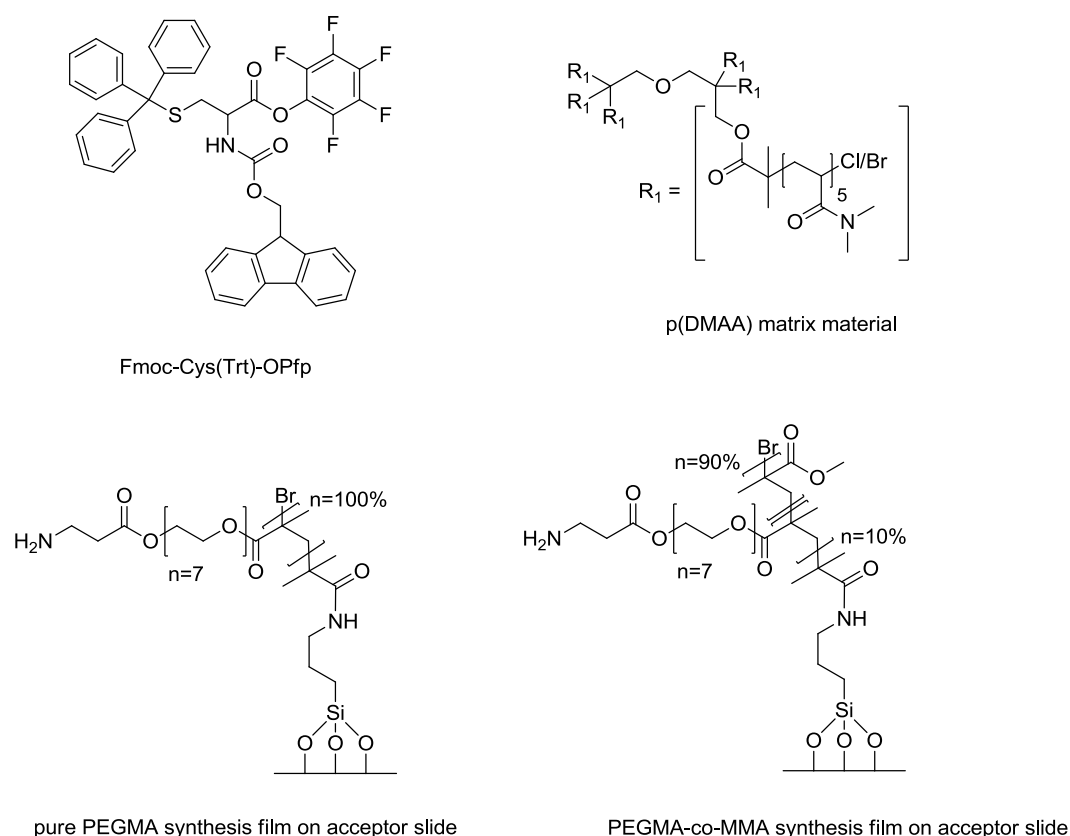
Figure 25: Molecular structures of the different components of the ToF-SIMS experiments: the model amino acid Fmoc-Cys(Trt)-OPfp, the matrix material p(DMAA), the synthesis film on the acceptor slides either pure PEGMA or PEGMA-co-MMA.

First, the effectiveness of the washing protocols to remove unreacted amino acid derivatives from the synthesis film was investigated. Acceptor slides were prepared by Fmoc-deprotection of two PEGMA-co-MMA synthesis slides carrying one Fmoc-ß-Ala. The control slide was capped directly after deprotection with a solution of acetic anhydride/ DIPEA/ DMF (10:20:70 vol-%) to cap all free amines, leaving the other slide only Fmoc-deprotected and still carrying free amines to which the activated amino acid derivatives should be able to bind. The donor slide was prepared by spin-coating a solution of Fmoc-Cys(Trt)-OPfp and p(DMAA) (**P1**) (10:90 wt-%) in DCM onto a polyimide foil covered glass slide. Using laser-induced forward transfer, both acceptor slides were patterned with rectangles consisting of eight overlapping spots (4 × 2) with pitch 40 μm, laser power 40% and pulse duration 10 ms. Subsequently, both slides were baked in the oven at 110 °C under argon atmosphere for 1.5 h. Then they were washed by flushing thoroughly with DCM and then rocking in DCM for 3 × 5min. Then the slides were placed in an ultrasonic sound bath for 30 sec followed by exchange of the DCM and 5 min rocking in DCM, this was repeated three times. After drying under a stream of argon, the slides were analyzed with ToF-SIMS (see Figure 26).
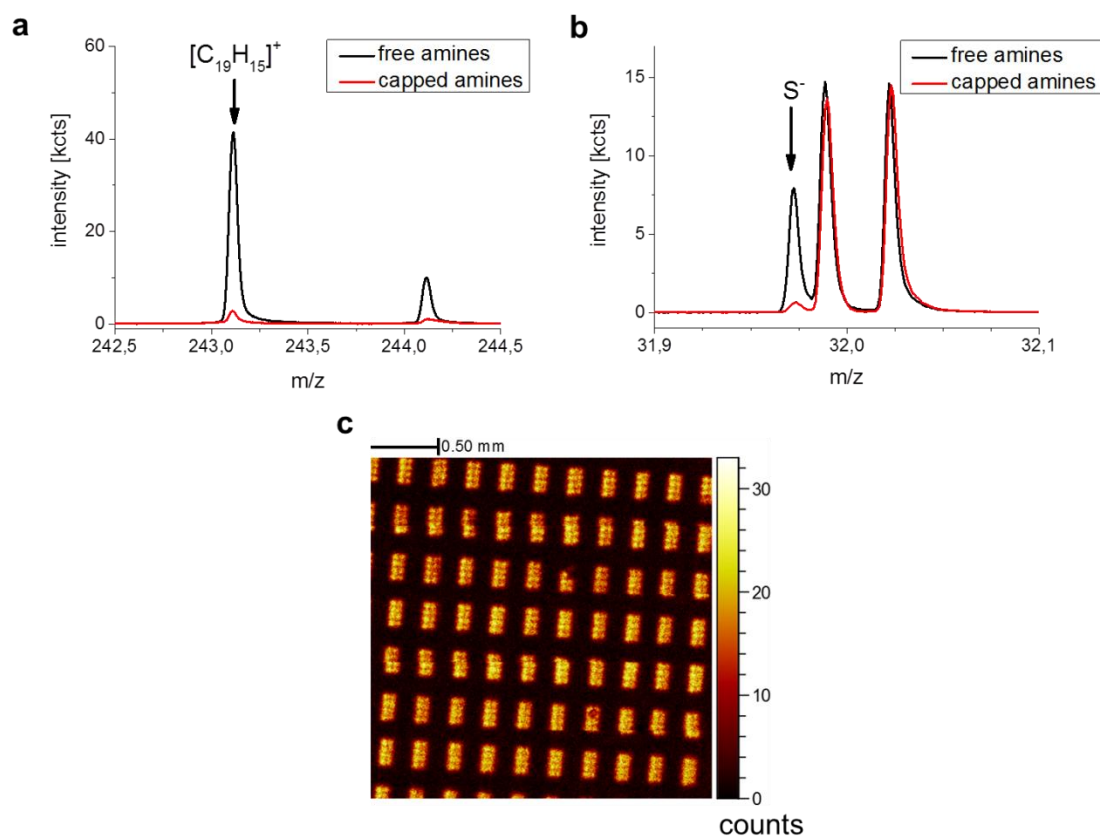
Figure 26: Fmoc-Cys(Trt)-OPfp coupling to PEGMA-co-MMA carrying one ß-alanine, ToF-SIMS analysis. (a) Trityl $[C_{19}H_{15}]^+$-fragments on acceptor with free amines (black) and an acceptor with capped amines (red), (b) sulfur signal on acceptor with free amines (black) and an acceptor with capped amines (red), (c) stage scan showing lateral distribution of trityl groups on an acceptor surface carrying free amines. All measurements conducted after laser transfer, followed by coupling at 110 °C and the washing protocol with DCM.

The ToF-SIMS analysis was focused on the side chain of the model amino acid Fmoc-Cys(Trt)-OPfp, which consists of a thiol, protected with a trityl group. The $[C_{19}H_{15}]^+$-fragment originates from the trityl group and the S⁻-ion originates from the thiol. For the acceptor surface with free amines, a strong signal could be detected for both fragments (black curves in Figure 26 a, b). For the capped surface, the detected signals were negligible (red curves in Figure 26 a, b). From these results it can be concluded that the amino acid derivative binds to the surface when using p(DMAA) six-arm star polymers as the matrix material. Furthermore, the washing protocol effectively removes uncoupled amino acids from the synthesis film and no unspecific intercalation takes place. This is a necessary requirement for the synthesis of peptide arrays in order to prevent the formation of false sequences. By doing a stage scan it could also be shown that the structuring is successful over a larger area as the lased pattern appears clearly in the measured area (see Figure 26 c).

In the next step it was investigated if the amino acid derivatives are able to penetrate into the synthesis film when using p(DMAA) six-arm star polymers as the matrix material, by doing depth profiling studies with ToF-SIMS. For these investigations, the acceptor surface was changed from PEGMA-co-MMA to pure PEGMA, as only these films can be grown to a thickness of around 100 nm. The thicker synthesis films are necessary to ensure that the sputtering gun of the ToF-SIMS is able to measure in steps and does not completely penetrate the synthesis film in the first sputter step. Also pure PEGMA films have already proven to be suitable substrates for this kind of sputtering and depth profiling measurements.[47] Again Fmoc-Cys(Trt)-OPfp was used as the model amino acid. The trityl side chain protecting group was used to monitor the penetration depth of the amino acid derivative. The major advantage of the trityl group is that it does not show any forward implantation of the intact fragment and that upon ion bombardment a characteristic fragment can be detected with satisfactory intensity.[47] For the donor slide preparation, a mixture of Fmoc-Cys(Trt)-OPfp and p(DMAA) (**P4**) (10:90 wt-%) in DCM was spin-coated onto a polyimide covered glass slide. Two pure PEGMA synthesis slides functionalized with one Fmoc-ß-Ala were Fmoc-deprotected to serve as acceptor slides. Then laser-induced forward transfer was performed from the donor to the acceptor using the same parameters as for experiments investigating the effectiveness of the washing protocol. Subsequently, one of the slides was baked in an oven at 110 °C under argon atmosphere for 1.5 h. Finally, both slides were analyzed with ToF-SIMS without performing any washing steps prior to the measurement (see Figure 27).
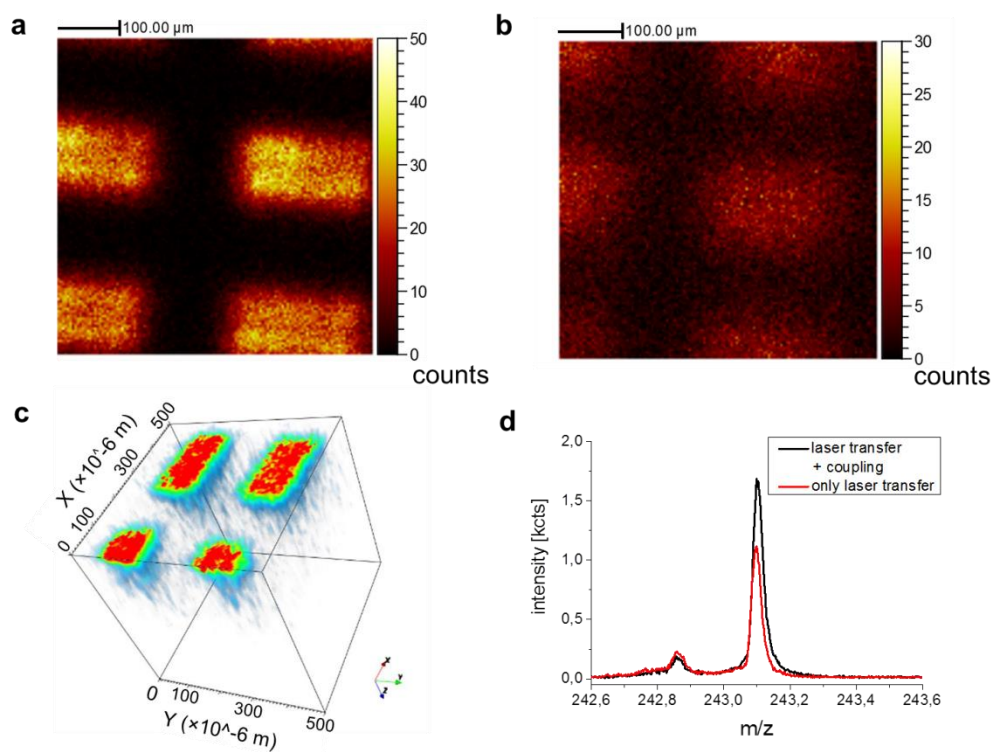
Figure 27: (a) Static-SIMS mapping of the surface distribution of trityl fragments $[C_{19}H_{15}]^+$ on the surface of a PEGMA/ ß-Ala acceptor layer, sample directly after laser based transfer. (b) Static SIMS mapping of the surface distribution of trityl fragments, on an acceptor surface patterned as before and 110 °C oven treatment. (c) Dynamic SIMS 3d model based on distribution of trityl fragments in PEGMA/ß-Ala acceptor layer, directly after laser based transfer (z axis not to scale, highest intensity red, lowest intensity blue) (d) Integrated trityl signal from dynamic SIMS from the total polymer thickness (black: after laser based transfer and coupling; red only laser based transfer).

The sample directly after the lasing step compared to the sample after lasing and an additional oven step shows more trityl signal on the surface (see Figure 27 a, b). This could indicate that the amino acid derivative diffuses into the synthesis film during the coupling step in the oven. However, the two slides were lased one by one, independent from each other; therefore an alternative explanation could be differences in the amount of transferred amino acid derivatives.

When looking at the depth profiles of the trityl group for the two samples (red curves in Figure 28 a, b), for both samples, there is a high signal of the $[C_{19}H_{15}]^+$-fragment in the upper part of the synthesis film, which drops rapidly going deeper.
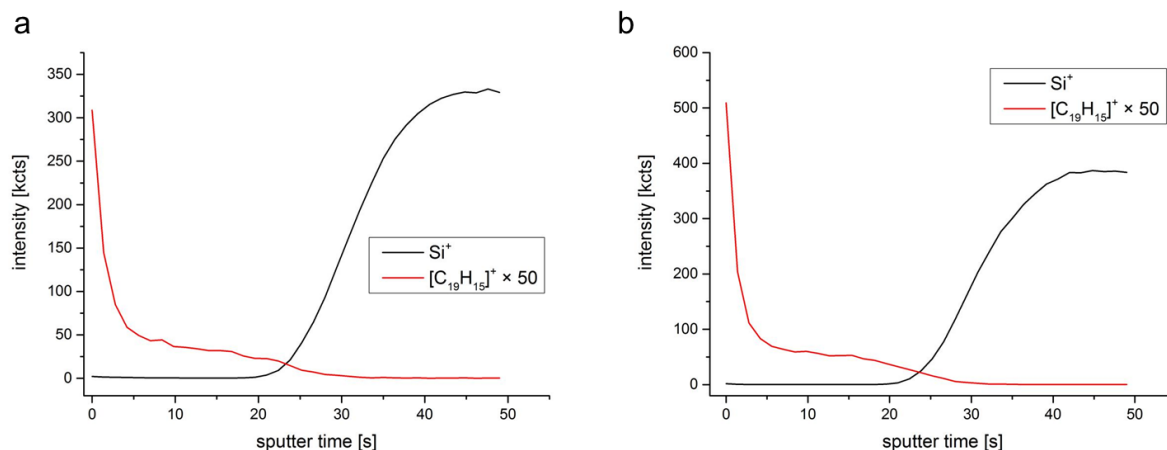
Figure 28: Depth profile of trityl fragment $[C_{19}H_{15}]^+$ in a pure PEGMA synthesis film on glass; (a) after transfer (b) after transfer and oven baking

This could be an indication that the amino acid derivatives only bind in the upper part of the synthesis film. When performing the laser based transfer, only very small amounts of matrix material and amino acid derivative are transferred. The pure PEGMA film has 90% more functional groups compared to the PEGMA-co-MMA synthesis film, each of which are possible binding partners to the activated amino acid derivatives. Therefore, it is probable that all of the transferred amino acid derivatives couple in the upper parts of the synthesis film and do not have the chance to diffuse into the lower parts. This lack of penetration should not be a problem for peptide array synthesis as the usual PEGMA-co-MMA synthesis films are normally only 13 to 25 nm thick. In addition, antibodies are large molecules, which anyway are not likely to diffuse into the synthesis film. Therefore, antibody binding events are anyway only likely to take place at the surface of the synthesis film. The static SIMS measurements on the surface of the samples suggested that during the oven step, the amino acid derivatives diffuse into the synthesis film and the depth profiling showed that the amino acid derivatives only diffuse into the upper parts of the synthesis film. To rule out that the difference in trityl signal measured between the oven sample and the unbaked sample was not caused by different amounts of transferred material, the depth profile signals were integrated over the complete depth to calculate the total amount of trityl group present in each sample (see Figure 27 d). The integrated trityl signals collected from the dynamic SIMS depth profiling experiment show no significant difference between the oven-baked sample and the unbaked sample. It can thus be ruled out that the difference in surface trityl signal concentration is caused by varying amounts of transferred material. This means that the amino acid derivatives diffuse into the synthesis film during the oven step but only into the upper part, where they probably react completely to the outmost layer of the synthesis film.

The analysis of the ToF-SIMS measurements was extended to also investigate the presence of the pentafluorophenol leaving group coming from the amino acid. Surprisingly, no $C_6F_5^-$ signal, representing the pentafluorophenol group, could be detected. A fluorine signal could be detected, but this signal was uniformly distributed over the surface and not reflecting the lased pattern (see Figure 29). The fluorine signal, which was measured over the whole sample, might be caused by contaminations. ToF-SIMS is a very sensitive surface analysis technique and therefore especially suffers even from small contaminations.[90] In contrast, the trityl signal showed the successful transfer of the pattern (see Figure 27 a), ruling out an error in the laser based transfer step.
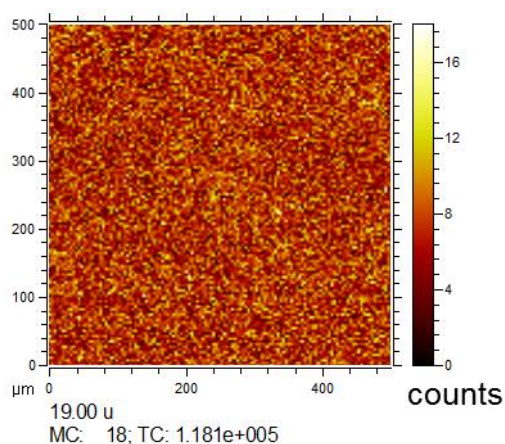
Figure 29: Static-SIMS mapping of the surface distribution of F$^-$, on the surface of a PEGMA/ ß-Ala acceptor layer, sample directly after laser based transfer

Drop cast samples of pure Fmoc-Cys(Trt)-OPfp and of the transfer mixture Fmoc-Cys(Trt)-OPfp and **P4** p(DMAA) (10:90 wt-%) were analyzed additionally to investigate the integrity of the amino acid derivative. The $C_6F_5^-$ fragment, which would indicate the presence of the OPfp ester, can be detected in the two drop cast samples. The boiling point of the pentafluorophenol leaving group is 143 °C.[111] Therefore, during the oven step, which takes place at 110 °C, it should not evaporate.

It might be that so little amounts are transferred that the pentafluorophenol falls underneath some detection limit in the case of the sample of a laser-induced forward transfer onto a pure PEGMA synthesis slide. Indeed, the drop cast sample of the amino acid derivative embedded into the p(DMAA) matrix material, the $C_6F_5^-$ signal is already very low and the drop cast samples were done on a bare wafer. So when even less material is present and additionally the synthesis film hinders the ionization of the $C_6F_5^-$ fragment, it might be possible that no fragments can be detected at all. The fact that the

surroundings play a major role in the ion formation probability is described as the matrix effect, where the same analyte ionizes in a different yield when the substrate or the surroundings e.g. embedded into another material change.[88]

This finding requires further investigation, which might lead to valuable information about the process of the laser-induced forward transfer.

As discussed above, the amino acid derivatives could only be found in the upper parts of the polymeric synthesis film. It would be interesting to also investigate the penetration behavior of the matrix material into the synthesis film. This could give valuable insight into the transfer of materials by combinatorial laser-induced forward transfer which is still not fully understood.

In order to do so, the matrix material must be distinguishable from the polymeric synthesis film on the acceptor slide in ToF-SIMS measurements. Drop-cast samples of p(DMAA) as example for the matrix material and a sample of the a PEGMA-co-MMA functionalized synthesis film were measured and compared to see if any characteristic fragments were present, that could only be found in one of the samples (see Figure 30).
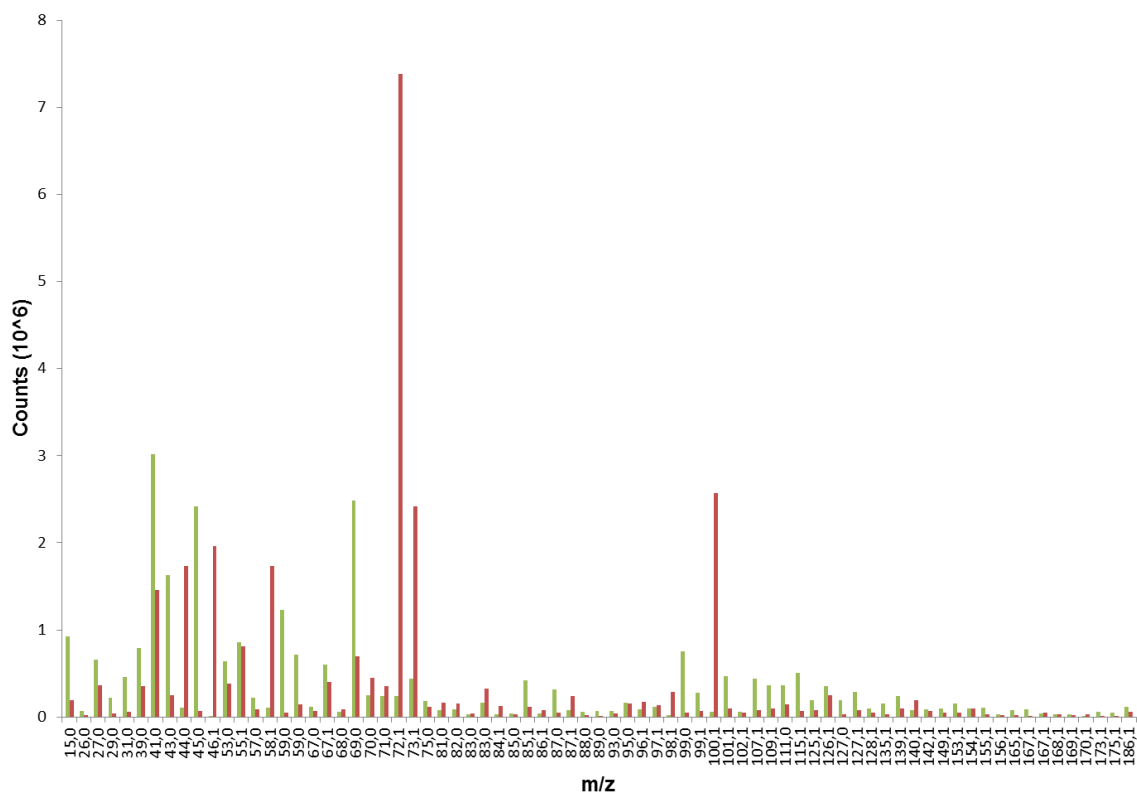
Figure 30: ToF-SIMS measurement of the positive ions of the p(DMAA) drop-cast (red) and a PEGMA-co-MMA synthesis slide (green)

In the positive spectrum as well as in the negative spectrum (not depicted), no fragments could be found which could be solely assigned to either the p(DMAA) matrix material or the PEGMA-co-MMA synthesis film. There are some fragments which have higher counts for either of the materials, but because all detected fragments could originate from either the matrix material or the synthesis film, the two polymers are not distinguishable and the spectra cannot be deconvoluted. To get more information about the interaction between the matrix material and the synthesis film it would be necessary to find fragments, which can be assigned solely to the matrix material, finger print pattern,[88] and which have high intensities. This could give valuable insight into the penetration behavior of the matrix material into the synthesis film and whether this influences the coupling depth of the amino acids. A possible solution to this might be labeling of the matrix material.

3.7. Investigations into the laser-induced forward transfer and the role of the matrix material

The mechanism of the laser-induced forward transfer is not understood yet. Experiments were performed to investigate if the coupling yield is improved by the coupling step in the oven and the use of a matrix material or not.

To investigate this hypothesis, two Fmoc-deprotected PEGMA-co-MMA surfaces carrying one ß-Ala as acceptor slides were lased using p(DMAA) (**P6**) as the matrix material and Fmoc-Cys(Trt)-OPfp as the amino acid derivative (10:90 wt-%) spin-coated onto a polyimide foil covered glass slide as a donor. One slide was baked in the oven under argon atmosphere for 1.5 h according to standard protocol, the other was left unbaked. Then both slides were washed and capped. Subsequently, the trityl protecting group was removed from the cysteine side chain and the thiol was stained with TAMRA maleimide. The stained slides were scanned (see Figure 31).
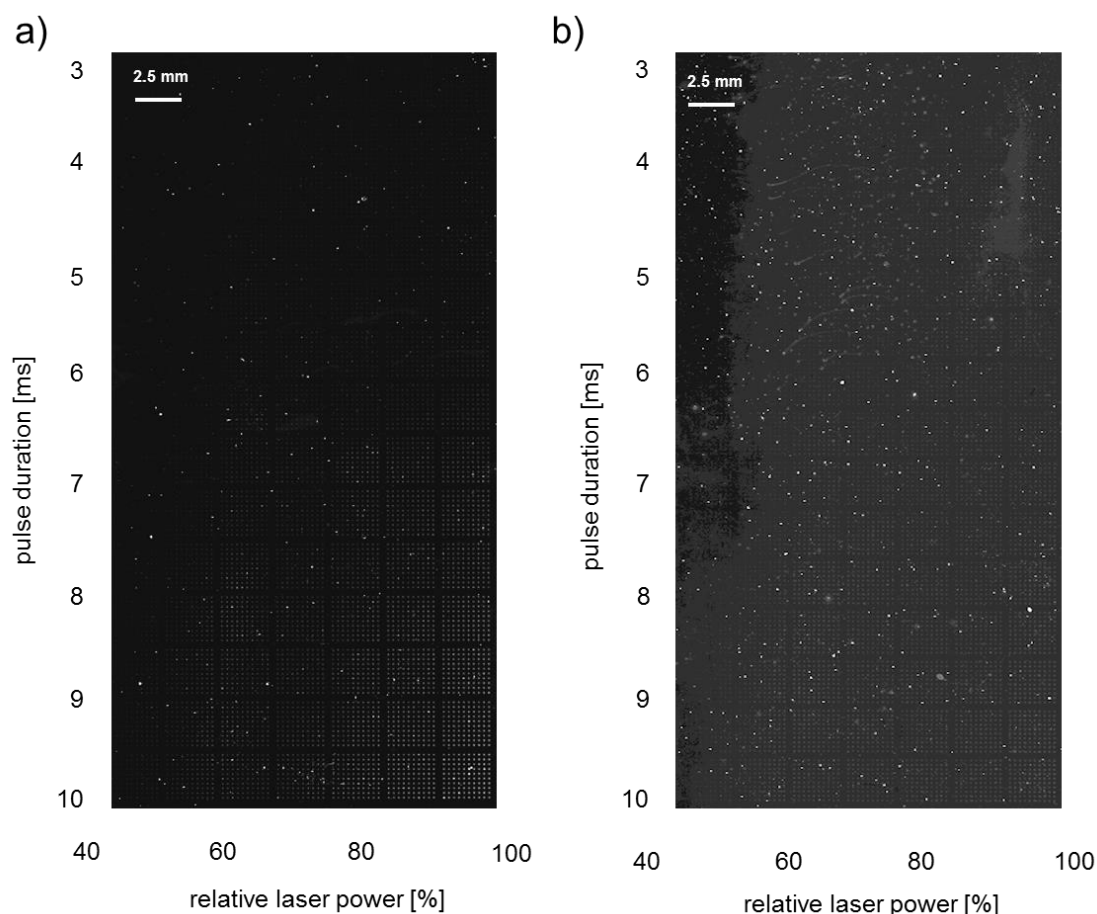
Figure 31: Fluorescence scans of spots at laser parameter variation: Laser parameters were varied: pulse duration from 3 to 10 ms (step size 0.05) and laser power from 37% to 100% (step size 0.8). Fmoc-Cys(Trt)-OPfp was transferred and coupled (a) with oven at 110 °C (b) without oven. The trityl side chain was removed and the thiol was stained with TAMRA maleimide. Both slides were scanned in the Genepix Scannner, contrast and brightness were adjusted.

A fluorescence signal is detected for both slides, but intensities are significantly higher for the slide with additional coupling in the oven. The laser beam heats the polyimide foil during the transfer; maybe this is enough to already couple a small amount of the activated amino acid derivatives directly during the lasing step. Although coupling is apparently possible with only the laser-induced forward transfer (and without the much longer oven step), these results suggest that it is necessary to do the oven step to obtain satisfactory yields.

In addition to the coupling experiments with and without oven it was also tested if it is possible to transfer amino acid derivatives without using any matrix material and to then couple them to the synthesis film. One polyimide foil covered glass slide was thus spin-coated with a mixture of Fmoc-Cys(Trt)-OPfp/ p(DMAA) (**P2**) (10:90 wt-%) as a donor. A second polyimide foil-covered glass slide was coated with only Fmoc-Cys(Trt)OPfp in

DCM solution. The solution was pipetted onto the slide and distributed by manually angling the slide in different directions until an even spread was reached and the DCM evaporated. Both slides were then used as donor slides in a laser-induced forward transfer onto Fmoc-deprotected PEGMA-co-MMA slides carrying one β-Ala. After coupling, washing, capping, side chain deprotection and staining with TAMRA maleimide, the slides were scanned (see Figure 32).
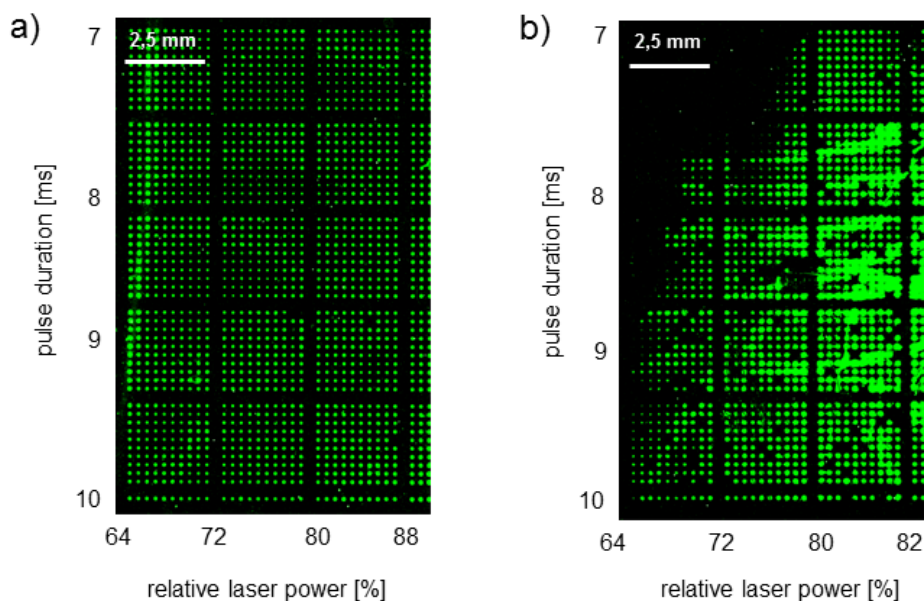
Figure 32: Fmoc-Cys(Trt)-OPfp transferred and coupled (a) using p(DMAA) as matrix material, (b) without matrix material. Both stained with TAMRA maleimide dye after side chain deprotection. Both slides were scanned in the GenePix scanner, contrast and brightness were adjusted.

The array that is produced with matrix material has smaller spots compared to the array synthesized without matrix material. Also visible spots were transferred down to lower pulse duration and intensity. Maybe the polymeric synthesis film takes over the role of the reaction medium/solvent when no matrix material is used. For the matrix-omitting protocol more missing spots in the grid and also a tendency towards blurry spots which mix with the neighboring spots can be observed. Using a matrix material seems to be necessary because smaller spots can be obtained, which is important when aiming for a higher spot density per cm^2 and when going to lower pitches. The transfer seems to be more reliable when using a matrix material. Either the matrix material supports a uniform transfer or the reason is the uniformity of the donor slide itself. Spin-coating was not possible for the donor slide without matrix material, as the material simply did not adhere to the slide. The drop-casting alternative, with manual distribution while the DCM was

evaporating, may not have yielded a coverage uniform enough for a consistent laser transfer.

According to the results shown above, using a matrix material as well as doing an oven step after the transfer considerably improve the quality and yield of coupling of the synthesized peptide array and are therefore necessary.

3.8. Conclusion

P(DMAA) polymers were examined as possible matrix materials for peptide array synthesis from 'solid' solvents with the laser-induced forward transfer method.

DSC measurements showed that amino acid derivatives are miscible with p(DMAA) polymers at temperatures above T_g of the matrix material, thereby fulfilling one of the key requirements for a matrix material. Moreover, the p(DMAA) makes good contact with the synthesis surface upon heating. Post-synthesis modifications of the p(DMAA) polymers are possible by end group functionalization. This could allow for optimization and adaptation of special application requirements in the future. In test reactions p(DMAA) could successfully be used as a matrix material to couple amino acid derivatives to a synthesis film structured by a laser-induced forward transfer. It was shown that coupling at 90 °C is possible. Also a small tripeptide could be successfully synthesized, which was proven by antibody staining. With the p(DMAA) as matrix material and laser-induced forward transfer spot densities can be increased to 20.000 spot per cm^2.

Different approaches to investigate the possibilities to lower the T_g and the coupling temperature were taken. Mixing in additives and end group functionalization were not very promising and therefore not deeply investigated. With the copolymerization approach, some first encouraging results were obtained, but these promising polymerization reactions were difficult to control and the yield of polymer was very low.

The coupling behavior of Fmoc-Cys(Trt)-OPfp as a model amino acid to the synthesis film when using p(DMAA) as the matrix material was investigated in detail by ToF-SIMS measurements. It was shown that the amino acid derivative couples to the film and that uncoupled amino acids can be removed almost completely from the synthesis film with the applied washing protocol. It was also shown that the transferred amino acid derivatives preferentially couple in the upper part of the synthesis film, where they are consumed completely.

The impact of the oven step and the matrix material on the resulting array were investigated. The oven step was shown to be beneficial for the peptide synthesis yield. Transfer without a matrix material is shown to be possible but the matrix material improves the transfer uniformity significantly and yields smaller spots.

P(DMMA) proved to be a very interesting matrix material candidate for peptide array synthesis by the 'solid' solvent approach in combination with laser-induced forward transfer structuring. If this is investigated and optimized further, significant improvements in spot density compared to the commercially available styrene-acrylic copolymer resin should be possible.

3.9. Outlook

For p(DMAA) to be used routinely as matrix material in peptide array synthesis, it is necessary to upscale the synthesis. This proved to be difficult because when a larger batch (**P1**) was synthesized, the polydispersity went up, which is undesirable for a defined product. An alternative to up-scaling might be to investigate the reuse of the donor slides, which has already been reported for the commercially available resin.[45] In this way, material could be saved and p(DMAA) could routinely be used as a matrix material for combinatorial laser-induced forward transfer.

Furthermore the lowering of p(DMAA)'s T_g proved to be challenging and will need further investigations. Probably, the best way forward is copolymerization of different monomers, as additives always add the risk of demixing effects and additional problems with irregularities during the transfer process.

The exact mechanism of the transfer process also needs to be investigated further. When better understanding of it is achieved, the matrix material can also be customized and improved further. One step in this direction might be to label the matrix material so that it is distinguishable from the synthesis film in ToF-SIMS, enabling the penetration behavior to be investigated further as well as the mechanism of the laser based transfer. P(DMAA) offers many possibilities as it is adjustable for these investigations.

4. The Ugi four component reaction on peptide arrays

In peptide array synthesis it is of great interest to couple special building blocks to side chains in post-modification steps, such as glycosylation. Generally, glycoconjugates play an important role in many intra- and intercellular mechanisms and are mainly recognized by proteins.[112]

For these kind of functionalization's MCRs, such as the U-4CR, are very good candidates as they are very selective and atom efficient.[54,55] The peptide-like structure of the U-4CR products makes them also very suitable for the incorporation into peptides.[54] The kind of peptidomimetics, where the backbone is not consisting strictly of peptide bonds, are of great value for protein-protein studies as they are often very stable *e.g.* no proteolysis takes place.[113] Proteins can bind to a peptidomimetic, as in most cases the binding event is depending on the side chains and their orientation and not on the backbone.[114,115]

Additionally, structural variations of U-4CR products can be achieved easily by variation of the different components. Therefore, the U-4CR is an interesting tool for creating peptidomimetics.[113] Another advantage is that the U-4CR is usually performed at room temperature.[116]

The U-4CR is also applied in the synthesis of peptide-like molecules on beads (SPPS) as a useful tool to generate libraries for screening, as often needed in pharmaceutical applications.[58,117,118] The U-4CR in the SPPS context is performed using the Fmoc-protection strategy for peptide synthesis.[119] Similarly to traditional SPPS, the amine functionality is bound to the beads and the other components are added from solution.

For screening purposes, it is also very interesting to have an array consisting of a library of molecules bound to a surface. In this way, many different molecules can be screened at the same time and be compared to each other. The compatibility of the U-4CR with small molecule arrays has already been demonstrated for cellulose substrates.[59–61] Macroarrays were thus synthesized by the SPOT method to create small molecule libraries.

Here, the two approaches of using the U-4CR in an analogous approach to SPPS for peptide synthesis and the array concept are combined. Peptide microarrays on glass slides functionalized with a polymeric synthesis film as substrates were investigated. The compatibility of the U-4CR reaction with these microarrays and *in situ* incorporation of

non-natural and demanding side chains into the peptides on the array were investigated.[**]

4.1. Side chain modification *via* the U-4CR

First, the compatibility of the U-4CR with the microarrays and with the environment of the PEGMA-co-MMA synthesis film was investigated. Since the amine proved to be a good choice as the anchor to the surface for the bead and cellulose based experiments with U-4CR,[58–61] it was chosen here as well. The PEGMA-co-MMA arrays, produced with the laser printing technique, were obtained from a commercial supplier carrying a ß-Ala-Asp-ß-Ala spacer, which was further functionalized with Ac-Lys(Boc) or Ac-Gly in alternating spots (see Figure 33 a). First the side chain protecting Boc of the lysine was removed to obtain an amino group (see Scheme 16). In the next step, this amino group was used as the amino component for the U-4CR and the other three components: Fmoc-ß-Ala-OH, hexanal and cyclohexyl isocyanide were thus added to the reaction from solution. The U-4CR was followed by a capping step so that unreacted amines were acetylated and could not react in the further steps to give false positive signals. The Fmoc protecting group of the U-4CR product was removed, yielding product (**1**), which was then stained with DyLight 680-NHS and the array was analyzed in a fluorescence scanner.
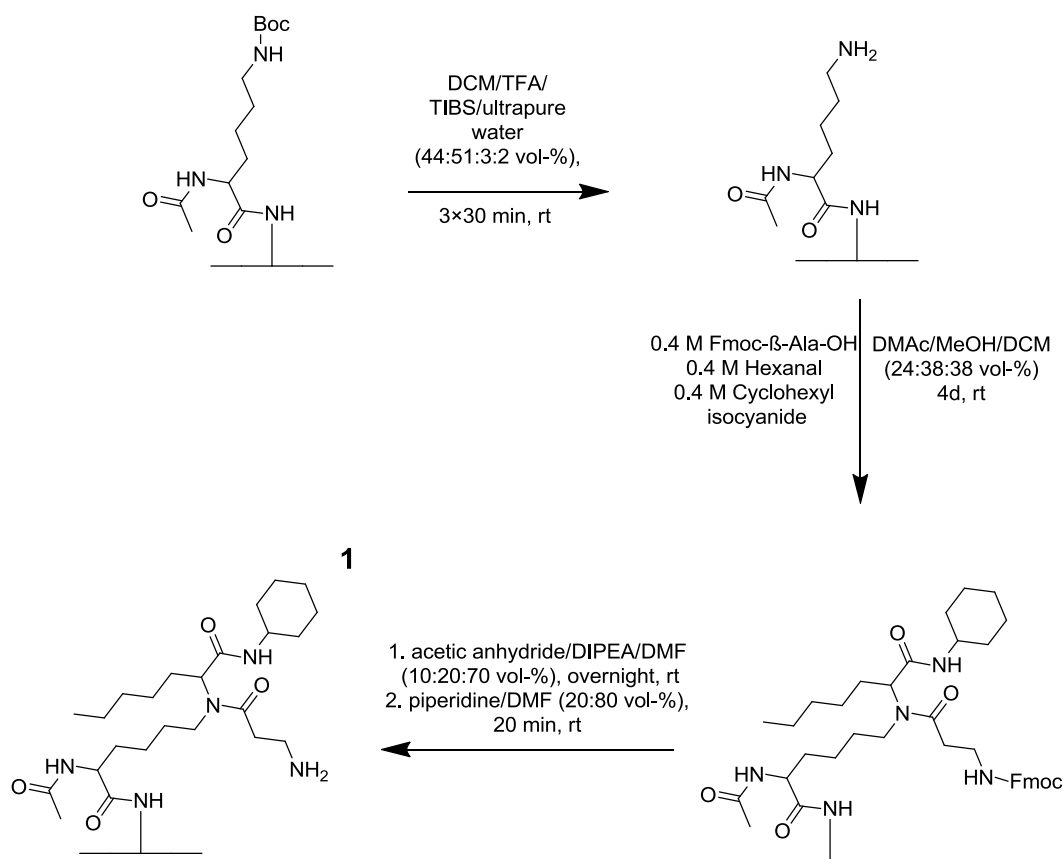
Scheme 16: Reaction scheme of the array side chain deprotection, U-4CR, capping and Fmoc-deprotection (exemplarily for MeOH/ DCM (50:50 vol-%) as the reaction solvent)

As the purchased peptide arrays are produced in batches with multiple array orders on one plate, it is not possible to obtain arrays which only carry one Fmoc-protected amino acid on top of a spacer. Therefore, lysine was chosen, as it carries an amino group in the side chain, which would be available for functionalization after removing the side chain protection group. The N-terminal group of the amino acids is not available for synthesis in this case, as it was capped with acetic anhydride. This is also the case for the N-terminus of the glycine spots, which could in this case be used as the negative control. No signal is expected to occur in these spots during validation of the reaction with fluorescent labeling. If a fluorescent signal is detected, this would be due to unspecific intercalation of unreacted Fmoc-ß-Ala-OH which could not be removed by the washing steps.

For a reaction to take place on an array, which consists of a glass substrate functionalized with a polymeric synthesis film to which the peptides are anchored, two requirements have to be fulfilled. First, all components of the reaction have to be soluble in the reaction solvent, which also needs to be able to promote the proceeding of the

reaction. Secondly, the solvent needs to swell the surface, so that diffusion of the different components into the synthesis film is possible.

The first step in this investigation was to find the right solvent mixture for the U-4CR on the arrays. Pure methanol (MeOH) and pure isopropanol were chosen as candidates because in literature for the combination of peptide synthesis and the U-4CR, alcohols are reported to be the most suitable solvents.[120] Also, a mixture of MeOH and DCM was applied, as this mixture was also described in literature to be suitable for U-4CR using an analogues approach to SPPS.[58] The DCM should support the swelling of the PEGMA-co-MMA synthesis film. For the first investigations, the side chain deprotected arrays were incubated with a solution containing Fmoc-ß-Ala-OH, cyclohexyl isocyanide and hexanal in MeOH, isopropanol or mixture of DCM/ MeOH (50:50 vol-%). *N,N*-Dimethylacetamide (DMAc) (24 vol-%) was added to each mixture to dissolve the Fmoc-ß-Ala-OH, which was used as the carboxylic acid component. The reactions were performed in a desiccator under argon atmosphere for four days. The arrays were capped overnight followed by an Fmoc-deprotection step in piperidine/ DMF (20:80 vol-%). Fluorescent staining was performed using DyLight 680-NHS. Subsequently, the slides were scanned in a fluorescence scanner (see Figure 33).

a

b

3 mm

c

3 mm

d

3 mm
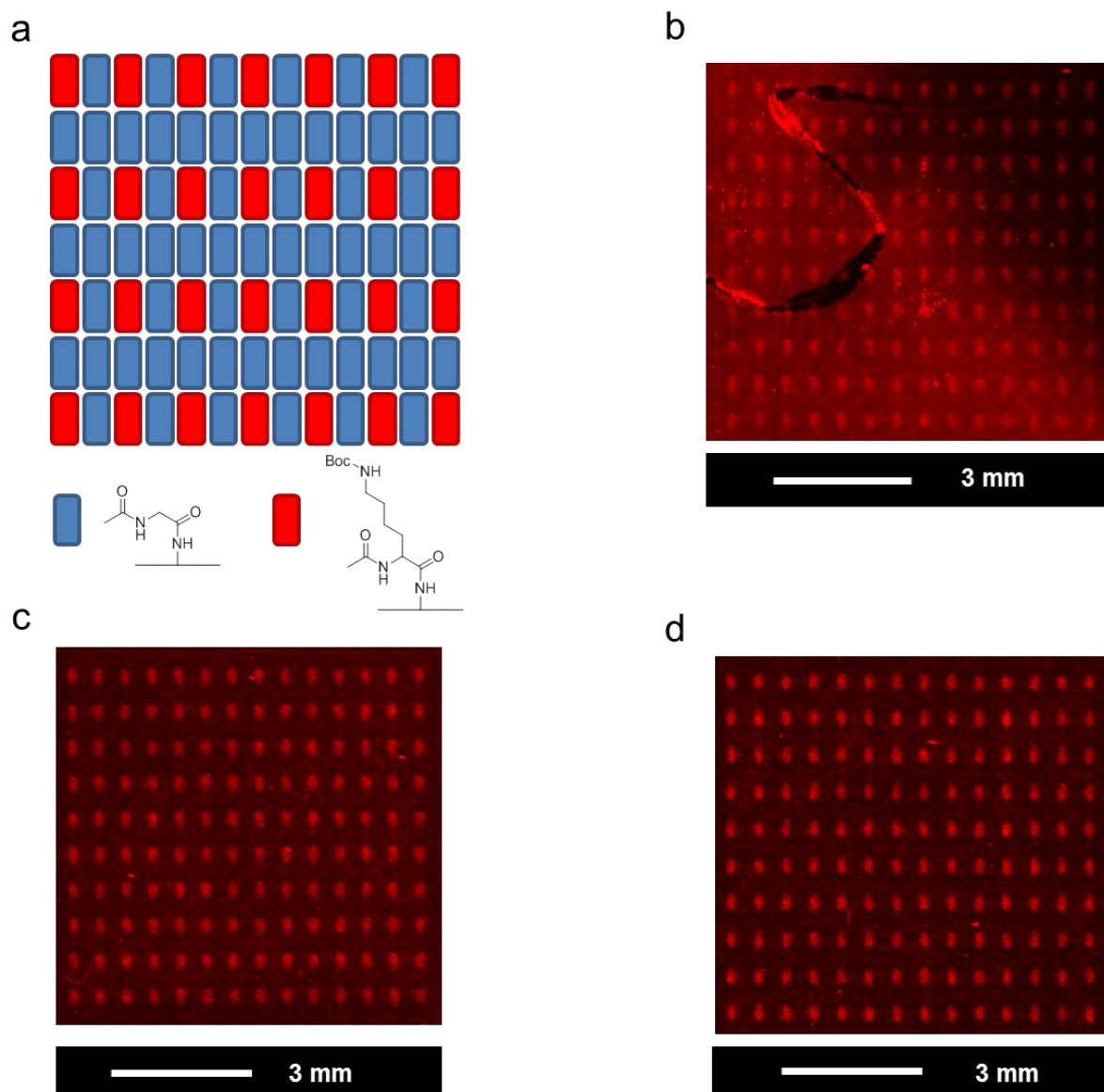
Figure 33: (a) Scheme of the array layout with alternating Ac-Lys (red) and Ac-Gly (blue) spots and fluorescence scans of the arrays (b-d), in the Odyssey scanner at intensity 3 and resolution 21 µm. An U-4CR with Fmoc-ß-Ala-OH, hexanal and cyclohexyl isocyanide was performed in different solvents: (b) MeOH, (c) Isopropanol, (d) MeOH/ DCM (50:50 vol-%). To all mixtures, DMAc (24 vol-%) was added. After a capping and an Fmoc-deprotection step, the amines were stained with DyLight 680-NHS. Contrast and brightness were adjusted.

For the array incubated with MeOH as the solvent, the background is very intense (see Figure 33 b); therefore the mixture was not investigated further. For the other two mixtures (see Figure 33 c, d) background and intensities are comparable, the background is still high for both, but not interfering with the spots too much. For further experiments the MeOH/ DCM mixture was preferred, as the DCM was expected to have better swelling properties of the synthesis film compared to isopropanol.

As the capping step, during array production, is usually only performed for a short period of time, it was tested if the background could be lowered by doing an overnight capping step, prior to the U-4CR. As a consequence, the background signal should only be high, if it was caused by reaction of the dye with amines on the surface still present due to an incomplete capping during array production. This additional capping did not reduce the background.

To prove the effectiveness of the capping step and to rule out unspecific intercalation of the Fmoc-ß-Ala-OH, an additional control experiment was performed, where the side chain deprotected array was incubated with the Fmoc-ß-Ala-OH without the isocyanide and the aldehyde component. Here, no significant fluorescent signals could be detected, strongly indicating that the U-4CR reaction took place and that the stained ß-Ala was covalently bound to the synthesis film and not just physisorbed. The background signals are probably caused by unspecific intercalation of the dye into the PEGMA-co-MMA synthesis film, which cannot be fully avoided.

After successfully proving that the U-4CR could be used on peptide arrays, the aldehyde and the isocyanide component were varied in further investigations.

4.2. Side-chain modification with the U-4CR with various aldehydes and isocyanides

Different combinations of aldehydes and isocyanides were investigated. All reactions were performed with Fmoc-ß-Ala-OH as the carboxylic acid component and in a solution of DMAc/ MeOH/ DCM (24:38:38 vol-%). As the aldehyde component either hexanal or isovaleraldehyde and as the isocyanide component either *tert*-butyl isocyanide, cyclohexyl isocyanide or benzyl isocyanide were used, resulting in six different surface modification possibilities (see Figure 34)
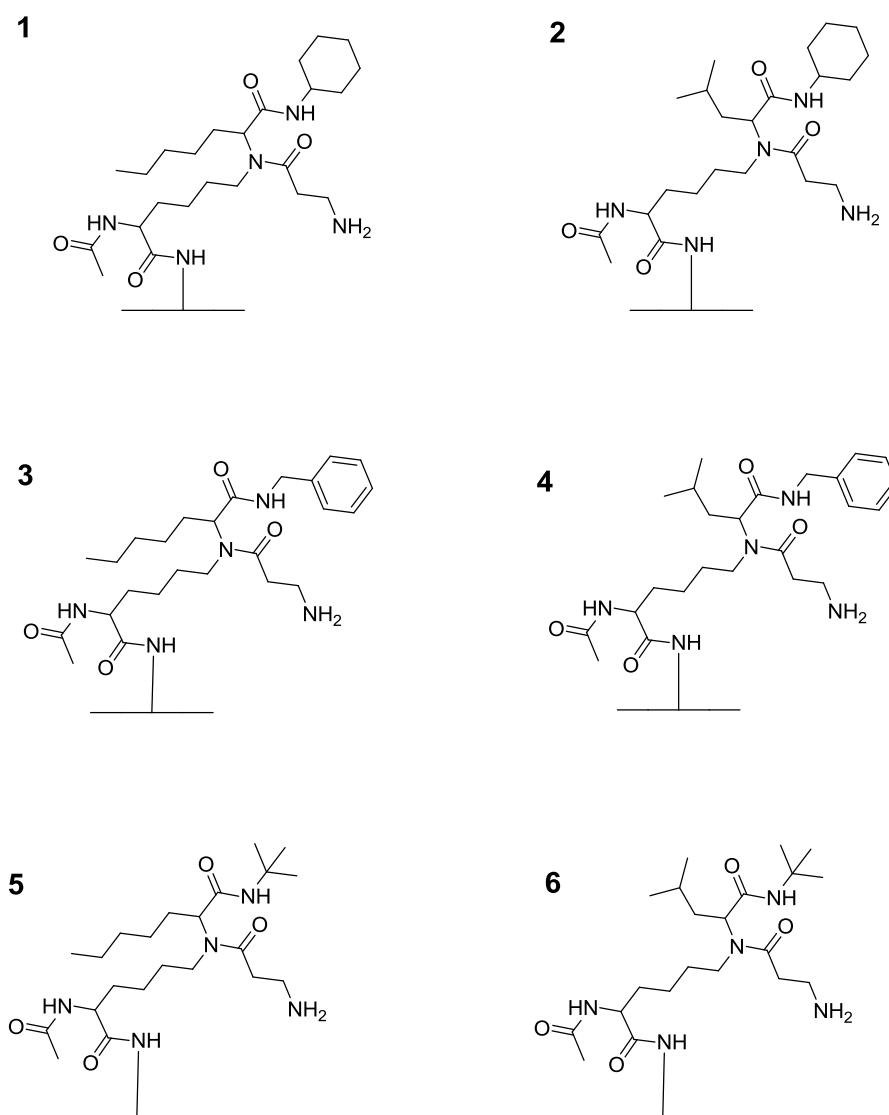
Figure 34: Products of the aldehyde and isocyanide variation experiments, all with the amino component from a side chain deprotected lysine bound to the array and with Fmoc-β-Ala-OH as the carboxylic acid, the aldehyde and the isocyanide component were varied: (1) hexanal and cyclohexyl isocyanide, (2) isovaleraldehyde and cyclohexyl isocyanide, (3) hexanal and benzyl isocyanide, (4) isovaleraldehyde and benzyl isocyanide, (5) hexanal and *tert*-butyl isocyanide, (6) isovaleraldehyde and *tert*-butyl isocyanide.

The arrays (schematically illustrated in Figure 33 a) with alternating lysine and glycine spots were side chain deprotected and then incubated with the different solutions to obtain different U-4CR products (see Figure 34). After an overnight capping step, the slides were Fmoc-deprotected and stained with DyLight 680-NHS (see Scheme 16 for schematic illustration of the synthesis steps). The slides were scanned and the mean of the grey value of the fluorescent signal over all spots was calculated (see Figure 35 a, b). For each spot, a background spot was analyzed in the same way (see Figure 35 a, b).

a

b
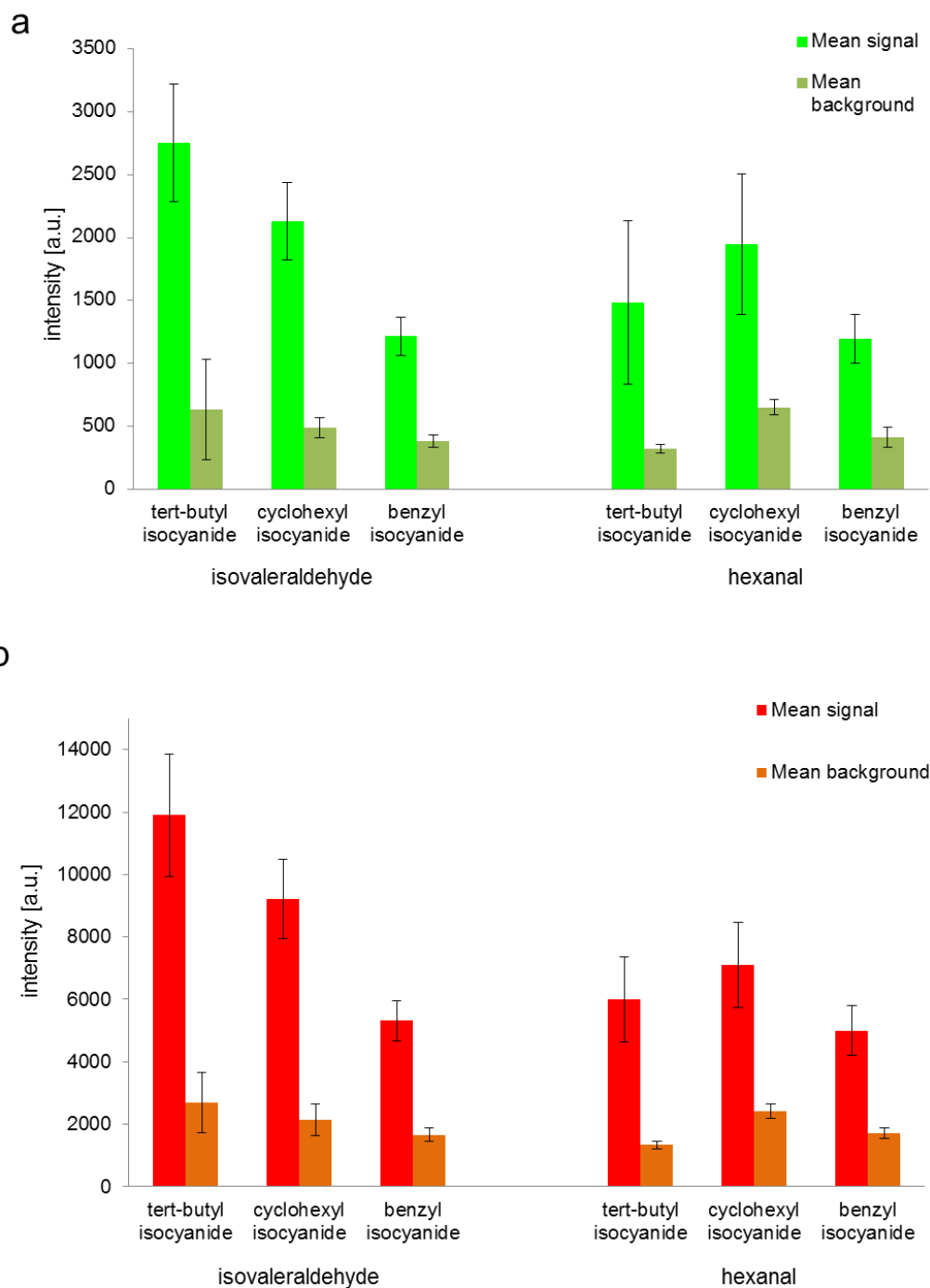
Figure 35: Plotted means of the determined grey values of the spots and the corresponding background spots for the U-4CR products between Fmoc-β-Ala-OH and different combinations of aldehydes and isocyanides. The amino group was generated by side chain deprotection of Ac-Lys(Boc), which was bound to the PEGMA-co-MMA surface. After capping and Fmoc-deprotection, the arrays were stained with DyLight 680-NHS and scanned in the Odyssey scanner at (a) intensity 5, (b) intensity 7, both with resolution 21 μm. For all, the grey values of each spot on the array (between 96 and 248 spots as the size of the arrays varied due to the shape of the slide) were determined and a corresponding background spot was analyzed.

The slides were scanned at different intensities, because to previous experience some artifacts can occur very rarely at certain intensities, due to unknown reasons. For both scan intensities the trends were the same, also the fluorescent signal was significantly higher than the background, which indicated that the U-4CR took place for all combinations (see Figure 35).

The highest intensities, in both scans, were obtained from the combination of *tert*-butyl isocyanide with isovaleraldehyde. For the other combinations lower intensities were observed, probably less product was formed due to steric hindrance. Remarkably benzyl isocyanide gave the lowest intensities and therefore lowest coupling yields. As the benzyl isocyanide is rather unstable, it might have degraded quickly, which was undesirable for the long reaction time of four days. Nevertheless, all investigated combinations showed a successful U-4CR on the peptide arrays.

The grey values of the fluorescent signal (intensity 5) for three representative spots of each array were also plotted as fluorescence height-intensity maps (see Figure 36) to investigate if the spots excel the background and if the rectangular shape of the print pattern was preserved.
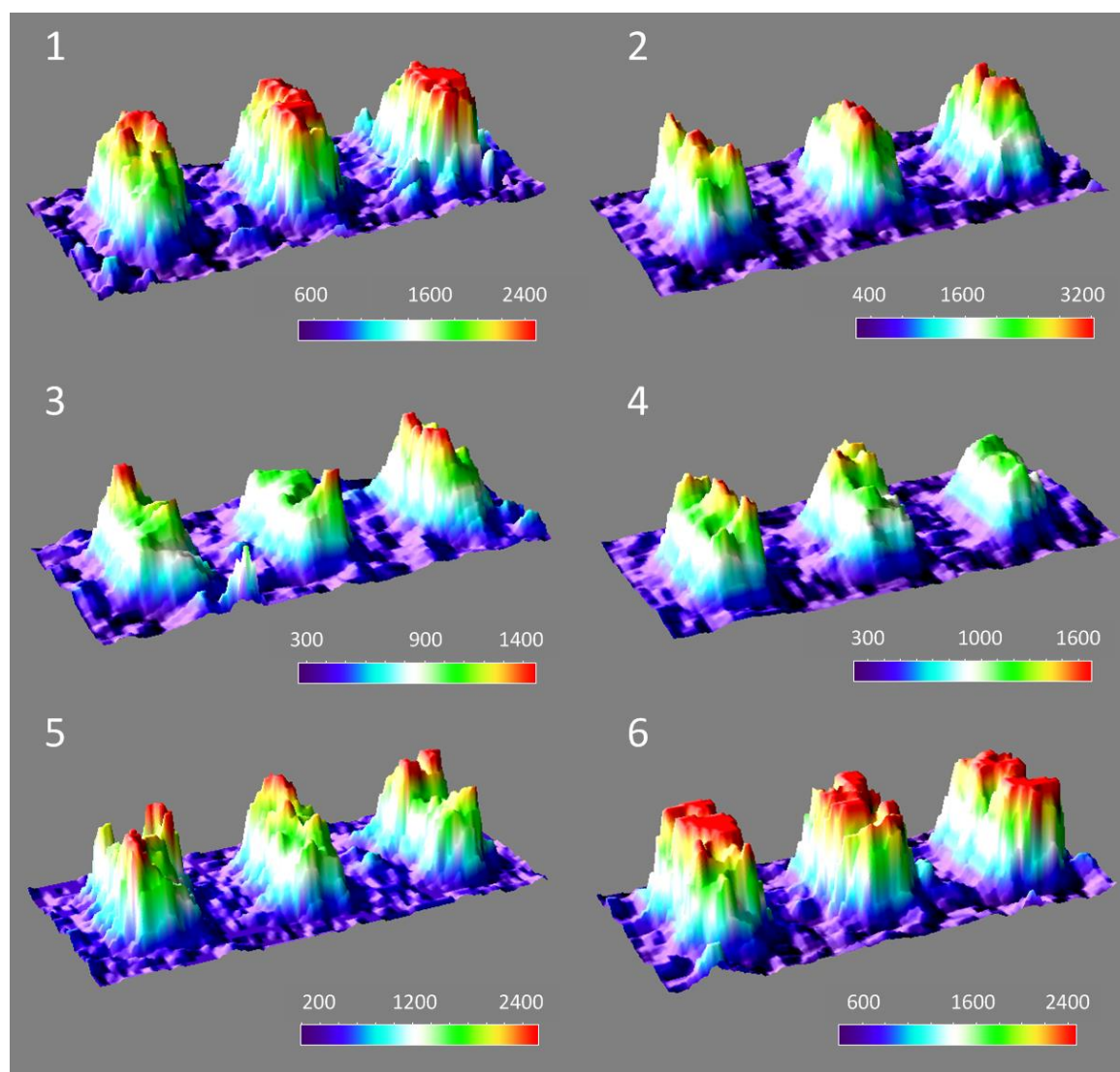
Figure 36: Height-intensity maps of the fluorescent signal for three exemplary spots of the U-4CR products between a side chain deprotected Ac-Lys, Fmoc-β-Ala-OH and different isocyanides and aldehydes: (1) cyclohexyl isocyanide and hexanal; (2) cyclohexyl isocyanide and isovaleraldehyde; (3) benzyl isocyanide and hexanal; (4) benzyl isocyanide and isovaleraldehyde; (5) *tert*-butyl isocyanide and hexanal; (6) *tert*-butyl isocyanide and isovaleraldehyde. All were stained with DyLight 680-NHS after an Fmoc-deprotection step and scanned at intensity 5. The grey values obtained from the scan were used as base for the 3D-models.

The spots could clearly be distinguished from the background in the expected rectangular shape. The same trends could be observed for the fluorescence intensity maps (see Figure 36) as from the means determined from all spots (see Figure 35) even though three spots have far less statistical power than the mean over all spots.

In the literature, improved yields and coupling speed of an U-4CR is reported by performing the reaction under microwave conditions.[121] For cellulose macroarrays this has already been shown.[59,60] For the microarrays functionalization with the U-4CR, this might be an interesting option as for now the reaction time is very long with four days,

which is not desirable when many different combinations need to be investigated. Still, investigation of the compatibility of the microwave reaction conditions with the polymeric synthesis film of the microarray are required. When performing the U-4CR for side chain functionalization, it has to be taken into account that functional side groups that carry functionalities that can participate in an U-4CR need to be protected orthogonally.

4.3. Mass determination of the U-4CR product

Until this point, the success of the U-4CR was only determined by fluorescent staining. Therefore, MALDI-ToF mass spectrometry was used to verify the presence of the U-4CR products on the surface.

As the analysis of a complete complex molecule is challenging with surface analysis techniques, the detachment of the product and subsequent analysis with mass spectrometry has been described in literature as a good alternative to prove that the complete, aimed for molecule is present on the surface.[42,45,46]

The surface has to be functionalized planar, not in spots to ensure that enough product is synthesized on the surface for the MALDI-ToF analysis. A PEGMA-co-MMA surface, carrying one Fmoc-β-Ala-OH, was deprotected and subsequently functionalized with an Fmoc-Rink amide linker (see Scheme 17). The slides were covered overnight with a DMF solution containing the Fmoc-Rink-amide-linker, DIC and pentafluorophenol.[45] After a capping and an Fmoc-deprotection step, the slides were functionalized with Fmoc-ß-Ala-OH. After another Fmoc-deprotection, an U-4CR was performed by immersing the slides in a solution of Fmoc-ß-Ala-OH combined with either isovaleraldehyde and *tert*-butyl isocyanide (see Figure 37 a) or hexanal and cyclohexyl isocyanide (see Figure 37 b) in DMAc/ DCM/ MeOH (24:38:38 vol-%). Both solutions were left standing under argon atmosphere for four days.
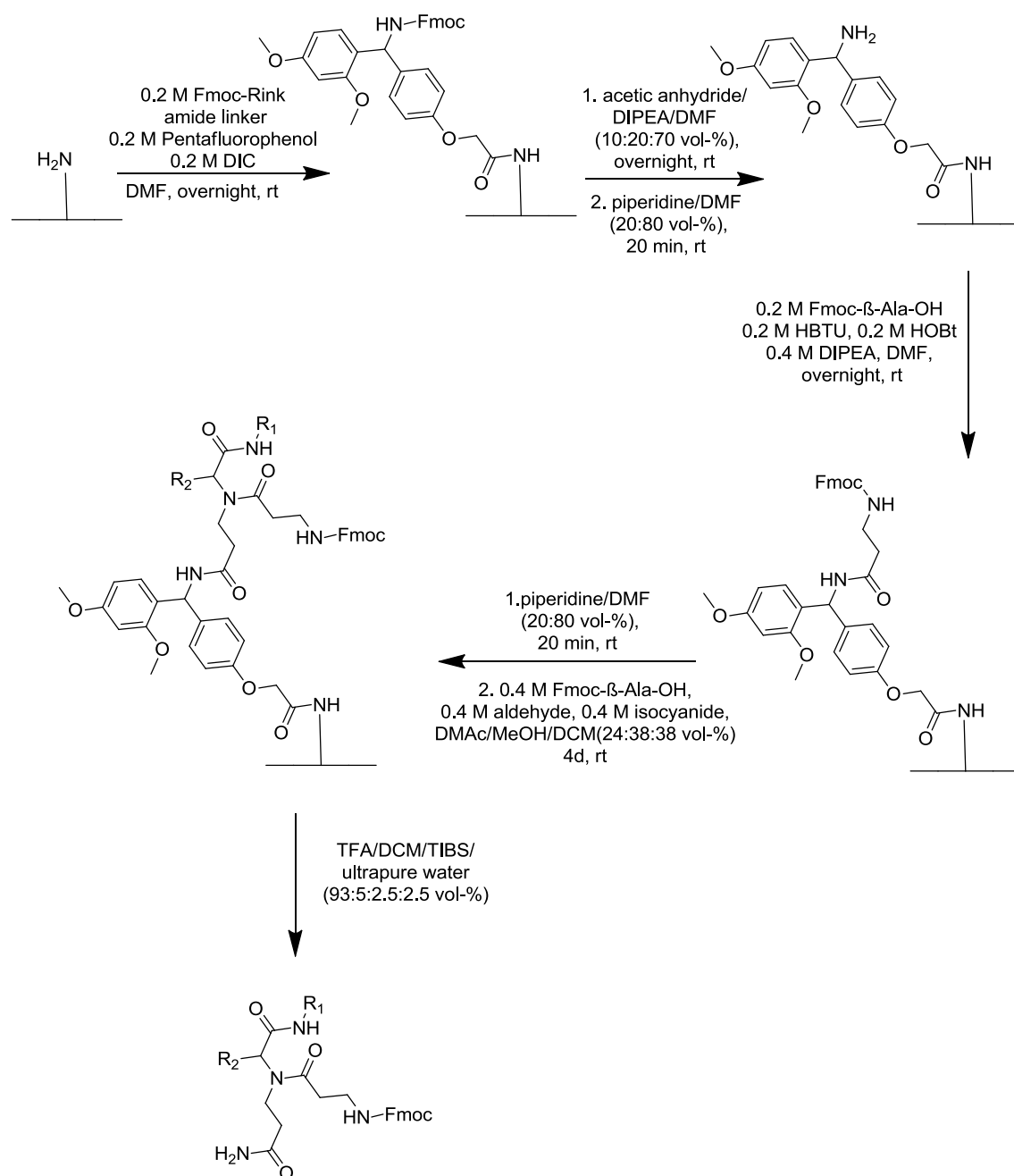
Scheme 17: Schematic illustration of the reaction steps for functionalizing the surface with an Fmoc-Rink amide linker, which then enables acidic detachment of the U-4CR reaction product from the surface.

The U-4CR product was detached from the surface with TFA and the resulting crude product was then analysed by MALDI-ToF. The masses of both products (Figure 37) were found in the respective samples proving that the U-4CR product was successfully synthesized on the surface.
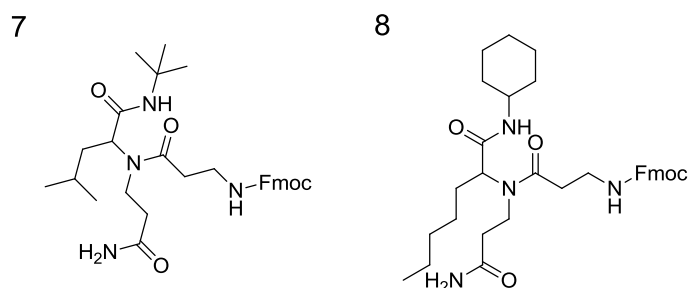
Figure 37: Schematic illustration of the reaction products from the surface functionalized with the Rink-amide linker after detachment. U-4CR with Fmoc-ß-Ala-OH, isovaleraldehyde and *tert*-butyl isocyanide (7) and U-4CR with Fmoc-ß-Ala-OH, hexanal and cyclohexyl isocyanide (8). The amino component was provided by an Fmoc-deprotected ß-Ala, which was coupled to the Rink-amide linker.

Additionally, the synthesis of more sterically demanding U-4CR products was investigated. In this case, instead of a PEGMA-co-MMA surface, a pure PEGMA surface was used, as more functional groups are present. In this way, it should be ensured that enough product was synthesized on the surface, even for reactions with a lower yield to enable the MALDI-ToF analysis. According to the already described reaction scheme (see Scheme 17), Fmoc-β-Ala-OH was used as the carboxylic acid and cyclohexyl isocyanide as the isocyanide component, as the aldehyde either 10-undecenal or bicyclo[2.2.1] hept-5-ene-2-carboxaldehyde was introduced (see Figure 38).
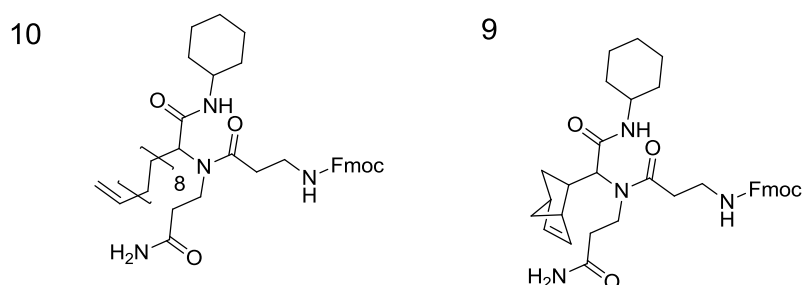
Figure 38: Schematic illustration of the reaction products from the surface functionalized with the Rink-amide linker after detachment. U-4CR with Fmoc-ß-Ala-OH, 10-undecenal and cyclohexyl isocyanide (10) and U-4CR with Fmoc-ß-Ala-OH, bicyclo[2.2.1] hept-5-ene-2-carboxaldehyde and cyclohexyl isocyanide (9). The amino component was provided by an Fmoc-deprotected ß-Ala, which was coupled to the Rink-amide linker.

The two products were detected by MALDI-ToF analysis. This showed that also sterically demanding molecules could be incorporated into the peptide array, which is a necessary requirement when *e.g.* sugars should be incorporated.

4.4. Incorporation of an U-4CR into a growing peptide chain

In the previous sections, the successful side chain functionalization of a peptide on a PEGMA-co-MMA synthesis surface as reaction environment has been shown. For peptidomimectis applications, it is necessary to investigate the incorporation of an U-4CR product into a peptide chain as a preliminary study.

First, it was investigated if the U-4CR product could be used as a base for a peptide chain. A PEGMA-co-MMA slide carrying one Fmoc-ß-Ala was functionalized with two additional ß-alanines to give a three β-Ala spacer. After an Fmoc-deprotection step, the U-4CR was performed using a solution of Fmoc-ß-Ala-OH, hexanal and cyclohexyl isocyanide in a DMAc/ DCM (dry)/ MeOH (dry) (24:38:38 vol-%) solvent mixture. Unreacted amines were capped overnight using the protocol described earlier for the standard Fmoc strategy. After this step, only the amines available for chain continuation were Fmoc-protected U-4CR products, all the unreacted amines had been capped. The slide was then Fmoc-deprotected and structured with the laser-induced forward transfer method described earlier. For the donor slide preparation, Fmoc-Gly-OPfp and resin (10:90 wt-%) were spin-coated onto a polyimide foil covered microscopy glass slide. The slide was baked in the oven under argon atmosphere at 110 °C for 1.5 h to couple the transferred Fmoc-Gly-OPfp to the deprotected Ugi product. After capping, the surface was Fmoc-deprotected and stained with 5-(6)-carboxytetramethylrhodamine *N*-succinimidyl ester (TAMRA-NHS) (see Scheme 18 for illustration of the synthesis pathway).
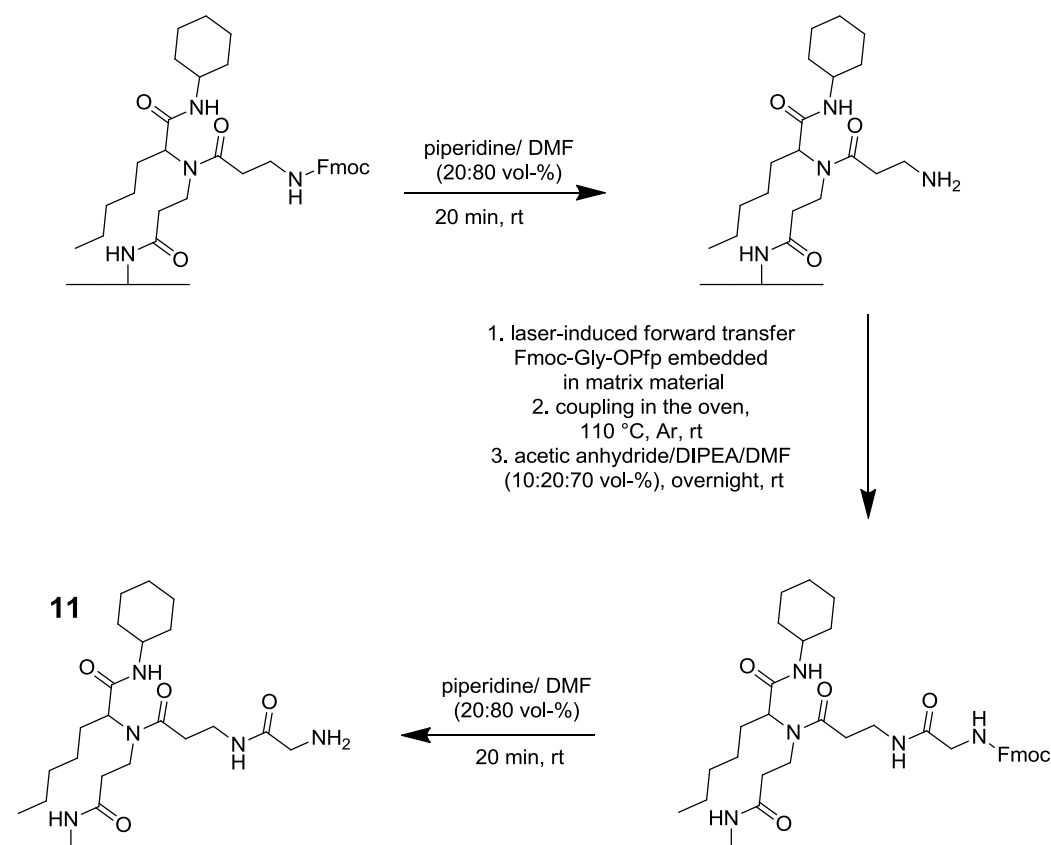
Scheme 18: Schematic illustration of the functionalization of an U-4CR product on a surface with Fmoc-Gly-OPfp by laser-induced forward transfer.

The fluorescently stained slide was then scanned (see Figure 39). The scan showed selective staining only for the completed chain. The U-4CR product is present and was Fmoc deprotected planarly all over the slide, but no staining was visible outside the spots. This indicates that the capping prior to the staining is effective also for the Ugi intermediates and thus all staining in the spots is selective for the complete product. These results proved that the U-4CR could be successfully used as the base of a growing peptide chain.
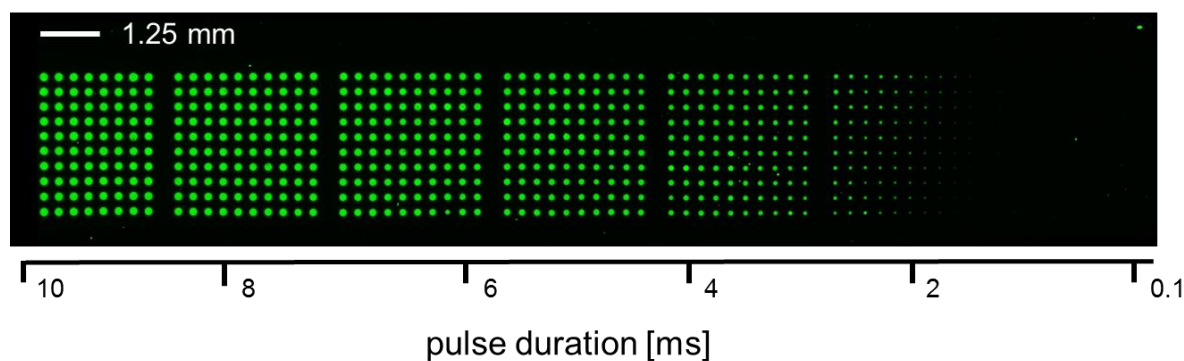
Figure 39: Fluorescence scan of spots at laser parameter variation. Fmoc-Gly-OPfp was transferred to an Fmoc-deprotected PEGMA-co-MMA slide functionalized with an U-4CR between hexanal, cyclohexyl isocyanide and Fmoc-β-Ala on a three β-Ala spacer. The coupling was performed at 110°C for 1.5 h. After capping and an Fmoc-deprotection, the N-terminus was stained with TAMRA-NHS. The slide was scanned in the GenePix Scanner. Contrast and brightness were adjusted.

In the next step it was investigated if an integration of the U-4CR product into a growing peptide chain is possible. Therefore an Fmoc-deprotected PEGMA-co-MMA synthesis slide functionalized with a three β-Ala spacer was functionalized with a solution of Fmoc-Lys(Boc)-OPfp in DMF. After an overnight capping and an Fmoc-deprotection step, the procedure was repeated with Fmoc-Gly-OPfp two times. After Fmoc-deprotection, the slide was then used for an U-4CR with a solution of Fmoc-ß-Ala-OH, hexanal and cyclohexyl isocyanide in a DMAc/ DCM (dry)/ MeOH (dry) (24:38:38 vol-%) solvent mixture for four days under argon atmosphere. After an overnight capping step the slide was structured by laser-induced forward transfer with the same donor slide and parameters as for the experiment described before. The slide was baked in the oven under argon atmosphere for 1.5 h at 90 °C. After washing, overnight capping and an Fmoc-deprotection, the slide was stained with TAMRA-NHS and scanned with a fluorescence scanner (see Figure 40). This incorporation was successful as well. The grey values were lower compared to the experiments where the U-4CR was used as the base of the peptide chain, but this was expected as the slide was functionalized with a spacer and a small tripeptide. The functionalization of each step is not going to full completion and therefore the concentration of functional groups on the surface drops with each additional amino acid in the peptide chain. All in all the U-4CR could be integrated into a peptide chain and is therefore a good candidate for further studies on the synthesis of peptidomimetics on microarrays.
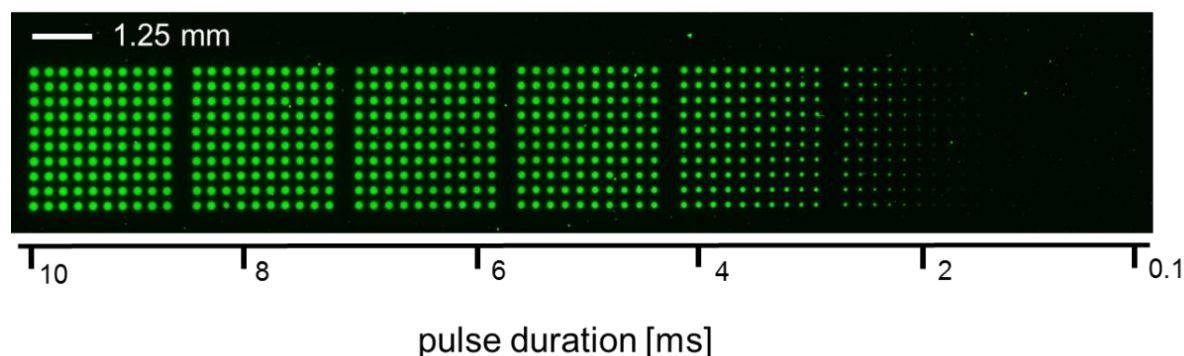
Figure 40: Fluorescence scan of spots at laser parameter variation. To an Fmoc-deprotected PEGMA-co-MMA slide functionalized with a spacer consisting of three β-Ala and Gly-Gly-Lys(Boc), further functionalized with an U-4CR of hexanal, cyclohexyl isocyanide and Fmoc-β-Ala, Fmoc-Gly-OPfp was transferred and coupled at 90°C. After an Fmoc-deprotection, the N-terminus was stained with TAMRA-NHS. The slide was scanned in the GenePix Scanner. Contrast and brightness were adjusted.

The slides stained with TAMRA-NHS showed less background fluorescence than the ones stained with DyLight 680-NHS. From earlier experiments it is known that DyLight interacts more with the synthesis film and therefore intercalates stronger in an unspecific fashion. Due to scanner limitations on the slide dimensions of the GenePix scanner, the array samples had to be scanned in the Odyssey scanner, which is not compatible with the excitation wavelength of TAMRA and therefore DyLight 680 had to be used.

4.5. Combinatorial U-4CR from 'solid' solvents in combination with laser-induced forward transfer

In all experiments until this point, the U-4CR was performed on arrays in solution. To achieve combinatorial freedom, it would be necessary to be able to perform different U-4CRs in different spots at the same time.

Various donor slides were thus prepared with p(DMAA) (**P3**) as the matrix material. One donor was prepared with Fmoc-Gly-OH and a second donor with 4-methoxyphenyl isocyanide and Boc-L-alaninal. The isocyanide and the aldehyde were chosen as they are solids, which is preferable for the donor slide preparation. For the lasing process, Fmoc-deprotected PEGMA-co-MMA synthesis slides with one Fmoc-β-Ala were used as acceptor slides. One acceptor was structured only with Fmoc-Gly-OH, as control experiment (see Figure 41 a). Then, one acceptor was functionalized by lasing first the donor containing the 4-methoxyphenyl isocyanide and Boc-L-alaninal, followed by lasing spots of the donor containing Fmoc-Gly-OH on top of the first layer (see Figure 41 b). This was also performed using the donor slide Fmoc-Gly-OH followed by the donor slide with 4-methoxyphenyl isocyanide and Boc-L-alaninal (see Figure 41 c).
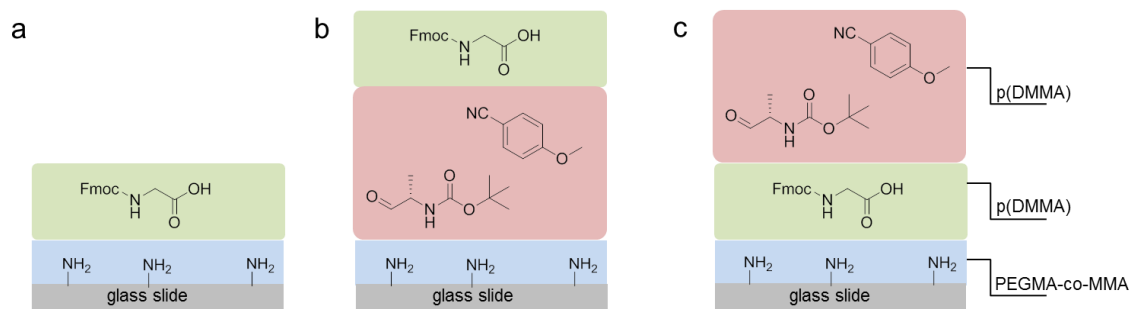
Figure 41: Scheme of the different layers deposited by laser-induced forward transfer. (a) Control containing only one layer of Fmoc-Gly-OH in p(DMAA) (P3); (b) 4-methoxyphenyl isocyanide and Boc-L-alaninal in p(DMAA) (P3) topped with Fmoc-Gly-OH in p(DMAA) (P3) (c) Fmoc-Gly-OH in p(DMAA) (P3) topped with 4-methoxyphenyl isocyanide and Boc-L-alaninal in p(DMAA) (P3).

The slides were baked in the oven at 110 °C for three hours under argon atmosphere. After a capping step and an Fmoc-deprotection step, the slides were scanned. Here, the signal of the control spots was about the same as for the spots were the U-4CR should have taken place. There could be several reasons why the functionalization was not successful. The matrix material was not suitable for the reaction and needs to be replaced. Another reason could be that the lasing step destroys the isocyanide and therefore one component is missing and the reaction cannot take place anymore. Additionally, it has to be investigated why the Fmoc-Gly-OH does intercalate unspecifically into the synthesis film and how it can be removed *e.g.* by improving the washing protocol.

4.6. Conclusions

The U-4CR could be successfully performed on arrays on PEGMA-co-MMA synthesis slides. Different side chain post-modification combinations could successfully be achieved by varying the aldehyde and the isocyanide component.

MALDI-ToF measurements clearly showed that the U-4CR product is present on the surface and successfully formed.

It was also possible to incorporate the product of an U-4CR into a growing peptide chain on the array and subsequently continue chain elongation by the combinatorial laser-induced forward transfer method.

The U-4CR from the 'solid' solvent approach with p(DMAA) as the matrix material was not successful and needs further investigation.

All in all, the U-4CR is a promising reaction for post-modification of side chains of peptide immobilized on a PEGMA-co-MMA synthesis surface. Furthermore, the U-4CR product could be successfully incorporated into a peptide chain which makes it a good candidate reaction for the synthesis of peptidomimetics on the array.

4.7. Outlook

It was clearly shown that peptide arrays with various post-synthesis side chain modifications can be produced *via* the U-4CR. Thereby, *e.g.* sugar molecules might be added to the side chains or sterically demanding side groups. However, investigations with antibodies that specifically bind such molecules still must be performed to prove that point. Especially, the amino acids in proximity to the U-4CR product could be varied to investigate the possible influence of the changes in the peptide chain around the U-4CR product. As indeed with different aldehyde and isocyanide components a successful U-4CR was performed, the incorporation of further components should proceed easily. Moreover, a shorter reaction time of less than four days could be investigated by performing the reaction under microwave conditions.

Furthermore, it was clearly shown that the U-4CR product can be integrated into a growing peptide chain. This finding should open possibilities to the synthesis of peptidomimetics with special conformations on the array.

However, up to now, the 'solid' solvent approach gave disappointing results. It is not yet clear whether this was due to a decomposed isocyanide component or due to the unsuitability of the matrix material. To synthesize truly combinatorial arrays, however, it is necessary to have different Ugi products in different spots of one layer. This could be achieved by investigating the possibilities of the stacking method of the laser-induced forward transfer further, by using a polyimide layer that absorbs all the light to protect light-sensitive components from laser-induced decay. Another option would be to surround the small spots – where the synthesis takes place – with a material that blocks lateral diffusion. Then the reaction in the 'solid'matrix material could be promoted by a saturated atmosphere of an additional solvent such as DCM or MeOH, maybe even in combination with the microwave-assisted approach.

Another alternative might be to switch to the lithographic approach, where the coupling steps take place in solution, albeit only for one selected reaction at the time.

5. Surface structuring in z-direction by molecular layer deposition

The first two chapters focused on surface functionalization in the field of peptide arrays, which are structured in the xy-direction and belong to the area of bio-materials. In this chapter, structuring in z-direction is addressed. The structuring is achieved by successive covalent linking of bifunctional molecules to set up a multilayer and multifunctional, hierarchical surface structure. To achieve this, the formation of dense self-assembled monolayers (SAMs) is necessary. Generally, Thiol-X chemistry is known to be a versatile tool for establishing functional monolayers or for the chemical modification of existing monolayers under mild conditions by photoinitiation. Dithiols in combination with dienes have been reported to be useful for a multi-layer system with alternating layers of thiol and diene,[86] but here the bifunctional molecules used were either aliphatic or benzylic and thus very nonpolar. If thiols and dienes with different chemical properties, e.g. of a certain polarity, would be used this could enable tuning of the properties inside a specific layer. Chemically differently modified layers can for instance limit permeability to polar solvents, although still maintaining an effectively polar surface. Another possibility is the protecting of base materials from aggressive reagents, while keeping a catalytic agent at the interface. To achieve well-defined layers it is of special importance that each layer shows a high grafting density, so no mix-up between the layers can take place. To achieve this, a precise characterization of each layer in terms of density and grafting is crucial.[††]

5.1. Substitution on a bromine terminated surface

In a first step, a silicon wafer was functionalized with 11-bromoundecyltrimethoxysilane. Then, a substitution reaction was planned with tetra(ethylene glycol) dithiol (see Scheme 19), where the bromine group should act as a marker atom for surface analysis by ToF-SIMS and XPS. If the bromine signal intensity drops or nearly disappears, this strongly indicates that the thiol acted as a nucleophile and the targeted nucleophilic substitution was successful.
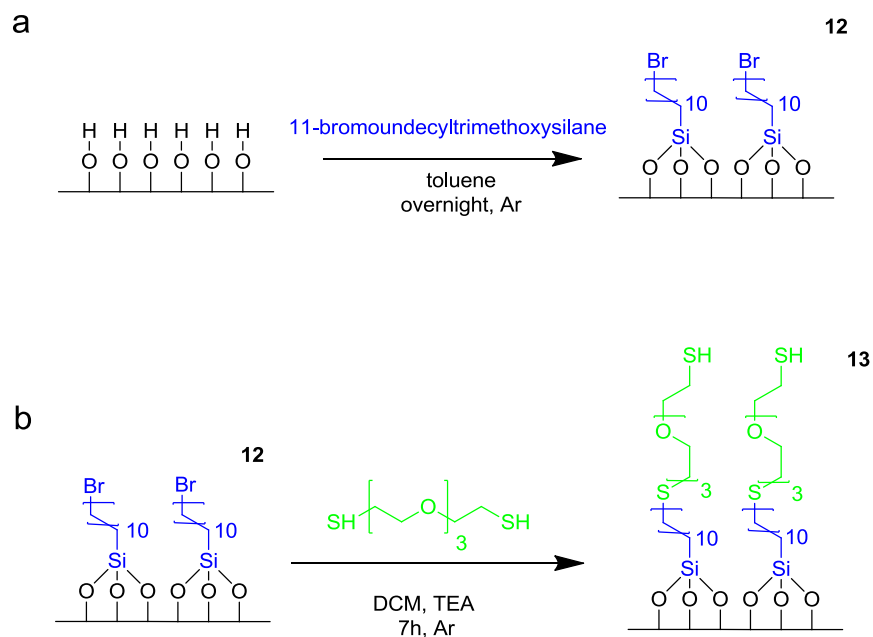
Scheme 19: Functionalization of a silicon wafer substrate with (a) 11-bromoundecyltrimethoxysilane and (b) subsequent substitution reaction with tetra(ethylene glycol) dithiol

The cleaned wafer pieces were immersed in a solution of 11-bromoundecyltrimethoxysilane in toluene overnight. After washing steps with toluene, acetone and ethanol (EtOH), one wafer piece was further functionalized *via* a substitution reaction with a solution of tetra(ethylene glycol) dithiol/ TEA/ DCM (24:9:67 vol-%). First the samples were analyzed by XPS (see Figure 42).
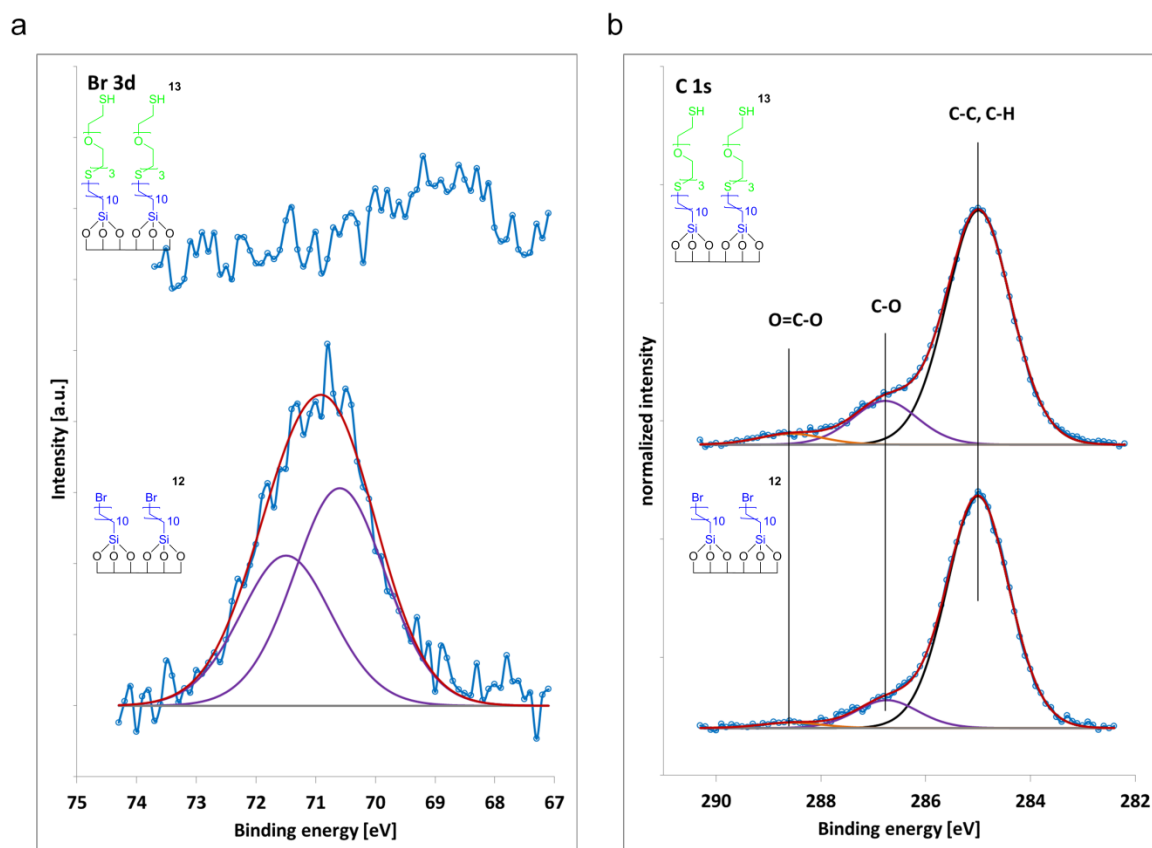
Figure 42: (a) Br 3d and (b) C 1s XPS spectra of a silicon wafer after functionalization with 11-bromoundecyltrimethoxysilane and subsequent substitution reaction with tetra(ethylene glycol) dithiol. The signals were normalized to the peak with the maximum intensity.

The successful functionalization of the silicon wafer with 11-bromoundecyltrimethoxysilane was proved by the presence of a Br 3d doublet with Br $3d_{5/2}$ at 70.5 eV (see Figure 42 a, bottom) attributed to a bromine bound to a carbon atom.[122]

For the sample on which the substitution reaction was performed, the bromine signal cannot be detected anymore (see Figure 42 a, top), which is expected since the bromine is the leaving group.

In the sample before the substitution of the bromine, the O=C-O and the C-O signal should not be present, the observed signals here are probably due to contaminations. Despite this background signal it can still be seen that the substitution reaction took place as the intensity of the C 1s peak at 286.8 eV attributed to C-O clearly increased (see Figure 42 b).

In a second step, ToF-SIMS measurements (see Figure 43) were performed to verify the results obtained from the XPS experiments (see Figure 42).
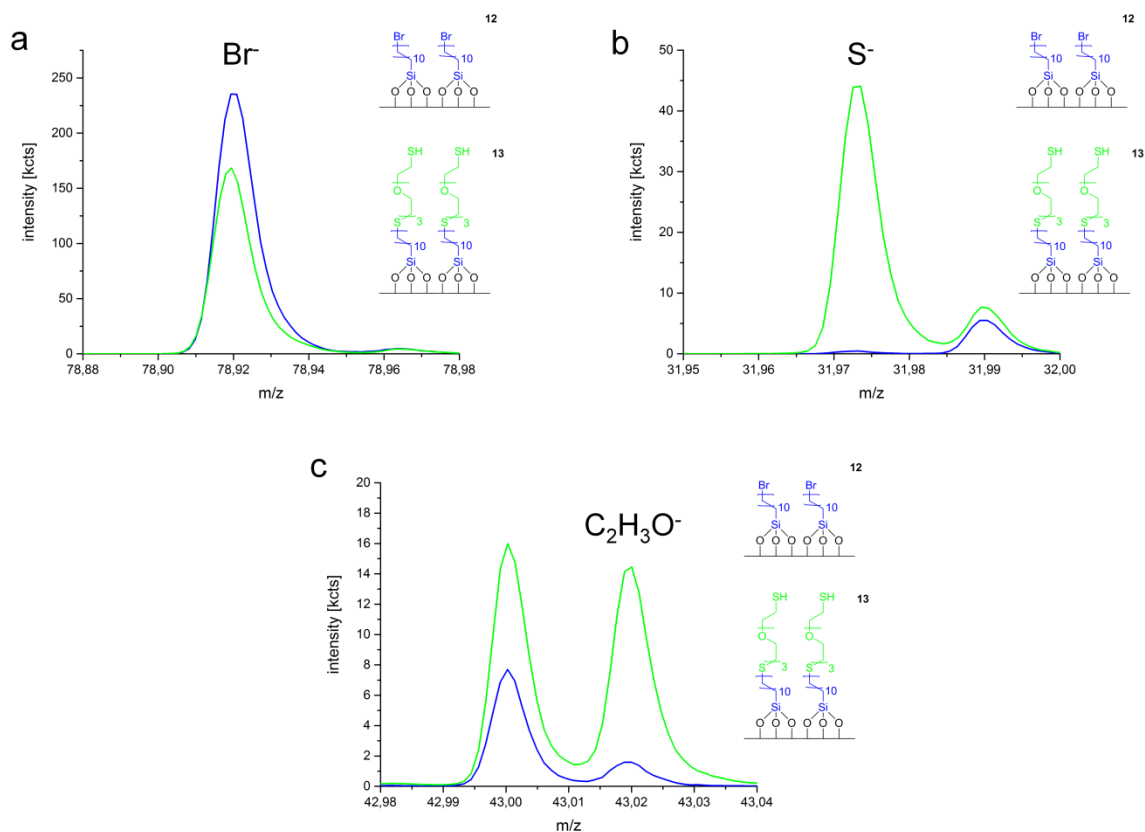
Figure 43: ToF-SIMS measurements (negative polarity) of the functionalization of a silicon wafer substrate with 11–bromoundecyltrimethoxysilane (12) (blue line) and subsequent substitution reaction with tetra(ethylene glycol) dithiol (13) (green line). Comparison of spectra counts of (a) Br$^-$ signal, (b) S$^-$ signal and (c) $C_2H_3O^-$ signal. Data is shown as measured (uncorrected counts, fixed primary ion dose).

The successful functionalization of the silicon wafer with the 11-bromoundecyltrimethoxysilane was confirmed by a bromine signal in the ToF-SIMS measurement. After the substitution reaction with the dithiol, the ToF-SIMS measurements showed a decrease of the bromine signal, but it did not disappear completely (see Figure 43 a). As ToF-SIMS is not a quantitative surface analysis technique,[2,88] the decrease in the bromine signal cannot be quantified. It indicated that the substitution reaction took place, but was probably not driven to completion. It could also be that the bromine was not properly removed from the surface by the washing steps. Literature reports that nucleophilic substitution reactions with bromine terminated alkyl chains bound to a surface are problematic due to their low reactivity.[123] The thiol group of the tetra(ethylene glycol) dithiol could not be shown and quantified by XPS, as the peak lies underneath the plasmon loss structure of the silicon. In the ToF-SIMS measurements, an S$^-$ peak appears after the substitution reaction (see Figure 43 b). Also the signal increase of the $C_2H_3O^-$ fragments (see Figure 43 c) could be detected. Taking all these changes of the mentioned signals into account, this indicates a successful, but

incomplete, substitution reaction. The XPS and the ToF-SIMS results are in good agreement.

The deposition of the second layer looked promising, but attempts to attach a third layer by a Thiol-Ene reaction were inconclusive when the surfaces were analyzed by ToF-SIMS and XPS. Therefore, silanization and second layer deposition were investigated with AFM measurements to verify the height of the monolayers before continuing the stacking process. By height determination, the thickness of the monolayer can be determined and insights can be gained into the grafting density.[124] If the grafting density is low, the height will be lower than the calculated theoretical height, because the chains are not dense enough on the surface to straighten each other up. Instead they collapse onto the surface. Another reason for lower heights than expected might be that the end groups of the bifunctional molecules bend over and react with functional groups on the surface or the layer below.[84] Especially the dithiol can be prone to this, which could explain why it was not possible to attach a third layer.

To determine the exact height of the layers, a special AFM technique called polymer blend lithography (PBL) was used.[125] To prepare the samples, a mixture of polystyrene (PS) and poly(methyl methacrylate) (PMMA) is spin-coated onto a substrate wafer piece. The two materials phase-separate on the surface, where droplets of PS are formed within a PMMA surrounding. The PMMA is then removed by selective washing with acetic acid. Subsequently, the now uncovered parts of the surface are functionalized with 1*H*,1*H*,2*H*,2*H*-perfluorodecyltrichlorosilane (FDTS). In the last step, the PS is removed, leaving behind spots of bare wafer substrate surrounded by FDTS. The empty space can now be functionalized *e.g.* with an organosilane (see Figure 44 for illustration of empty and filled holes).
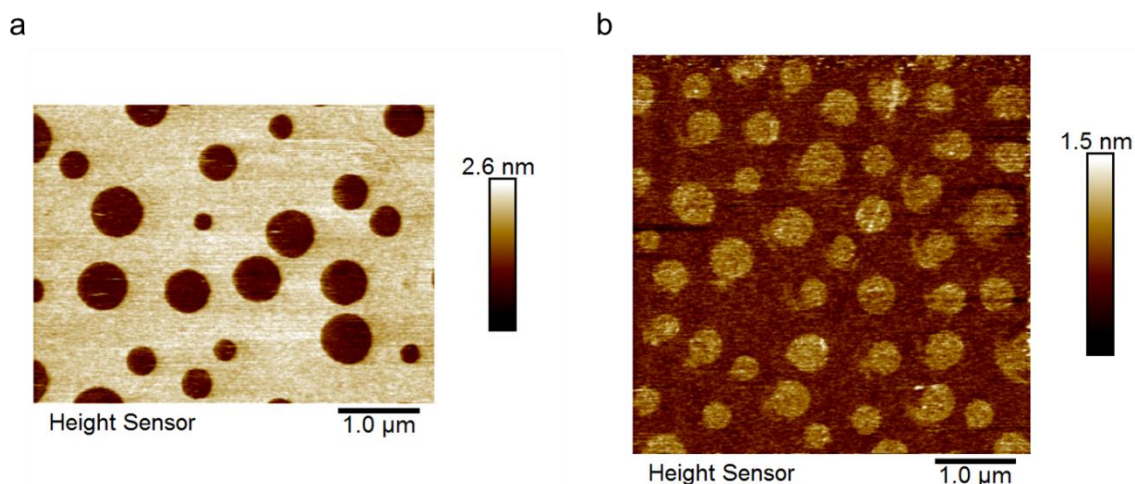
Figure 44: Example of a surface structured with PBL, (a) FDTS as matrix with empty holes, (b) FDTS as matrix, holes functionalized with 10-undecenyltrichlorosilane.

As the exact height of the FDTS is known, the height of the molecules in the holes can be determined. The correct height of the molecular film can be gained by subtraction or addition of the known FDTS height with the measured height in the holes

Wafer pieces nano-patterned by the above procedure were provided by Dr. J. Berson. The freshly prepared wafer pieces were immersed in a solution of 11-bromoundecyltrimethoxysilane in toluene overnight. The expected height would be 1.6 nm, but the measured height was 1.0 nm. This indicated the grafting density was probably not very high and the molecules partially collapsed onto the surface. The substitution reaction was also investigated. Instead of the expected 1.3 nm, the height only increased by 0.3 nm. The reaction was probably not very efficient, leading to a low density of molecules on the surface. Additionally, the molecules might have collapsed on the surface because of the low grafting density. It was tried to add an additional layer, but this was not successful, maybe the bifunctional thiols bend over and react with another functional group of the first layer that an additional layer could not be attached anymore.

5.2. Surface functionalization with different silanes

The success of a silanization reaction depends on various parameters, such as the substrate, the deposition method, thermal curing and the reaction time.[126] Additionally, the length of the alkyl chain influences the silanization result: longer alkyl chains should result in denser and more defined monolayer due to the stronger Van-der-Waals interactions between their chains.[127,128]

As the substitution reaction with the bromine could not be driven to completion and the loss in functional groups was probably too high to add a third layer, different silanes as candidates for the base layer were tested: 10-undecenyltrichlorosilane, allyltrimethoxysilane and 3-mercaptopropyltrimethoxysilane (see Figure 45).
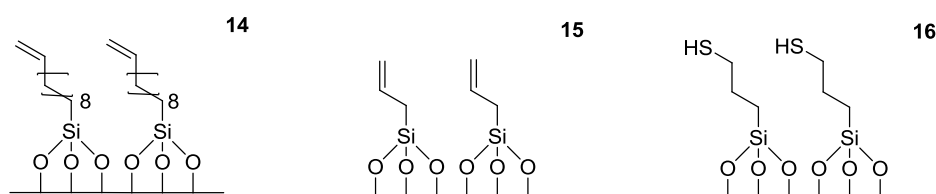
Figure 45: Schematic illustration of a surface functionalized with 10-undecenyltrichlorosilane (14), allyltrimethoxysilane (15) and 3-mercaptopropyltrimethoxysilane (16).

With these molecules, a direct Thiol-Ene reaction on the surface should be possible and the incomplete substitution step could be eliminated.

For the silanization, the wafer pieces were immersed in a solution of the respective silane in toluene under controlled humidity conditions.[129] Then, the samples were analyzed by ToF-SIMS (see Figure 46).
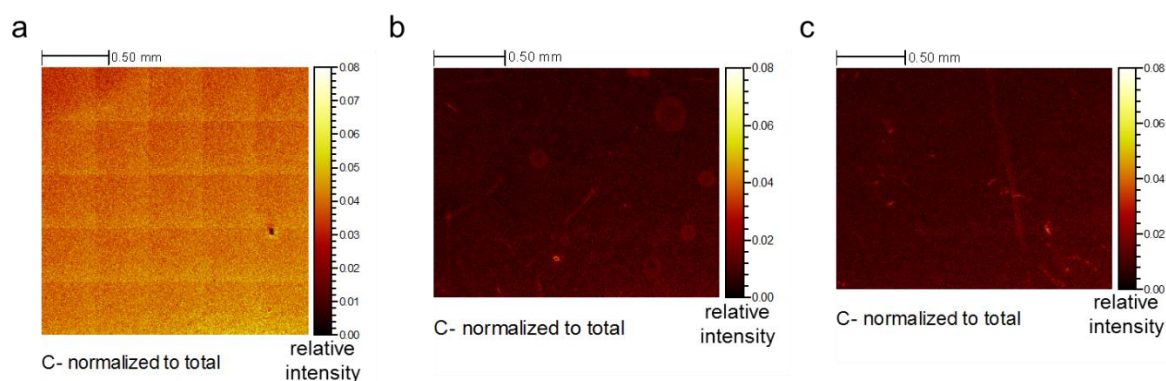
Figure 46: Large stage raster ToF-SIMS surface measurements (negative polarity) of the C⁻ signal after functionalization with (a) 10-undecenyltrichlorosilane (14), (b) 3-mercaptopropyltrimethoxysilane (16) and (c) allyltrimethoxysilane (15). All images are normalized to the total ion intensity. For (b) and (c) slightly smaller areas (2 × 1.6 mm) were measured compared to (a) (2 × 2 mm).

In the 10-undecenyltrichlorosilane sample, the C⁻ signal is uniformly distributed and also the highest relative intensities were measured. For the other two samples, the intensities were very low indicating that almost no carbon is bound to the surface. As the image scans show relative intensities, one explanation could be that these molecules are smaller than the 10-undecenyl and contain less carbon. For the 3-mercaptopropyltrimethoxysilane, also the sulfur signal was investigated and it was also very low. This indicated that the functionalization was not dense and probably no monolayer was formed. As the SAM is directly on top of the bare silicon wafer, a not very dense monolayer should result in a less shielded substrate and therefore still high numbers of Si^+ counts should be detected (see Figure 47).
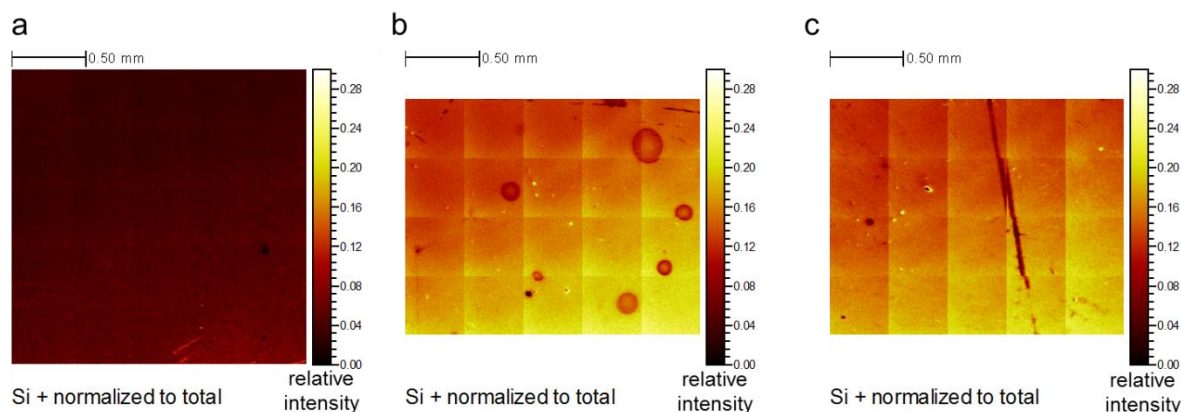
Figure 47: Large stage raster ToF-SIMS surface measurements (positive polarity) of the Si$^+$ signal after functionalization with (a) 10-undecenyltrichlorosilane (14), (b) 3-mercaptopropyltrimethoxysilane (16) and (c) allyltrimethoxysilane (15). All images are normalized to the total ion intensity. For (b) and (c) slightly smaller areas (2 × 1.6 mm) were measured compared to (a) (2 × 2 mm).

The Si$^+$ signal is the weakest (dark color, lower relative intensity) for the wafer functionalized with 10-undecenyltrichlorosilane, indicating a uniform and dense covered surface. For the other two samples, the relative Si$^+$ signal intensity is significantly higher, indicating that the surface was not covered densely. Moreover, inhomogeneities were observed.

Additionally FDTS nano-patterned samples were functionalized in the same way and the height of the formed monolayers was determined by AFM to investigate the density of the formed monolayers.

Table 5: Height measurements of the monolayers obtained with different silanes with AFM

Silane	Theoretical height (nm)	Measured height (nm)
10-undecenyltrichlorosilane	1.4	1.3
3-mercaptopropyltrimethoxysilane	0.5	0
allyltrimethoxysilane	0.4	0.2

Again, the best results were obtained for the 10-undecenyltrichlorosilane as the measured height barely differed from the theoretical height (see Table 5) indicating the formation of a dense monolayer. For the allyltrimethoxysilane, the measured height was half of the theoretical height, indicating that the formed layer was not very dense. This is in accordance with the ToF-SIMS results, where only low intensities were measured.

For the 3-mercaptotrimethoxysilane, no layer formation was observed, which is in accordance with the ToF-SIMS results, where very low counts for carbon and sulfur were measured. A possible improvement of the monolayer formation for the 3-mercaptotrimethoxysilane was investigated by changing the reaction protocol and using the one for the 11-bromoundecyltrimethoxysilane, where the wafer pieces were immersed overnight in a 0.4 M solution. AFM measurements were performed on these samples and showed that large aggregates were formed and not the desired monolayer. This kind of polymerization is described in literature for 3-aminopropyltriethoxysilane (APTES), where the nucleophilic nitrogen attacks the triethoxysilane.[127] As the thiol group also has a nucleophilic nature, it is possible that the aggregates and the thick layers were caused by a similar polymerization of the silane.

With the 10-undecenyltrichlorosilane reaction, the best layers could be achieved. Therefore, for all further experiments this layer was the base layer for the layer system. A possible explanation for the good results might be that the 10-undecenyltrichlorosilane carries the longest alkyl chains. It is known that longer alkyl chains form denser monolayers, because of the stronger Van-der-Waals interactions between the chains, which keep the chains upright perpendicular to the surface and lead to a denser packing.[127]

5.3. Thiol-Ene reactions

The next step in building up a layer system was to investigate whether a Thiol-Ene reaction on the silicon wafer samples functionalized with 10-undecenyl can be executed or not (see Scheme 20). As the layers should be different in their structure and layer properties, 2,2′-(ethylenedioxy)diethanethiol was chosen for the second layer. This molecule was chosen instead of tetra(ethylene glycol) dithiol, because it is shorter and therefore should be less prone to bend over.
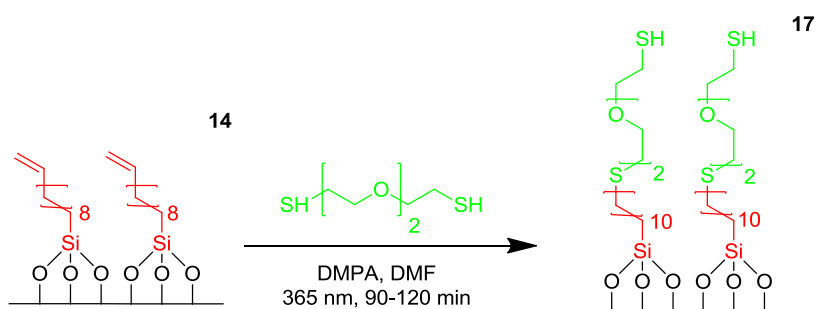
Scheme 20: Thiol-Ene reaction on a 10-undecenyltrichlorosilane functionalized silicon wafer substrate with 2,2′-(ethylenedioxy)diethanethiol.

10-undecenyl terminated silicon wafers were immersed in pure 2,2′-(ethylenedioxy)diethanethiol and a few of drops of DMF were added. Then, the samples were illuminated under a 15 W UV-lamp at a wavelength of 365 nm for different times. It was also tested if addition of the radical initiator 2,2-dimethoxy-2-phenylacetophenone (DMPA) could improve the Thiol-Ene reaction (see Table 6 for reaction conditions).

Table 6: Reaction conditions for the Thiol-ene reactions

Sample	Illumination time (min)	DMPA (mg)
a	120	5
b	120	0
c	90	10

After cleaning in the ultrasonic sound bath, all samples were analyzed with XPS, ToF-SIMS and AFM. Especially the sulfur signal was an important reference signal, as its appearance indicated a successful reaction. In the XPS measurements of the S 2s spectra a signal at 228 eV could be detected for all three samples (see Figure 48). This sulfur binding energy is addressed to a thiol bond (S-C). This signal was not detected on the blank wafer or on the silane functionalized wafer.
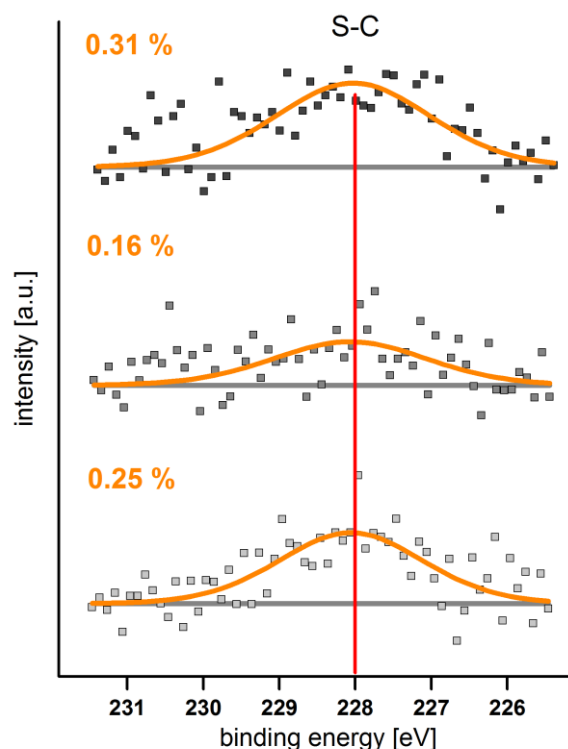
Figure 48: XPS measurements of S 2s spectra after a Thiol-Ene reaction on a 10-undecenyltrichlorosilane functionalized silicon wafer substrate with 2,2′-(ethylenedioxy)diethanethiol. The S 2s spectra was taken instead of the S 2p, as the plasmon features of the silicon substrate overlapped with the small S 2p signals. The reaction was performed under illumination with UV-light (365 nm) under different conditions: (a) reaction with addition of DMPA (5 mg) for 120 min (a); (b) reaction without addition of DMPA for 120 min (b); (c) reaction with addition of DMPA (10 mg) for 90 min (c). All fits were performed to the same boundary conditions and measurements were referenced to the C 1s C-C peak at 285.0 eV. This approach ensures comparability of the measurements.

To compare the XPS measurements all spectra were fitted in the same way. This enables comparison of the signals. The S-C signal is low on all samples with a poor signal to noise ratio. For sample **b**, the signal and the noise are within the same order of magnitude. These results were therefore compared to surface images taken with ToF-SIMS. It was tested whether the differences obtained with XPS could also be seen in the distribution of the sulfur signals in the ToF-SIMS measurement (see Figure 49).
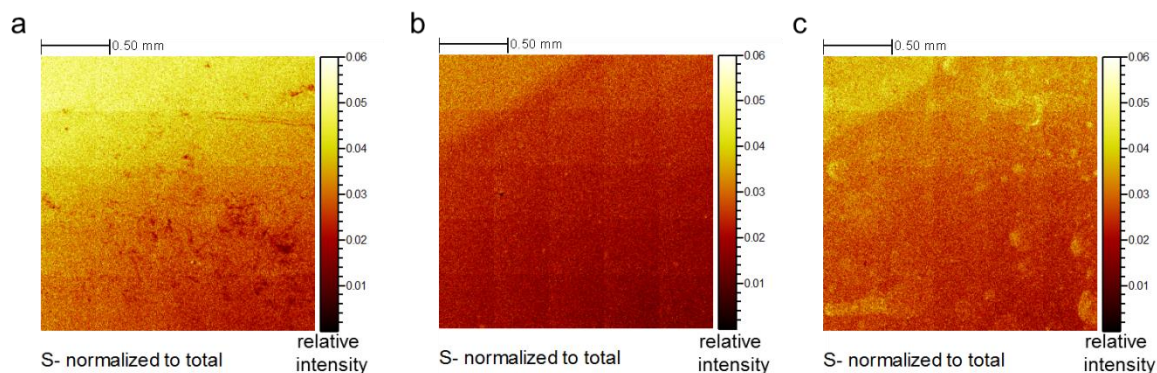
Figure 49: ToF-SIMS measurements (negative polarity) of the S^{-} signal after a Thiol-Ene reaction on a 10-undecenyltrichlorosilane functionalized silicon wafer substrate with 2,2′-(ethylenedioxy)diethanethiol. The reaction was performed under illumination with UV-light (365 nm) under different conditions: (a) reaction with addition of DMPA (5 mg) for 120 min (a); (b) reaction without addition of DMPA for 120 min (b); (c) reaction with addition of DMPA (10 mg) for 90 min (c). All images are normalized to the total ion intensity with the same intensity sale and show an area of 2 ˣ2 mm.

Sulfur was detected on all three samples. The trend that was observed in the XPS results could also be found in the ToF-SIMS measurements. The lowest amount of sulfur is present in sample **b**, where no DMPA initiator was used. The other two samples differ less in the sulfur concentration, but in sample **a**, the overall intensity distribution is higher than in sample **c**.

To investigate the grafting density, the change in height for the different Thiol-Ene reaction conditions was measured by AFM. FDTS nano-patterned wafer pieces functionalized with 10-undecenyltrichlorosilane were used to perform Thiol-Ene reactions and afterwards analysed by AFM to determine the height increase by addition of the next layer (see Table 7).

Table 7: Results of layer height determination after Thiol-Ene reaction under different reaction conditions on a 10-undecenyl terminated FDTS patterned wafer pieces.

Reaction conditions	Theoretical height (nm)	Measured height (nm)
a	1.3	0.7
b	1.3	0.6
c	1.3	0.5

For all samples, the measured height was lower than the theoretical height. The highest increase in height was observed for method **a**, which was also the most promising method according to the XPS and ToF-SIMS results. For the other two methods, in the

height increased more for method **b** than for method **c**, whereas in the ToF-SIMS and XPS results method **c** looked more promising than method **c**.

As the FDTS nano-patterned wafers show a different surface structure than the flat wafers, it might be that the differences of height and signal intensity occur due to the different surface geometries.

Overall the differences in height increase were minimal and only half or less than the theoretical value, indicating that the grafting density was not sufficient for the molecules to straighten up. It could be that the molecules are still too long and bend over so that they react with both functional sides with the surface, which is described in literature as a major problem for longer flexible molecules.[86]

5.4. Conclusion

The goal was to establish a system, which would allow for structural control and control over chemical and physical properties in z-direction by covalent layer-by-layer deposition of bifunctional molecules *via* Thiol-Ene chemistry. Therefore, a base layer has to be established, which is covalently bound to the synthesis surface, a silicon wafer.

First, a functionalization with 11-bromoundecyltrimethoxysilane followed by a substitution reaction with tetra(ethylene glycol) dithiol was investigated. A complete substitution could not be achieved, probably due to the low reactivity of bromine terminated alkyl chains functionalized surfaces. Therefore, this approach was discarded.

In the second approach, different silanes were compared to functionalize either with an alkene or a thiol. The 3-mercaptosilane either polymerized instead of forming a SAM or the grafting density was very low. From the two alkene terminated silanes, the longest, 10-undecenyltrichlorosilane, gave the best surface coverage and highest grafting density according to ToF-SIMS and AFM experiments. Therefore, it was decided to continue with this molecule as the base for the first Thiol-Ene reaction with 2,2′-(ethylenedioxy)diethanethiol. Different reaction conditions for Thiol-Ene chemistry were investigated with XPS, ToF-SIMS and AFM. Here, a second layer could be added to the first, but the height of the second layer was lower than expected. This might be due to bending over of the molecules and needs further investigations or the use of a more rigid molecule.

In summary, 10-undecenyltrichlorosilane is a very promising base layer for the overall layer system. The addition of the second layer was proven to be possible. Furthermore, a thorough characterization procedure with the combination of ToF-SIMS, XPS and height determination of the layers by AFM has been established, which is suitable for future investigation when additional layers are added.

5.5. Outlook

The reaction conditions of the Thiol-Ene reaction need further optimization. Maybe it is advisable to take even shorter and stiffer molecules to eliminate the bending over of molecules and the resulting loss of active groups. Another solution might be a protection strategy, where one side of the bifunctional molecule is protected followed by a subsequent deprotection step prior to addition of the next layer.

The most important step is to add more layers and start to build up the layered system. Loss of functional groups due to incomplete functionalization might be compensated by performing Thiol-Yne reactions instead of Thiol-Ene.

6. Materials and methods

6.1. Materials

Chemicals and solvents from the following suppliers were used: all amino acids and amino acid derivatives from Iris Biotech (Marktredwitz/ Germany); resin (S-LEC-P LT 7552) from Sekisui Chemical Co. Ltd. (Osaka/ Japan); silanes from acbr GmbH (Karlsruhe/ Germany); Cu(I)Cl and dry MeOH from Alfa Aeser (Karlsruhe/ Germany); linear p(DMAA) from Polymer Source Inc. (Dorval/ Canada); DCM, DIPEA, DMF, MeOH and piperidine from Merck (Darmstadt / Germany); Blocking Buffer for Fluorescent Western Blotting – MB-070 from Rockland (Gilbertsville/ USA); all residual chemicals and solvents from Sigma Aldrich Chemie GmbH (Steinheim/ Germany). All used solvents were of analytical purity grade.

Benzyl isocyanide was provided by Rebecca Seim (Institute of Organic Chemistry, KIT, Karlsruhe/ Germany).

DCM (dry) and DMF (dry) were stored above 4 Å molar sieve.

Before ATRP polymerization, all monomers were passed over a short basic alumina oxide column to remove the inhibitor.

Monoclonal mouse Anti-FLAG M2 antibodies were bought from Sigma Aldrich Chemie GmbH (Steinheim/ Germany). The anti-bodies were labeled fluorescently with NHS-esters or a Lightning-Link® Rapid conjugation kit by Dr. Ralf Bischoff at the German Cancer Research Institute (DKFZ, Heidelberg/ Germany).

All PEGMA-co-MMA synthesis slides, the pure PEGMA slides for the trimer peptide synthesis and the arrays with the alternating lysine and glycine spots were obtained from PEPperPRINT GmbH (Heidelberg/ Germany).

Silicon wafers were bought from Si-Mat Silicon Materials (Kaufering/ Germany).

Dialysis membranes Spectra/Por® 7 MWCO 1000 were bought from Carl Roth GmbH +Co. KG (Karlsruhe/ Germany). Polyimide Kapton foil was bought from CMC Klebetechnik GmbH (Frankenthal/ Germany).

Ultrapure water was produced with a Synergy® Water Purification System equipped with a Synergy Pak 2 from Merck (Darmstadt / Germany).

The wafers used for the AFM experiments with PBL were obtained already nano-patterned with FDTS from Dr. J. Berson (Institute for Nanotechnology, KIT, Karlsruhe/ Germany).

6.2. Polymer synthesis

6.2.1. p(DMAA) (P1-P6)
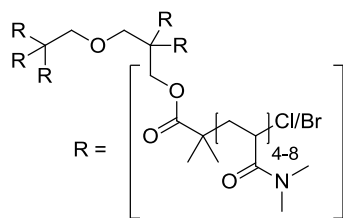
Cu(I)Cl (450 µmol, 45.0 mg, 3.00 eqv.) was added to a Schlenk tube equipped with a stirring bar under argon atmosphere. Dipentaerithritol hexakis (2-bromoisobutyrate) (150 µmol, 172 mg, 1.00 eqv.), Me$_6$Tren (450 µmol, 104 mg, 121 µL, 3.00 eqv.) and toluene (1.50 mL) were added to another Schlenk flask against a stream of argon. The mixture was bubbled through with argon for 5 min. Subsequently the mixture was transferred into the first Schlenk tube by syringe and the resulting mixture was stirred thoroughly for about 10 min. DMAA (7.25 mmol, 720 mg, 750 µL, 48.0 eqv.) and toluene (1.00 mL) were placed in a third Schlenk flask. This mixture was also degassed by bubbling through with argon for 10 min. Subsequently the solution was added to the reaction flask by syringe. The reaction mixture was stirred at room temperature for 24 to 48 h. The reaction was stopped by adding ultrapure water (about 5 mL) and exposing the reaction mixture to the air. The reaction mixture was dialyzed against ultrapure water for one to three days, where the water was exchanged about two times. Finally the remaining solvent was removed by rotary evaporation or by lyophilization.

For **P1** and **P3**, a quadrupled reaction mixture was used. For **P4**, 200 µmol of initiator were used instead of 150 µmol. For **P5** and **P6**, the reaction mixture was doubled.

The products were obtained as white solids in the following yields after purification by dialysis: 2.18 g (62%) (**P1**), 437 mg (50%) (**P2**), 1.15 g (33%) (**P3**), 409 mg (42%) (**P4**), 327 mg (19%) (**P5**), 400 mg (23%) (**P6**).

^{1}H-NMR **P1** (500 MHz, CDCl$_3$) δ: 5.13 (t (br), C*H*Br), 4.13 to 3.68 (m (br), C*H$_2$*-C-O-C=O), 3.35 (s (br), O-C*H$_2$*), 3.15 to 2.74 (m (br), *H* (dimethylacrylamide)), 2.74 to 1.96 (m (br), *H* back bone), 1.96 to 1.15 (m, (br), C*H$_2$* backbone), 1.15 to 0.87 (m (br), O=C-(C*H$_3$*)$_2$) ppm.

^{1}H-NMR **P2** (300 MHz, CDCl$_3$) δ: 5.11 (t (br), 6H, C*H*Br), 4.43 to 3.67 (m (br), 12H, C*H$_2$*-C-O-C=O), 3.35 (s (br), O-C*H$_2$*), 3.27 to 2.78 (m (br), *H* (dimethylacrylamide)), 2.76 to 2.20 (m (br), C*H$_2$* back bone), 2.18 to 1.45 (m, (br), *H* backbone), 1.24 to 0.90 (m (br), O=C-(C*H$_3$*)$_2$) ppm.

^{1}H-NMR **P3** (300 MHz, CDCl$_3$) δ: 5.17 (t (br), C*H*Br), 4.49 to 3.60 (m (br), C*H$_2$*-C-O-C=O), 3.42 (s (br), O-C*H$_2$*), 3.19 to 2.78 (m (br), *H* (dimethylacrylamide)), 2.78 to 2.36 (m (br), C*H$_2$* back bone), 2.34 to 1.39 (m, (br), *H* backbone), 1.19 to 0.97 (m (br), O=C-(C*H$_3$*)$_2$) ppm.

^{1}H-NMR **P4** (300 MHz, CDCl$_3$) δ: 5.11 (t (br), C*H*Br), 4.47 to 3.35 (m (br) C*H$_2$*-C-O-C=O), 3.36 (s (br), O-C*H$_2$*), 3.26 to 2.77 (m (br), *H* (dimethylacrylamide)), 2.77 to 2.19 (m (br), C*H$_2$* back bone), 1.98 to 1.43 (m, (br), *H* backbone), 1.21 to 0.93 (m (br), O=C-(C*H$_3$*)$_2$) ppm.

^{1}H-NMR **P5** (300 MHz, CDCl$_3$) δ: 5.06 (d (br), C*H*Br), 4.36 to 3.87 (m (br), C*H$_2$*-C-O-C=O), 3.34 (s (br), O-C*H$_2$*), 3.19 to 2.77 (m (br), *H* (dimethylacrylamide)), 2.77 to 2.34 (m (br), *H* back bone), 2.34 to 1.43 (m, (br), C*H$_2$* backbone), 1.43 to 0.92 (m (br), O=C-(C*H$_3$*)$_2$) ppm.

^{1}H-NMR **P6** (300 MHz, CDCl$_3$) δ: 5.06 (d (br), C*H*Br), 4.87 to 3.88 (m (br), C*H$_2$*-C-O-C=O), 3.43 (s (br), O-C*H$_2$*), 3.20 to 2.80 (m (br), *H* (dimethylacrylamide)), 2.78 to 2.43 (m (br), *H* back bone), 2.36 to 1.46 (m, (br), C*H$_2$* backbone), 1.36 to 0.96 (m (br), O=C-(C*H$_3$*)$_2$) ppm.

T$_g$: 107.3 °C (**P1**); 107.5 °C (**P2**); 81.1 °C (**P3**); 98.8 °C (**P4**); 104.2 °C (**P5**); 88.5 °C (**P6**)

M$_n$ (SEC): 6300 (**P1**); 6100 (**P2**); 3250 (**P3**); 3850 (**P4**); 6450 (**P5**); 4250 (**P6**)

Đ (SEC): 1.5 (**P1**); 1.3 (**P2**); 1.2 (**P3**); 1.2 (**P4**); 1.3 (**P5**); 1.3 (**P6**)

DP (per arm) (SEC): 8 (**P1**); 8 (**P2**); 4 (**P3**); 5 (**P4**); 8 (**P5**); 5 (**P6**)

DP (per arm) (NMR): 7 (**P1**); 7 (**P2**); 3 (**P3**); 5 (**P4**); 6 (**P5**); 3 (**P6**)

6.2.2. p(DMAA) end group functionalized with 2-methyl-2-propanethiol (P7)
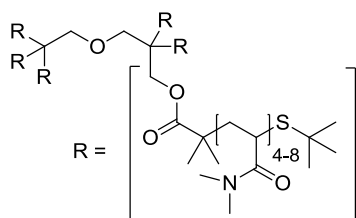
P(DMAA) (**P5**) (47.0 µmol, 50.0 mg, 1.00 eqv.) was dissolved in DCM (dry) (250 µL). Subsequently TEA (dried over magnesium sulfate) (112 µmol, 11.3 mg, 15.5 µL, 2.38 eqv.) and 2-methyl-2-propanethiol (47.0 µmol, 4.23 mg, 5.29 µL, 1.00 eqv.) were added. The mixture was stirred for 7 h. The solvent was removed and the crude was

dialyzed against ultrapure water for two days. Finally the solvent was removed by lyophilization. The product was obtained as a white solid in a yield of 40.6 mg (78%) after dialysis.

^{1}H-NMR (500 MHz, CDCl$_3$) δ: 5.34 (t (br), CHBr), 4.42 to 3.80 (m (br), CH_2-C-O-C=O), 3.38 (s (br), O-CH_2), 3.18 to 2.77 (m (br), H (dimethylacrylamide)), 2.77 to 2.33 (m (br), CH_2 back bone), 2.33 to 1.44 (m, (br), H backbone), 1.44 to 1.97 (m (br), O=C-(CH_3)$_2$), 0.89 to 0.77 (m (br), (CH_3)$_3$) ppm.

T$_g$: 111.4 C

6.2.3. p(DMAA) end group functionalized with 3-methyl-1-butanethiol (P8)
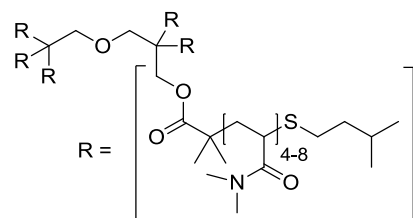
P(DMAA) (**P5**) (47.0 µmol, 50.0 mg, 1.00 eqv.) was dissolved in DCM (dry) (250 µmL). Subsequently TEA (dried over magnesium sulfate) (112 µmol, 11.3 mg, 15.5 µL, 2.38 eqv.) and 3-methyl-1-butanethiol (47.0 µmol, 4.90 mg, 5.80 µL, 1.00 eqv.) were added. The mixture was stirred for 7 h. The solvent was removed and the crude was dialyzed against ultrapure water for two days. Finally the solvent was removed by lyophilization. The product was obtained as a white solid in a yield of 42.7 mg (81%) after dialysis.

^{1}H-NMR (500 MHz, CDCl$_3$) δ: 4.46 to 3.81 (m (br), CH_2-C-O-C=O), 3.46 (s (br), O-CH_2), 3.22 to 2.76 (m (br), H (dimethylacrylamide)), 2.77 to 2.31 (m (br), CH_2 back bone), 2.31 to 1.46 (m, (br), H backbone), 1.46 to 1.02 (m (br), O=C-(CH_3)$_2$), 0.99 to 0.91 (m (br), SCH$_2$CH(CH_3)$_2$) ppm.

T$_g$: 108.2 C

6.2.4. p(DMAA-co-2-ethylhexylacrylate) (P9)
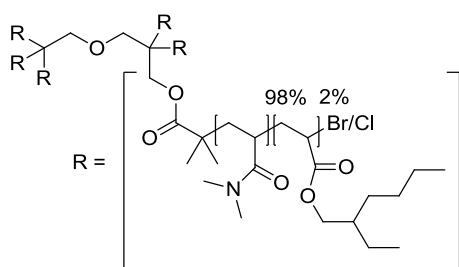
Cu(I)Cl (900 µmol, 90.0 mg, 3.00 eqv.) was added to a Schlenk tube equipped with a stirring bar under argon atmosphere. Dipentaerithritol hexakis (2-bromoisobutyrate) (300 µmol, 344 mg, 1.00 eqv.), Me₆Tren (900 µmol, 208 mg, 242 µL, 3.00 eqv.) and toluene (3.00 mL) were added to another Schlenk flask against a stream of argon. The mixture was bubbled through with argon for 5 min. Subsequently the mixture was transferred into the first Schlenk tube by syringe and the resulting mixture was stirred thoroughly for about 10 min. DMAA (14.5 mmol, 1.44 g, 1.20 mL, 48.0 eqv.), 2-ethylhexylacrylate (300 µmol, 55.2 mg, 49.0 µL, 1.00 eqv.) and toluene (2.00 mL) were placed in a third Schlenk flask. This mixture was also degassed by bubbling through with argon for 10 min. Subsequently the solution was added to the reaction flask by syringe. The reaction mixture was stirred at room temperature for about 12 h. The polymerization was terminated at this point, as overnight a green solid had precipitated. The reaction was stopped by adding ultrapure water (about 5 mL) and exposing the reaction mixture to the air. The reaction mixture was dialyzed against ultrapure water for about one day, where the water was exchanged two times. Finally the remaining solvent was removed by rotary evaporation. The product was obtained as a white product in a yield of 160 mg (9%) after dialysis.

^{1}H-NMR (300 MHz, CDCl$_3$) δ: 5.06 (d (br), C*H*Br), 4.16 to 3.81 (m (br), C*H₂*-C-O-C=O), 3.41 (s (br), O-C*H₂*), 3.24 to 2.78 (m (br), *H* (dimethylacrylamide)), 2.75 to 2.36 (m (br), *H* back bone), 2.30 to 1.42 (m, (br), C*H₂* back bone), 1.43 to 0.94 (m (br), O=C-(C*H₃*)$_2$; C*H₂* (ethylhexylacrylate)), 0.88(s, (br) C*H₃* (ethylhexylacrylate)) ppm.

T$_g$: 93.9 C

M$_n$ (SEC): 7800

Đ (SEC): 1.61

DP (per arm) (SEC): 11

DP (per arm) (NMR): 3

6.2.5. p(DEAA-co-DMAA) (P10)
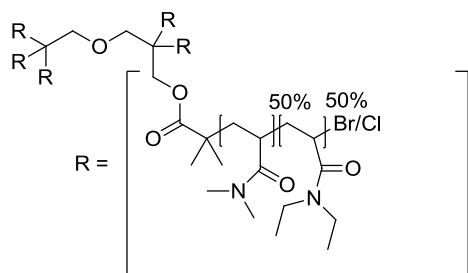
Cu(I)Cl (900 µmol, 90.0 mg, 3.00 eqv) was added to a Schlenk tube equipped with a stirring bar under argon atmosphere. Dipentaerithritol hexakis (2-bromoisobutyrate) (300 µmol, 344 mg, 1.00 eqv.), Me$_6$Tren (900 µmol, 208 mg, 242 µL, 3.00 eqv.) and toluene (1.50 mL) were added to another Schlenk flask against a stream of argon. The mixture was bubbled through with argon for 5 min. Subsequently the mixture was transferred into the first Schlenk tube by syringe and the resulting mixture was stirred thoroughly for about 10 min. DEAA (7.25 mmol, 922 mg, 1.07 mL, 24.0 eqv.), DMAA (7.25 mmol, 720 mg, 750 µL, 24.0 eqv.) and toluene (1.00 mL) were placed in a third Schlenk flask. This mixture was also degassed by bubbling through with argon for 10 min. Subsequently the solution was added to the reaction flask by syringe. The reaction mixture was stirred at room temperature for about 24 h. The reaction was stopped by adding ultrapure water (about 5 mL) and exposing the reaction mixture to the air. The reaction mixture was dialyzed against ultrapure water for about 1 d, where the water was exchanged two times. Finally the remaining solvent was removed by rotary evaporation. The product was obtained as a white solid in a yield of 1.38 g (71%) after dialysis.

^{1}H-NMR (300 MHz, CDCl$_3$) δ: 5.00 (br, CHBr), 4.01 to 3.37 (m (br), CH_2-C-O-C=O), 3.37 (s (br), O-CH_2), 3.26 to 2.69 (m (br), CH_3), 2.69 to 2.21 (m (br), H back bone), 1.94 to 1.53 (m, (br), CH_2 backbone), 1.43 to 0.92 (m (br), CH_2(CH$_3$)$_3$ and O=C-(CH_3)$_2$) ppm.

T$_g$: 90.7 C

M$_n$ (SEC): 8650

Đ (SEC): 1.3

DP (per arm) (SEC): 11

115

6.2.6. poly(N-[-3(Dimethylamino)propyl] methacrylate) (P11)
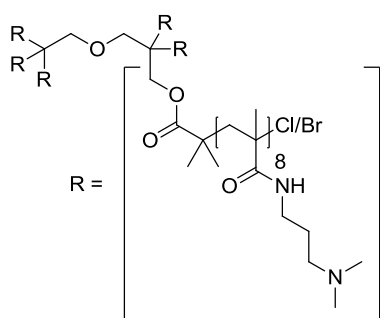
Cu(I)Cl (450 µmol, 45.0 mg, 3.00 eqv.) was added to a Schlenk tube equipped with a stirring bar under argon atmosphere. Dipentaerithritol hexakis (2-bromoisobutyrate) (150 µmol, 172 mg, 1.00 eqv.), Me$_6$Tren (450 µmol, 104 mg, 121 µL, 3.00 eqv.) and toluene (1.50 mL) were added to another Schlenk flask against a stream of argon. The mixture was bubbled through with argon for 5 min. Subsequently the mixture was transferred into the first Schlenk tube by syringe and the resulting mixture was stirred thoroughly for about 10 min. N-[-3(Dimethylamino)propyl] methacrylate (7.25 mmol, 1.23 g, 1.30 mL, 24.0 eqv.) and toluene (1.00 mL) were placed in a third Schlenk flask. This mixture was also degassed by bubbling through with argon for 10 min. Subsequently the solution was added to the reaction flask by syringe. The reaction mixture was stirred at room temperature for about 48 h. The reaction was stopped by adding ultrapure water (about 10 mL) and exposing the reaction mixture to the air. The reaction mixture was dialyzed against ultrapure water for about one day, where the water was exchanged two times. Finally the remaining solvent was removed by rotary evaporation. The product was obtained as a colorless solid in a yield of 397 mg (29%) after dialysis.

^{1}H-NMR (300 MHz, CDCl$_3$) δ: 7.61 (s,(br), NH), 4.00- 3.54(m (br), CH_2-C-O-C=O), 3.17 (m (br), O=C-NCH_2), 2.82 (s (br), O-CH_2), 2.56 to 2.13 (m (br), N(CH_3)$_2$, NCH_2), 1.92 to 1.55 (m, (br), CH_2 backbone), 1.30 to 0.95 (m (br), O=C-(CH_3)$_2$, CH_3) ppm.

T$_g$: 33.1 C

M$_n$ (SEC): 990

Đ (SEC): 1.13

6.2.7. poly(N-[-3(Dimethylamino)propyl] methacrylate-co-diethylacrylamide) (P12)
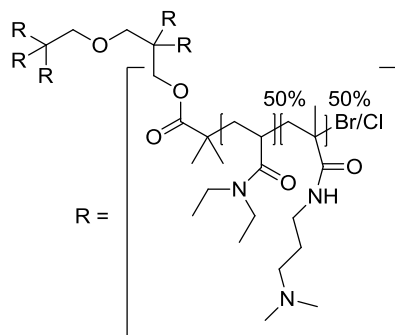
Cu(I)Cl (450 µmol, 45.0 mg, 3.00 eqv.) was added to a Schlenk tube equipped with a stirring bar under argon atmosphere. Dipentaerithritol hexakis (2-bromoisobutyrate) (150 µmol, 172 mg, 1.00 eqv.), Me$_6$Tren (450 µmol, 104 mg, 121 µL, 3.00 eqv.) and toluene (1.50 mL) were added to another Schlenk flask against a stream of argon. The mixture was bubbled through with argon for 5 min. Subsequently the mixture was transferred into the first Schlenk tube by syringe and the resulting mixture was stirred thoroughly for about 10 min. DEAA (3.63 mmol, 461 mg, 500 µL, 24.00 eqv.), N-[-3(Dimethylamino)propyl] methacrylate (3.63 mmol, 617 mg, 650 µL, 24 eqv.) and toluene (1.00 mL) were placed in a third Schlenk flask. This mixture was also degassed by bubbling through with argon for 10 min. Subsequently the solution was added to the reaction flask by syringe. The reaction mixture was stirred at room temperature for about 48 h. The reaction was stopped by adding ultrapure water (about 5 mL) and exposing the reaction mixture to the air. The reaction mixture was dialyzed against ultrapure water for about one day, where the water was exchanged two times. Finally the remaining solvent was removed by rotary evaporation. The product was obtained as a colorless solid in a yield of 249 mg (20%) after dialysis.

^{1}H-NMR (300 MHz, CDCl$_3$) δ: 4.08 to 3.37 (m (br), CH_2-C-O-C=O), 3.21 (s (br), O-CH_2, N-(CH_2)$_2$), 2.78 (m (br), H (dimethyl acryl amide)), 2.07 to 2.53 (m (br), H backbone, N(CH_3)$_2$, NCH_2) 2.03 to 1.05 (m, (br), CH_2 backbone), 1.29 to 0.9 (m (br), O=C-(CH_3)$_2$, CH_3(DMAA), CH_3) ppm.

T$_g$: 35.9 C

M$_n$ (SEC): 1300

Đ (SEC): 1.15

6.3. Peptide array synthesis

6.3.1. Fmoc-deprotection

A PEGMA-co-MMA or pure PEGMA surface functionalized with a least one Fmoc-ß-Ala or an Fmoc-protected growing peptide chain was deprotected by gently rocking the slide in a freshly prepared solution of piperidine/ DMF (dry) (20:80 vol-%) for 20 min. Subsequently the slide was washed by rocking it in DMF 3 × 5 min followed by MeOH 2 × 3 min, each time the solvent was refreshed. Finally the slides were dried under a stream of argon.[7,45,47]

6.3.2. Deposition of amino acid derivatives embedded in matrix material by laser-induced forward transfer

The same lasing set-up as already described in literature was used for the laser-induced forward transfer.[45] It consists of a green laser at wavelength 532 nm (FSDL-532-1000T, 1W; Frankfurt Laser Company, Friedrichsdorf/ Germany) which is switched by an AOM (1002AF1; Polytec GmbH, Waldbronn/ Germany). A laser scanning system (hurrySCAN 10; Scanlab AG, Puchheim/ Germany) is moving the beam over an x-y microscope stage (SCANplus 100_100; Maerzhaeuser, Wetzlar/ Germany) on which the donor and acceptor pair is placed. First the acceptor is put into the holder of the microscope stage with the functionalized side facing upwards. Then the donor is placed on top of the acceptor with the spin-coated side facing downwards. Additionally the set-up is equipped with a camera (DCC1645C; Thorlabs Inc., Newton/ USA) with a microscope lens (PLN 4XCY; Olympus GmbH, Hamburg/ Germany). The 1 W laser (340 mW at the scanhead) was operated at 5 V.

6.3.2.1. Laser-induced forward transfer with p(DMAA) and its copolymers as matrix material

As acceptor slides Fmoc-deprotected either PEGMA-co-MMA or pure PEGMA surfaces functionalized with one Fmoc-ß-Ala were used if not stated otherwise. The acceptor slide was Fmoc-deprotected prior to the lasing step.

To prepare the donor slide for the laser based deposition of the amino acids: 1.00 mL of a mixture of an Fmoc-protected and OPfp-activated amino acid derivative and p(DMAA) (10:90 wt-%) (**P1**, **P2**, **P3** or **P4**) in DCM (123 mg.mL^{-1}) was spin-coated onto a polyimide

foil covered microscopy slide with the following parameters: 50 rps for 10 sec followed by 100 rps for 40 sec.

For the parameter variation coupled at 110 °C (see Figure 15), the additive experiment (see Figure 22), testing of poly(-N-[-3(Dimethylamino)propyl] methacrylate-co-diethylacrylamide) (**P12**) as matrix material (see Figure 24) and comparison transfer with and without matrix material (see Figure 32): pitch 250 µm, relative laser power from 30% to 100% (step size 0.8) and pulse duration from 1 to 10 ms (step size 0.05).

For the parameter variation coupled at 90 °C (see Figure 16): pitch 250 µm, relative laser power from 30% to 100%(step size 1) and pulse duration from 1 to 10 ms (step size 0.075).

For the coupling tests investigating the necessity of the oven step (see Figure 31): pitch 250 µm, relative laser power from 37% to 100% (step size 0.8) and pulse duration from 3 to 10 ms (step size 0.05).

For the FLAG epitope synthesis different parts of the array were lased with different parameters (see Figure 18). It was then zoomed in on the different areas to analyze them further:

Parameter variation (see Figure 20 a): pitch 250 µm, relative laser power from 37% to 100% (step size 0.9), pulse duration from 2.86 to 10 ms (step size 0.06).

KIT logo (see Figure 20 b): pitch 250 µm, relative laser power 60%, pulse duration 6 ms.

KIT logo (see Figure 19 c, Figure 20 c): pitch 75 µm, relative laser power 100%, pulse duration 2 ms.

QR code (see Figure 19 a, Figure 20 d): pitch 100 µm, relative laser power 100%, pulse duration 3 ms.

Grid pattern (see Figure 19 b, Figure 21 a): pitch 50 µm, laser power 100%, pulse duration 2 ms.

For the ToF-SIMS experiments investigating the effectiveness of the washing protocol (see Figure 26) and the coupling depth and behavior (see Figure 27 and Figure 28), eight spots were deposited next to each other to give a rectangular pattern, pitch 50 µm, relative laser power 40% and pulse duration 10 ms.

6.3.2.2. Structuring of U-4CR functionalized surface with Fmoc-Gly-OPfp

On an Fmoc-deprotected PEGMA-co-MMA surface functionalized with three β-Ala's and a surface with β-Ala-β-Ala-β-Ala-Lys(Boc)-Gly-Gly an U-4CR with Fmoc-β-Ala-OH, hexanal and cyclohexyl isocyanide was performed. The slides were immersed in a solution of 0.4 M Fmoc-ß-Ala-OH, 0.4 M cyclohexyl isocyanide and 0.4 M hexanal in DMAc/ DCM (dry)/ MeOH (dry) (24:38:38 vol-%) and kept under argon atmosphere for four days in a desiccator. Subsequently the slides were washed with DMF 5 × 5 min. After a capping step the slides were Fmoc-deprotected and used as acceptor slides for laser-induced forward transfer

To prepare the donor slide for the laser based deposition of the amino acids: 1.00 mL of a mixture of an Fmoc-Gly-OPfp and S-LEC-P LT 75 52 (10:90 wt-%) in DCM (123 mg.mL^{-1}) was spin-coated onto a polyimide foil covered microscopy slide with the following parameters: 50 rps for 10 sec followed by 100 rps for 40 sec.

The following laser parameters were used: relative laser power 100%, pulse duration 0.1 to 10 ms (step size 0.14) (see Figure 39 and Figure 40)

6.3.2.3. U-4CR from 'solid' solvent

As acceptor slides Fmoc-deprotected PEGMA-co-MMA surfaces functionalized with one Fmoc-ß-Ala were used. The acceptor slide was Fmoc-deprotected prior to the lasing step.

To prepare the donor slide for the laser based deposition: 1.00 mL of a mixture of an Fmoc-Gly-OH and p(DMAA) (**P3**) (5:95 wt-%) in DCM (131 mg.mL^{-1}) and was spin-coated onto a polyimide foil covered microscopy slide with the following parameters: 50 rps for 10 sec followed by 100 rps for 40 sec. 1.00 mL of a mixture of a Boc-L-alaninal, 4-methoxyphenylisocyanide and p(DMAA) (**P3**) (3:2:95 wt-%) in DCM (131 mg.mL^{-1}) and was spin-coated onto a polyimide foil covered microscopy slide with the following parameters: 50 rps for 10 sec followed by 100 rps for 40 sec.

The following laser parameters were used: relative laser power 100%, pulse duration 0.1 to 10 ms (step size 0.14)

6.3.3. Coupling of amino acid derivatives to the synthesis film

6.3.3.1. Coupling procedures performed in the oven

After the lasing step, the acceptor slides were baked in an oven at 110 °C or 90 °C, for 1.5 h (if not stated otherwise) under argon atmosphere. After a cooling down period, the slides were flushed thoroughly with DCM and rocked in DCM for 3 × 5min. Then the slides were placed in an ultrasonic sound bath for 30 sec followed by 5 min rocking in fresh DCM, the ultrasonic sound bath step followed by rocking in fresh DCM was repeated three times. Finally the slides were dried in a stream of argon. Each coupling step was followed by a capping step.

6.3.3.2. Coupling procedures from solution

The Fmoc-deprotected PEGMA-co-MMA or pure PEGMA synthesis slides functionalized with at least one Fmoc-ß-Ala were covered with 1.00 mL of a 0.2 M solution of the Fmoc-protected and OPfp-activated amino acid in DMF (dry). The solution was left standing in a desiccator under argon atmosphere at room temperature for 3 to 10 h. Subsequently the slides were washed with DMF, 3 × 5 min, directly followed by a capping step.

6.3.3.3. Coupling of Fmoc-β-Ala-OH to the synthesis film from solution

For the synthesis of the FLAG epitope and the U-4CR followed by functionalization with Fmoc-Gly-OPfp with the 'solid' solvent approach, the synthesis film was functionalized with two additional β-alanines before starting the synthesis of the sequence. A solution of 0.2 M Fmoc-β-Ala-OH in DMF (dry) was prepared in a Schlenk flask, then 1.2 eqv. of DIC were added. The solution was degassed gently and refilled with argon. After stirring the mixture for about 5 min, 0.4 M 1-methylimidazole was added by syringe. The solution was stirred for an additional minute and poured over an Fmoc-deprotected synthesis slide. The slide was kept in a desiccator for at least 2 h under argon atmosphere, when the first Fmoc-β-Ala was coupled to the hydroxyl groups of the PEGMA, the reaction was performed overnight. Then the slide was washed 3 × 5 min with DMF and 2 × 3 min with MeOH. Finally the slide was dried under a stream of argon.[47] The synthesis slide was then Fmoc-deprotected and the procedure was repeated until the desired length of ß-Ala's for the spacer was reached or it was proceeded with coupling of the next amino acid.

6.3.4. Capping of unreacted amines

To cap the unreacted free amino groups on the surface, they were acetylated. For this, the slide was treated with a solution of acetic anhydride/ DIPEA/ DMF (dry) (10:20:70 vol-%) for at least 3 h to overnight reaction time in a desiccator under argon atmosphere. Afterwards the slides were washed with DMF, 5 × 5 min and MeOH 2 × 3 min.[45,47] The capping step was followed by an Fmoc-deprotection step, if the peptide chain synthesis was finished; a side chain deprotection step was done additionally after the Fmoc-deprotection.

6.3.5. Side chain deprotection

To remove the protective groups of the side chains, the synthesis slides were rocked in a solution, freshly prepared each time, of DCM/ TFA/ TIBS/ ultrapure water (44:51:3:2 vol-%) for 3 × 30 min. Then the slides were washed 2 × 5 min with DCM, 1 × 5 min with DMF, 1 × 30 min DIPEA/ DMF (5:95 vol-%), 2 × 5 min DMF and 2 × 3 min MeOH. Finally the slides were dried under a stream of argon.[19,45]

6.3.6. Staining protocols

6.3.6.1. Staining with TAMRA maleimide

After 10 min of pre-swelling in PBS-T buffer, the side chain deprotected acceptor slides were rocked in a solution of TAMRA maleimide in PBS-T buffer (4.00 µg per 10.0 mL) for 2 h. Afterwards the slides were washed 5 × 5 min with PBS-T and then flushed thoroughly with ultrapure water. The slides were dried under a stream of argon.

6.3.6.2. Staining with TAMRA-NHS

The Fmoc-deprotected acceptor slides were pre-swollen with PBS-T buffer for 10 min, followed by a staining step rocking the slides in a solution of TAMRA-NHS in PBS-T (1.00 µg per 10.0 mL) for 2 h. Subsequently the slides were washed: with PBS-T buffer for 5 min, with ultrapure water for 2 min, with DMF for 5 min, with ethyl acetate for 5 min and finally the slide was flushed with DCM and dried under a stream of argon.

6.3.6.3. Staining with DyLight 680-NHS

The Fmoc-deprotected acceptor slides were pre-swollen with PBS-T buffer for 10 min, followed by a staining step rocking the slides in a solution of DyLight 680-NHS in PBS-T (1.00 µg per 10.0 mL) for 2 h. Subsequently the slides were washed: with PBS-T buffer for 5 min, with ultrapure water for 2 min, with DMF for 5 min, with ethyl acetate for 5 min and finally the slide was flushed with DCM and dried under a stream of argon.

6.3.6.4. Antibody staining

The slides were pre-swollen in phosphate buffered saline (PBS) buffer for 30 min. Then the slides were blocked in Rockland buffer for 1 h and washed with PBS-T for 5 min. Subsequently the slides were incubated with monoclonal mouse anti-FLAG M2-DyLight 800 antibodies, diluted 1:1000 in Rockland buffer/ PBS-T buffer (1:99 vol-%) for 1 h. The slides were washed 3 × 1 min in PBS-T and gently flushed with ultrapure water. Finally the slides were dried under a stream of argon and scanned.

After scanning, the slides were sonicated in chloroform 3 × 1 min, followed by washing in chloroform for 3 min to remove the antibodies from the surface and enable a second incubation with a differently labeled antibody. After washing, the slides were dried under a stream of argon.

For the second antibody incubation, the slides were pre-swollen in Rockland buffer/ PBS-T (10:90 vol-%) for 30 min. Then the slides were incubated with monoclonal mouse anti-FLAG M2-Cy3 antibodies diluted 1:1000 in Rockland buffer/ PBS-T (1:99 vol-%) for 1 h. Finally the slides were washed 3 × 1 min with PBS-T, flushed carefully with ultrapure water and dried under a stream of argon.

6.3.7. Synthesis pure PEGMA surfaces

Self-synthesized, pure PEGMA slides were used for ToF-SIMS experiments and for the U-4CR experiments, subsequently analysed with MALDI-ToF.

6.3.7.1. Silanization

Prior to functionalization, the glass slides were either cleaned in an ultrasonic sound bath: 5 min in EtOH, followed by 2 × 3 min in ultrapure water or no pre-cleaning was performed. The slides were gently rocked for 3 h a solution of 1 M KOH in isopropanol, after which, the slides were washed with deionized water 2 × 5 min, sonicated in

ultrapure water 5 × 1 min and finally washed with EtOH. The slides were then dried under a stream of argon and tempered at 120 °C for 30 min to 1 h. After cooling down, the slides were transferred into a desiccator under argon atmosphere and a solution of APTES/ ultrapure water/ EtOH (absolute) (2.9:2.4:94.7 vol-%) was poured over the slides. They were left standing overnight for at least 16 h. Then the reaction mixture was removed and the slides were immediately flushed thoroughly with EtOH, followed by 5 × 1 min washing steps in ultrasonic sound bath in EtOH. Finally the slides were baked in the oven for 1 h to 3 h at 120 °C under argon atmosphere.

6.3.7.2. Functionalization with α-bromoisobutyrylbromide

The APTES functionalized slides were placed in a desiccator under argon atmosphere. In a Schlenk flask under argon atmosphere, a solution of 0.6 mM DIPEA in DCM (dry) was cooled to 0 °C and α-bromoisobutyryl bromide was added against a stream of argon to result in a 0.2 mM solution. After a short stirring period, the solution was poured over the glass slides, which are left standing overnight for at least 16 h under argon atmosphere. Then the slides were washed 2 × 3 min with DCM, followed by 2 × 2 min with MeOH. Finally the slides were dried under a stream of argon.[47]

6.3.7.3. Si-ATRP polymerization synthesis

The slides were placed in a desiccator under argon atmosphere. To a Schlenk flask under argon atmosphere, which was evacuated and refilled with argon three times, PEGMA, ultrapure water and MeOH (33:33:33 vol-%) were added against a stream of argon. Subsequently 2,2'- bipyridine (50 mM) was added against a stream of argon. The resulting solution was stirred until the solid material was dissolved completely. Subsequently, copper(I)bromide (Cu(I)Br) (30 mM) was added also against a stream of argon and the solution was degassed. After an additional 5 min of stirring, the solution was poured over the glass slides under argon atmosphere. The slides were incubated overnight. Then they were washed, 1 × 5 min with MeOH/ ultrapure water (50:50 vol-%), 3 × 5 min with ultrapure water and 2 × 3 min with MeOH.[47] Finally the slides were dried under a stream of argon and they were kept under argon atmosphere at 4 °C until further use. The slides were then functionalized with the first ß-alanine according to the procedure described above.

6.4. U-4CR on arrays in solution

6.4.1. Side chain functionalization

6.4.1.1. Array functionalization with Fmoc-β-Ala-OH, hexanal and cyclohexyl isocyanide (1)
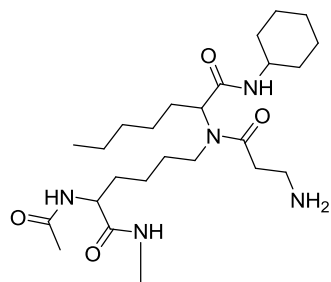
Side chain deprotected PEGMA-co-MMA arrays carrying alternating Lys and Gly spots were immersed in a solution of 0.4 M Fmoc-ß-Ala-OH, 0.4 M cyclohexyl isocyanide and 0.4 M hexanal in either DMAc/ DCM (dry)/ MeOH (dry) (24:38:38 vol-%), DMAc/ MeOH (24:66 vol-%) or DMAc/ isopropanol (24:66 vol-%) and kept under argon atmosphere for four days in a desiccator. Subsequently the slides were washed with DMF 5 × 5 min and capped directly afterwards. After the capping step, the slides were Fmoc-deprotected followed by a fluorescent staining step with DyLight 680-NHS.

6.4.1.2. Array functionalization with Fmoc-β-Ala-OH, isovaleraldehyde and cyclohexyl isocyanide (2)
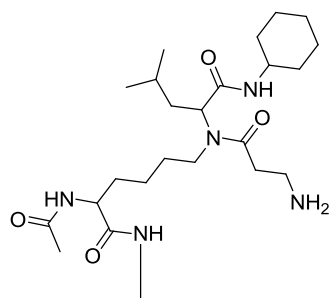
Side chain deprotected PEGMA-co-MMA arrays carrying alternating Lys and Gly spots were immersed in a solution of 0.4 M Fmoc-ß-Ala-OH, 0.4 M cyclohexyl isocyanide and 0.4 M isovaleraldehyde in DMAc/ DCM (dry)/ MeOH (dry) (24:38:38 vol-%) and kept under argon atmosphere for four days in a desiccator. Subsequently the slides were washed with DMF 5 × 5 min and capped directly afterwards. After the capping step, the slides were Fmoc-deprotected followed by a fluorescent staining step with DyLight 680-NHS.

6.4.1.3. Array functionalization with Fmoc-β-Ala-OH, hexanal and benzyl isocyanide (3)
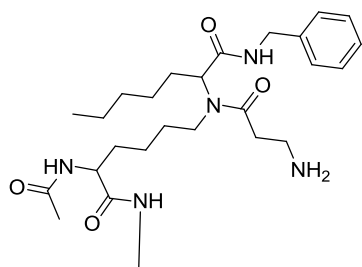
Side chain deprotected PEGMA-co-MMA arrays carrying alternating Lys and Gly spots were immersed in a solution of 0.4 M Fmoc-ß-Ala-OH, 0.4 M benzyl isocyanide and 0.4 M hexanal in DMAc/ DCM (dry)/ MeOH (dry) (24:38:38 vol-%) and kept under argon atmosphere for four days in a desiccator. Subsequently the slides were washed with DMF 5 × 5 min and capped directly afterwards. After the capping step, the slides were Fmoc-deprotected followed by a fluorescent staining step with DyLight 680-NHS.

6.4.1.4. Array functionalization with Fmoc-β-Ala-OH, isovaleraldehyde and benzyl isocyanide (4)
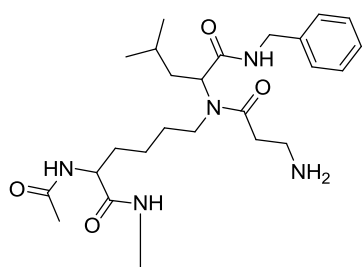
Side chain deprotected PEGMA-co-MMA arrays carrying alternating Lys and Gly spots were immersed in a solution of 0.4 M Fmoc-ß-Ala-OH, 0.4 M benzyl isocyanide and 0.4 M isovaleraldehyde in DMAc/ DCM (dry)/ MeOH (dry) (24:38:38 vol-%) and kept under argon atmosphere for four days in a desiccator. Subsequently the slides were washed with DMF 5 × 5 min and capped directly afterwards. After the capping step, the slides were Fmoc-deprotected followed by a fluorescent staining step with DyLight 680-NHS.

6.4.1.5. Array functionalization with Fmoc-β-Ala-OH, hexanal and *tert*-butyl isocyanide (5)
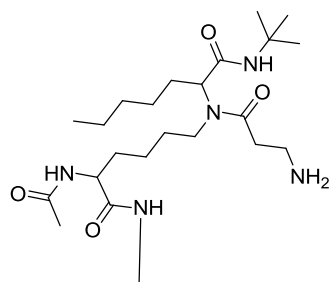
Side chain deprotected PEGMA-co-MMA arrays carrying alternating Lys and Gly spots were immersed in a solution of 0.4 M Fmoc-ß-Ala-OH, 0.4 M *tert*-butyl isocyanide and 0.4 M hexanal in DMAc/ DCM (dry)/ MeOH (dry) (24:38:38 vol-%) and kept under argon atmosphere for four days in a desiccator. Subsequently the slides were washed with DMF 5 × 5 min and capped directly afterwards. After the capping step, the slides were Fmoc-deprotected followed by a fluorescent staining step with DyLight 680-NHS.

6.4.1.6. Array functionalization with Fmoc-β-Ala-OH, isovaleraldehyde and *tert*-butyl isocyanide (6)
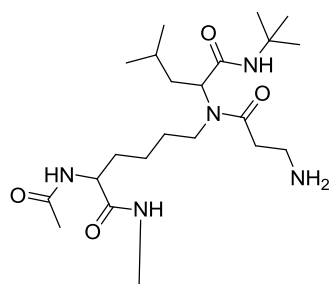
Side chain deprotected PEGMA-co-MMA arrays carrying alternating Lys and Gly spots were immersed in a solution of 0.4 M Fmoc-ß-Ala-OH, 0.4 M *tert*-butyl isocyanide and 0.4 M isovaleraldehyde in DMAc/ DCM (dry)/ MeOH (dry) (24:38:38 vol-%) and kept under argon atmosphere for four days in a desiccator. Subsequently the slides were washed with DMF 5 × 5 min and capped directly afterwards. After the capping step, the slides were Fmoc-deprotected followed by a fluorescent staining step with DyLight 680-NHS.

6.4.2. Fluorescence intensity of the different U-4CR products

All arrays with products **1**-**6** were scanned in the Odyssey scanner at resolution 21 µm and intensity 5 and 7. The grey values of each Lys spot (between 96 and 248 spots as

the size of the arrays varied due to the shape of the slide) and a corresponding background spot for each Lys spot were determined, separately for both intensities. Below the mean values of the fluorescence intensity of the spots and the background (see Table 8 and Table 9) belonging to the comparison diagram (see Figure 35) are given.

Table 8: Mean calculated for the fluorescence intensity of the spots and the background measured at intensity 5 and the respective standard deviations.

	Spot signals (Mean intensity)	Background signal (Mean intensity)
1	1947 ± 559	654 ± 63
2	2129 ± 309	490 ± 80
3	1198 ± 191	418 ± 80
4	1216 ± 149	385 ± 51
5	1488 ± 649	323 ± 32
6	2751 ± 470	634 ± 399

Table 9: Mean calculated for the fluorescence intensity of the spots and the background measured at intensity 7 and the respective standard deviations.

	Spot signals (Mean intensity)	Background signal (Mean intensity)
1	7098 ± 1372	2423 ± 231
2	9206 ± 1269	2146 ± 507
3	4992 ± 800	1720 ± 162
4	5310 ± 632	1654 ± 214
5	5996 ± 1372	1331 ± 126
6	11903 ± 1960	2698 ± 970

6.4.3. Surface functionalization for subsequent MALDI-ToF experiments

6.4.3.1. Functionalization with the Rink-amide linker and subsequent Fmoc-β-Ala-OH

An Fmoc deprotected PEGMA-co-MMA slide or a pure PEGMA slide functionalized with one ß-Ala was covered with a solution of 0.2 M 4'-{(R,S)-alpha-[1-(9-Fluorenyl)methoxycarbonylamino]-2,4-dimethoxybenzyl}-phenoxyacetic acid (Fmoc-Rink amide linker), 0.2 M pentafluorophenol and 0.2 M DIC in DMF (dry) overnight.[45] The slide was washed with DMF 3 × 5 min, followed by a 4 h capping step. In the next step the slide was Fmoc-deprotected and covered with a solution of 0.2 M Fmoc-ß-Ala-OH, 0.2 M *N,N,N',N'*-Tetramethyl-O-(1H-benzotriazol-1-yl)uronium hexafluorophosphate, 0.2 M HOBt or OxymaPure and 0.4 M DIPEA in DMF (dry) overnight. Afterwards the slide was washed with DMF 3 × 5 min and 2 × 3 min MeOH. Then the slide was flushed with DCM and dried under a stream of argon.

6.4.3.2. Surface functionalization with Fmoc-β-Ala-OH, isovaleraldehyde and *tert*-butyl isocyanide (7)

An Fmoc-β-Ala-Rink-amide linker functionalized slide was Fmoc-deprotected and immersed in a solution of 0.4 M Fmoc-ß-Ala-OH, 0.4 M *tert*-butyl isocyanide and 0.4 M isovaleraldehyde in DMAc/ DCM (dry)/ MeOH (dry) (24:38:38 vol-%) and kept under argon atmosphere for four days in a desiccator. Subsequently the slides were washed with DMF 5 × 5 min and 2 ×3 min with MeOH. Finally the slide was flushed with DCM and dried under a stream of argon.

The surface was incubated with 1.00 mL of DCM for 10 min, then the DCM was removed and 1.00 mL of TFA/ DCM/ TIBS/ ultrapure water (92:3:2.5:2.5 vol-%) was pipetted onto the surface, after 15 min additional solution was pipetted onto the slide so that it did not fall dry and it was incubated for an additional 15 min. Then the surface was washed three times with about 0.5 mL of DCM, followed by about 0.5 mL of MeOH.[45] After evaporation of the solvent, the remaining crude product was investigated with MALDI-ToF.

-MS (MALDI) (**7**): m/z cal. 550.7, measured 551.2 [(M+H)][+], 573.1 [(M+Na)][+], 589.1[(M+K)][+]

6.4.3.3. Array functionalization with Fmoc-β-Ala-OH, hexanal and cyclohexyl isocyanide (8)

An Fmoc-β-Ala-Rink-amide linker functionalized slide was Fmoc-deprotected and immersed in a solution of 0.4 M Fmoc-ß-Ala-OH, 0.4 M cyclohexyl isocyanide and 0.4 M hexanal in DMAc/ DCM (dry)/ MeOH (dry) (24:38:38 vol-%) and kept under argon atmosphere for four days in a desiccator. Subsequently the slides were washed with DMF 5 × 5 min and 2 ×3 min with MeOH. Finally the slide was flushed with DCM and dried under a stream of argon.

The surface was incubated with 1.00 mL of DCM for 10 min, then the DCM was removed and 1.00 mL of TFA/ DCM/ TIBS/ ultrapure water (92:3:2.5:2.5 vol-%) was pipetted onto the surface, after 15 min additional solution was pipetted onto the slide so that it did not fall dry and it was incubated for an additional 15 min. Then the surface was washed three times with about 0.5 mL of DCM, followed by about 0.5 mL of MeOH.[45] After evaporation of the solvent, the remaining crude product was investigated with MALDI-ToF.

-MS (MALDI) (**8**): m/z cal. 590.8, measured 591.3[(M+H)][+], 613.3 [(M+Na)][+], 629.2[(M+K)][+]

6.4.3.4. Array functionalization with Fmoc-β-Ala-OH, bicyclo[2.2.1] hept-5-ene-2-carboxaldehyde and cyclohexyl isocyanide (9)
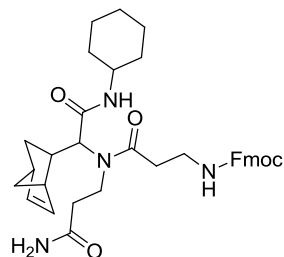
An Fmoc-β-Ala-Rink-amide linker functionalized slide was Fmoc-deprotected and immersed in a solution of 0.4 M Fmoc-ß-Ala-OH, 0.4 M cyclohexyl isocyanide and 0.4 M bicyclo[2.2.1] hept-5-ene-2-carboxaldehyde in DMAc/ DCM (dry)/ MeOH (dry) (24:38:38 vol-%) and kept under argon atmosphere for four days in a desiccator. Subsequently the slides were washed with DMF 5 × 5 min and 2 ×3 min with MeOH. Finally the slide was flushed with DCM and dried under a stream of argon.

The surface was incubated with 1.00 mL of DCM for 10 min, then the DCM was removed and 1.00 mL of TFA/ DCM/ TIBS/ ultrapure water (92:3:2.5:2.5 vol-%) was pipetted onto the surface, after 15 min additional solution was pipetted onto the slide so that it did not fall dry and it was incubated for an additional 15 min. Then the surface was washed three times with about 0.5 mL of DCM, followed by about 0.5 mL of MeOH.[45] After evaporation of the solvent, the remaining crude product was investigated with MALDI-ToF.

-MS (MALDI) (**10**): m/z cal. 658.9, measured 659.3 [(M+H)]$^+$, 681.3 [(M+Na)]$^+$

6.4.3.5. Array functionalization with Fmoc-β-Ala-OH, 10-undecenal and cyclohexyl isocyanide (10)
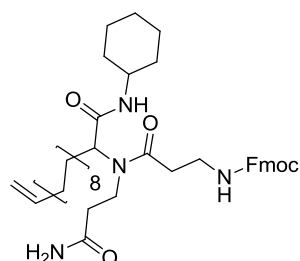
An Fmoc-β-Ala-Rink-amide linker functionalized slide was Fmoc-deprotected and immersed in a solution of 0.4 M Fmoc-ß-Ala-OH, 0.4 M cyclohexyl isocyanide and 0.4 M 10-undecenal in DMAc/ DCM (dry)/MeOH (dry) (24:38:38 vol-%) and kept under

argon atmosphere for four days in a desiccator. Subsequently the slides were washed with DMF 5 × 5 min and 2 ×3 min with MeOH. Finally the slide was flushed with DCM and dried under a stream of argon.

The surface was incubated with 1.00 mL of DCM for 10 min, then the DCM was removed and a 1.00 mL of a solution of TFA/DCM/TIBS/ultrapure water (92:3:2.5:2.5 vol-%) was pipetted onto the surface, after 15 min additional solution was pipetted onto the slide so that it did not fall dry and it was incubated for an additional 15 min. Then the surface was washed three times with about 0.5 mL of DCM, followed by about 0.5 mL of MeOH.[45] After evaporation of the solvent, the remaining crude product was investigated with MALDI-ToF.

-MS (MALDI) (**9**): m/z cal. 612.8, measured 613.2 [(M+H)]$^+$, 635.2 [(M+Na)]$^+$

6.5. Molecular layer deposition

6.5.1. Silanization with 11-bromoundecyltrimethoxysilane (12)
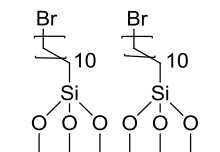
Silicon wafers pieces of about 1.5 × 1.5 cm size were cut and used as delivered with their native oxide layer. The slides were placed in oxygen plasma for 5 or 10 min. Then the wafer pieces were cleaned in a solution of ammonia (25%)/ hydrogen peroxide (30%)/ ultrapure water (14:14:72 vol-%) at about 60 °C for 30 min. After washing with ultrapure water, the wafer pieces were immersed in a solution sulfuric acid (95%)/ hydrogen peroxide (30%)/ ultrapure water (14:14:72 vol-%) for 30 min. Subsequently the wafer pieces were washed with ultrapure water and dried under a stream of argon. Then a 0.4 M solution of 11-bromoundecyltrimethoxysilane in toluene (dry) was poured over them and they were left standing overnight under argon atmosphere. The next day, they were rinsed, followed by a 10 min sonification step, first with toluene, then with acetone and finally with EtOH, after which they were dried under a stream of argon.

6.5.2. Thiol reaction with bromine terminated wafer (13)
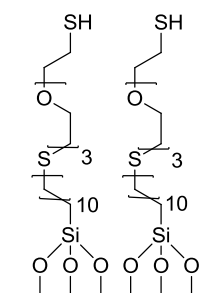
The bromine terminated wafer pieces were immersed in a solution of tetra(ethylene glycol) dithiol/ TEA (dried over magnesium sulfate)/ DCM (dry) (24:9:67 vol-%) and rocked gently for 7 h under argon atmosphere. Subsequently they were rinsed with DCM, sonicated 3 × 1 min in DCM (refreshed each time) and dried under a stream of argon.

6.5.3. Protocols silanization tests

Silicon wafers with their native oxide layer were cut into pieces of 1 × 1cm, followed by cleaning with a Snow Jet model K4-05 (Tectra, Frankfurt/ Germany) to remove surface contaminations.[130] The samples for the ToF-SIMS measurements were used directly after cleaning. Samples for the AFM analysis were additionally structured by Dr. J. Berson with polymer blend lithography to create holes of exactly defined depth.[125] A FDTS matrix was used in order to accurately determine the sample height.

6.5.3.1. Functionalization with 10-undecenyltrichlorosilane (14)
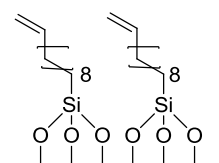
For the functionalization with 10-undecenyltrichlorosilane the wafer pieces were immersed in a 8.4 mM solution in toluene (dry) for 1.5 h in a glove box with 28-33% humidity. Subsequently the wafer pieces were washed a couple of times with $CHCl_3$, followed by a 5 min sonication step in $CHCl_3$ and soaking in cyclohexane at 60 °C for 10 min.[129] Finally the wafer pieces were dried under a stream of argon.

6.5.3.2. Functionalization with allyltrimethoxysilane (15)
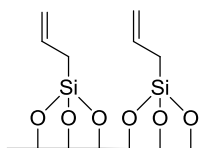
For the functionalization with allyltrimethoxysilane the wafer pieces were immersed in an 8.4 mM solution in toluene (dry) for 1.5 h in a glove box with 28-33% humidity. Subsequently the wafer pieces were washed a couple of times with $CHCl_3$, followed by a 5 min sonication step in $CHCl_3$ and soaking in cyclohexane at 60 °C for 10 min.[129] Finally the wafer pieces were dried under a stream of argon.

6.5.3.3. Functionalization with 3-mercaptopropyltrimethoxysilane (16)
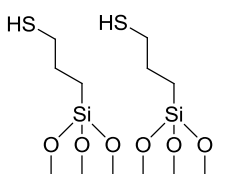
For the functionalization with 3-mercaptopropyltrimethoxysilane the wafer pieces were immersed in a 8.4 mM solution in toluene (dry) for 1.5 h in a glove box with 28-33% humidity. Subsequently the wafer pieces were washed a couple of times with $CHCl_3$, followed by a 5 min sonication step in $CHCl_3$ and soaking in cyclohexane at 60 °C for 10 min.[129] Finally the wafer pieces were dried under a stream of argon.

For an additional AFM experiment, a fresh wafer piece was immersed in a 0.4 M solution of 3-mercaptopropyltrimethoxysilane in toluene overnight under argon atmosphere. The next day the wafer piece was rinsed with toluene, followed by a 10 min sonification step in toluene, rinsed with acetone and ethanol and sonicated in ethanol for 10 min. Finally it was dried under a stream of argon.

6.5.4. Thiol-Ene reactions (17)
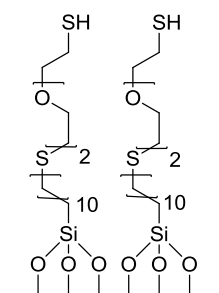
The silicon wafer pieces functionalized with 10-undecenyltrichlorosilane (**14**) were immersed in 2,2′-(ethylenedioxy)diethanethiol. DMF (3 µL.mL^{-1}) was added to ensure coverage of the surface with the solution. Additionally DMPA (0, 5 or 10 mg.mL^{-1}) was added (see Table 6). Then the samples were placed under a UV-lamp (VL-115.L, 15 W, Vilber Lourmat GmbH, Eberhardzell/ Germany) and irradiated for 90 or 120 min (see table Table 6) with light of the wavelength 365 nm.

Table 6: Reaction conditions for the Thiol-Ene reactions

Sample	Illumination time (min)	DMPA (mg)
a	120	5
b	120	0
c	90	10

Finally the slide was cleaned by flushing it with toluene, followed by a 2 min sonification step in toluene. Finally the slides were dried under a stream of argon.

6.6. Instruments

6.6.1. ^{1}H-NMR

^{1}H-NMR spectra were measured on a Bruker Avance 300 at 300 MHz or on a Bruker Avance 500 at 500 MHz from the Bruker Corporation (Billerica/ USA) in CDCl$_3$.

6.6.2. SEC

Synthesized polymers were analyzed by SEC using a Polymer Laboratories PL-GPC 50 plus integrated system equipped with an auto sampler by Agilent (Santa Clara/ USA), a PLgel 25 µm bead-size guard column (50 × 7.5 mm), followed by three PLgel 5 µm

MixedC columns (300 × 7.5 mm) and a refractive index detector. DMAc with 0.03 wt-% Lithiumbromide was used as the eluent with a flow rate of 1 mL.min^{-1}. For sample preparation, 2 g.L^{-1} of polymer was dissolved. Subsequently the solution was passed through a polytetrafluorethylene syringe filter prior to measurement. As a standard a linear poly(methyl methacrylate) standard was used.

6.6.3. DSC

Glass transition temperatures were analyzed on a Differential Scanning Calorimeter 204 F1 Phoenix by NETZSCH Gerätebau GmbH (Selb/ Germany). Samples were measured in an aluminum pans by Netzsch (Selb/ Germany). The measurements were executed in two heating and cooling cycles ranging from -20 °C to 200 °C. The used heating and cooling rates were 10°K.min^{-1}, where at the minimum and maximum temperatures an isothermal element of 10 min was integrated.[108] Only the second heating cycle was analyzed to ensure the same thermal history for all samples.

6.6.4. Fluorescence scans

Analysis of fluorescently labeled synthesis surfaces was performed with an Odyssey Infrared Imager by LICOR Biosciences (Lincoln/ USA). Slides were scanned with a resolution of 21 µm, at intensity 3, 5 or 7 in the 700 nm channel for DyLight 680 staining or at intensity 7 in the 800 nm channel for antibody staining. Most slides were analyzed with a GenePIX 4000B microarray scanner by Molecular Devices (Sunnyvale/ USA). These slides were scanned with a resolution of 5 µm, photo multiplier tube gain 450, laser intensity 33% in the 532 nm channel. Either ImageJ or the respective software of the scanner was used to enhance contrast and brightness of the scanned objects after scanning. ImageJ was also used to determine the grey values of the scans from the unmodified images and make 3D-models of spots.

6.6.5. ToF-SIMS measurements

ToF-SIMS was performed on a TOF.SIMS^5 instrument (ION-TOF GmbH, Münster / Germany). This spectrometer is equipped with a Bi cluster primary ion source and a reflectron type time-of-flight analyzer. Ultra-high vacuum base pressure was < 5×10^{-9} mbar, during analysis in the 10^{-8} mbar range.

For high mass resolution, the Bi source was operated in the "high current bunched" mode providing short Bi_3^+ primary ion pulses at 10 kHz and 25 keV energy, a lateral resolution of approximately 4 µm, and a target current of 0.4 pA. The short pulse length of 0.9 ns allowed for high mass resolution.

6.6.5.1. Peptide array analysis and molecular layer deposition (substitution experiments)

The primary ion beam was rastered across a 500 × 500 µm² field of view on the sample, and 128 × 128 data points were recorded (Figure 27 a, b, Figure 29 and Figure 43). Images larger than the maximum deflection range of the primary ion gun (Figure 26) were obtained using the manipulator stage scan mode at 150 points/mm.

Unless stated otherwise, primary ion doses were kept below 10^{11} ions/cm² (static SIMS limit). If charge compensation was necessary, an electron flood gun providing electrons of 21 eV was applied and the secondary ion reflectron tuned accordingly. Spectra were calibrated on the omnipresent C^-, CH^-, CH_2^-, C_2^-, or on the C^+, CH^+, CH_2^+, and CH_3^+ peaks. Based on these datasets, the chemical assignments for characteristic fragments were determined.

6.6.5.2. Molecular layer deposition (silanization and Thiol-Ene experiments)

The primary ion beam was rastered across a 2000 × 2000 µm respectively a 2000 × 1600 µm area (see Figure 46, Figure 47 and Figure 49). In this stage raster measurement mode smaller areas of 400 µm in square are subsequently measured to cover the whole large area scan. For these scans a resolution of 200 point/mm was used. This fits quite well to the diameter of the high-current bunched Bismuth ion beam of about 5 to 7 µm.

Unless stated otherwise, primary ion doses were kept below 10^{11} ions/cm² (static SIMS limit). If charge compensation was necessary, an electron flood gun providing electrons was used. Spectra were calibrated on the omnipresent C^-, C_2^-, C_4^-, C_8^- or on the C^+, Si^+ and SiO^+ peaks. Based on these datasets, the chemical assignments for characteristic fragments were determined.

6.6.5.3. Depth profiling

For depth profiling, dynamic SIMS (Figure 27c, d, Figure 28 a, b), a dual beam analysis was performed in non-interlaced mode: The primary ion source was again operated in "high current bunched" mode with a scanned area of 500 × 500 µm² (20 frames) and a

sputter gun (operated with C_{60}^+ ions, 20 keV, scanned over a concentric field of 850×850 µm^2, target current 1.3 nA) was applied to erode the sample for 1.4 sec followed by a 0.2 sec pause. Thereby, the sputter ion dose density was > 50 times higher than the Bi ion dose density and molecular secondary ions like $C_{19}H_{15}^+$ were preserved. To avoid artifacts due to geometrical effects, data presented in Figure 28 a, b were extracted from a 350×250 µm^2 field of view centered on one lased array spot.

6.6.6. Contact angle measurements

Contact angle measurements were performed using an OCA40 (DataPhysics, Filderstadt/ Germany). The heating facility was created by equipping the moveable table with a copper heating block equipped with a temperature sensor. The power supply for heating was a EA-PS 2042-10B constant current box, equipped with a Eurotherm 2404 control element.

6.6.7. XPS

XPS investigation was performed in a K-Alpha+ spectrometer (ThermoFisher Scientific, East Grinstead/ UK) using a microfocused, monochromated Al Kα X-ray source (400 µm spot size). The K-Alpha charge compensation system was employed during analysis, using electrons of 8 eV energy, and low-energy argon ions to prevent any localized charge build-up. The kinetic energy of the electrons was measured by a 180° hemispherical energy analyzer operated in the constant analyzer energy mode at 50 eV pass energy for elemental spectra. Data acquisition and processing using the Thermo Avantage software is described elsewhere,[131] and Scofield sensitivity factors were applied for quantification.[132] The spectra were fitted with one or more Voigt profiles (BE uncertainty: $\pm$0.2 eV). All spectra were referenced to the C 1s peak (C-C, C-H) at 285.0 eV binding energy controlled by means of the well-known photoelectron peaks of Cu, Ag and Au respectively.

6.6.8. AFM

AFM imaging was carried out in contact mode under liquid using a Bruker Dimension ICON system (Billerica/ USA). The tip used was a Mikromasch HQ:CSC37/Pt (typical force constant: 0.3 N/m) (Sofia/ Bulgaria).

6.6.9. MALDI-ToF

MALDI-ToF measurements were performed at the DKFZ in Heidelberg on an Ultraflex[TM] TOFTOF I instrument (Bruker Daltonik, Bremen/ Germany) equipped with a nitrogen laser. The instrument was operated with positive-ion reflecton mode, ion source voltage 1 (ion acceleration voltage) 25.0 kV, ion source voltage 2 (first extraction plate) 21.9 kV, ion source lens voltage 6 kV and reflectron voltage 26.3 kV.

As the matrix, one droplet of 2.5-dihydroxybenzoic acid (Bruker, Daltonik) (20 mg.mL^{-1}) was dissolved in acetonitrile/ 0.1%TFA in water (30:70 vol-%) and placed on a ground steel target. A peptide calibration standard II from Bruker Daltonik was used. The used software was FlexControl version 2.4 for instrument control and FlexAnalysis version 2.4 for spectrum processing.

7. Literature

(1)   Breitling, F.; Felgenhauer, T.; Nesterov, A.; Lindenstruth, V.; Stadler, V.; Bischoff, F. R. *ChemBioChem* **2009**, *10* (5), 803.

(2)   *Surface Analysis Methods in Materials Science*, 2nd ed.; O'Conner, D. J., Ed.; Springer Series in Surface Sciences; Springer Berlin: Berlin, 2010.

(3)   Lehninger, A. L.; Nelson, D. L.; Cox, M. M. *Lehninger principles of biochemistry*, 4th ed.; W.H. Freeman: New York, 2005.

(4)   Ambrogelly, A.; Palioura, S.; Söll, D. *Nat. Chem. Biol.* **2007**, *3* (1), 29.

(5)   Berg, J. M.; Tymoczko, J. L.; Stryer, L.; Gatto, G. J. *Biochemie*, 7. Aufl., Nachdr.; Lehrbuch; Springer Spektrum: Berlin, 2014.

(6)   Coin, I.; Beyermann, M.; Bienert, M. *Nat. Protoc.* **2007**, *2* (12), 3247.

(7)   Sewald, N.; Jakubke, H.-D. *Peptides: chemistry and biology*, 2nd ed.; Wiley-VCH: Weinheim, 2009.

(8)   Han, S.-Y.; Kim, Y.-A. *Tetrahedron* **2004**, *60* (11), 2447.

(9)   Montalbetti, C. A. G. N.; Falque, V. *Tetrahedron* **2005**, *61* (46), 10827.

(10) Sheehan, J. C.; Hess, G. P. *J. Am. Chem. Soc.* **1955**, *77* (4), 1067.

(11) Valeur, E.; Bradley, M. *Chem Soc Rev* **2009**, *38* (2), 606.

(12) Castro, B.; Dormoy, J. R. *Tetrahedron Lett.* **1972**, *13* (47), 4747.

(13) Castro, B.; Dormoy, J. R. *Tetrahedron Lett.* **1973**, *14* (35), 3243.

(14) Castro, B.; Dormoy, J. R.; Evin, G.; Selve, C. *Tetrahedron Lett.* **1975**, *16* (14), 1219.

(15) Wiley: Handbook of Reagents for Organic Synthesis, Activating Agents and Protecting Groups - Anthony J. Pearson, William R. Roush http://eu.wiley.com/WileyCDA/WileyTitle/productCd-0471979279.html (accessed Sep 8, 2016).

(16) Kent, S. B. H. *Annu. Rev. Biochem.* **1988**, *57* (1), 957.

(17) Amblard, M.; Fehrentz, J.-A.; Martinez, J.; Subra, G. *Mol. Biotechnol.* **2006**, *33* (3), 239.

(18) Carpino, L. A.; Han, G. Y. *J. Org. Chem.* **1972**, *37* (22), 3404.

(19) Jones, J. *Amino acid and peptide synthesis*, 2nd ed.; Oxford chemistry primers; Oxford University Press: Oxford ; New York, 2002.

(20) Behrendt, R.; White, P.; Offer, J. *J. Pept. Sci.* **2016**, *22* (1), 4.

(21) Merrifield, R. B. *Science* **1965**, *150* (3693), 178.

(22) Atherton, E.; Fox, H.; Harkiss, D.; Logan, C. J.; Sheppard, R. C.; Williams, B. J. *J. Chem. Soc. Chem. Commun.* **1978**, No. 13, 537.

(23) Breitling, F.; Nesterov, A.; Stadler, V.; Felgenhauer, T.; Bischoff, F. R. *Mol. Biosyst.* **2009**, *5* (3), 224.

(24) Gao, X.; Pellois, J. P.; Na, Y.; Kim, Y.; Gulari, E.; Zhou, X. *Mol. Divers.* **2004**, *8* (3), 177.

(25) Legutki, J. B.; Johnston, S. A. *Proc. Natl. Acad. Sci.* **2013**, *110* (46), 18614.

(26) Cretich, M.; Damin, F.; Pirri, G.; Chiari, M. *Biomol. Eng.* **2006**, *23* (2–3), 77.

(27) Andresen, H.; Grötzinger, C.; Zarse, K.; Kreuzer, O. J.; Ehrentreich-Förster, E.; Bier, F. F. *PROTEOMICS* **2006**, *6* (5), 1376.

(28) Reineke, U.; Volkmer-Engert, R.; Schneider-Mergener, J. *Curr. Opin. Biotechnol.* **2001**, *12* (1), 59.

(29) PEPperPRINT: Conformational Epitope Mapping http://www.pepperprint.com/applications/conformational-epitope-mapping/ (accessed Aug 19, 2016).

(30) Katz, C.; Levy-Beladev, L.; Rotem-Bamberger, S.; Rito, T.; Rüdiger, S. G. D.; Friedler, A. *Chem. Soc. Rev.* **2011**, *40* (5), 2131.

(31) Frank, R. *Tetrahedron* **1992**, *48* (42), 9217.

(32) Hilpert, K.; Winkler, D. F.; Hancock, R. E. *Nat. Protoc.* **2007**, *2* (6), 1333.

(33) Frank, R. *J. Immunol. Methods* **2002**, *267* (1), 13.

(34) Reimer, U.; Reineke, U.; Schneider-Mergener, J. *Curr. Opin. Biotechnol.* **2002**, *13* (4), 315.

(35) Fodor, S.; Read, J.; Pirrung, M.; Stryer, L.; Lu, A.; Solas, D. *Science* **1991**, *251* (4995), 767.

(36) Reineke, U.; Schneider-Mergener, J.; Schutkowski, M. In *BioMEMS and Biomedical Nanotechnology*; Ferrari, M., Ozkan, M., Heller, M. J., Eds.; Springer US, 2006; pp 161–282.

(37) Singh-Gasson, S.; Green, R. D.; Yue, Y.; Nelson, C.; Blattner, F.; Sussman, M. R.; Cerrina, F. *Nat. Biotechnol.* **1999**, *17* (10), 974.

(38) Pellois, J. P.; Zhou, X.; Srivannavit, O.; Zhou, T.; Gulari, E.; Gao, X. *Nat. Biotechnol.* **2002**, *20* (9), 922.

(39) Li, S.; Marthandan, N.; Bowerman, D.; Garner, H. R.; Kodadek, T. *Chem. Commun.* **2005**, No. 5, 581.

(40) Buus, S.; Rockberg, J.; Forsstrom, B.; Nilsson, P.; Uhlen, M.; Schafer-Nielsen, C. *Mol. Cell. Proteomics* **2012**, *11* (12), 1790.

(41) LC Sciences http://www.lcsciences.com/discovery/ (accessed Sep 9, 2016).

(42) Stadler, V.; Felgenhauer, T.; Beyer, M.; Fernandez, S.; Leibe, K.; Güttler, S.; Gröning, M.; König, K.; Torralba, G.; Hausmann, M.; Lindenstruth, V.; Nesterov, A.; Block, I.; Pipkorn, R.; Poustka, A.; Bischoff, F. R.; Breitling, F. *Angew. Chem. Int. Ed.* **2008**, *47* (37), 7132.

(43) Beyer, M.; Nesterov, A.; Block, I.; König, K.; Felgenhauer, T.; Fernandez, S.; Leibe, K.; Torralba, G.; Hausmann, M.; Trunk, U.; Lindenstruth, V.; Bischoff, F. R.; Stadler, V.; Breitling, F. *Science* **2007**, *318* (5858), 1888.

(44) Maerkle, F.; Loeffler, F. F.; Schillo, S.; Foertsch, T.; Muenster, B.; Striffler, J.; Schirwitz, C.; Bischoff, F. R.; Breitling, F.; Nesterov-Mueller, A. *Adv. Mater.* **2014**, *26* (22), 3730.

(45) Loeffler, F. F.; Foertsch, T. C.; Popov, R.; Mattes, D. S.; Schlageter, M.; Sedlmayr, M.; Ridder, B.; Dang, F.-X.; von Bojničić-Kninski, C.; Weber, L. K.; Fischer, A.; Greifenstein, J.; Bykovskaya, V.; Buliev, I.; Bischoff, F. R.; Hahn, L.; Meier, M. A. R.; Bräse, S.; Powell, A. K.; Balaban, T. S.; Breitling, F.; Nesterov-Mueller, A. *Nat. Commun.* **2016**, *7*, 11844.

(46) Beyer, M.; Felgenhauer, T.; Bischoff, R. F.; Breitling, F.; Stadler, V. *Biomaterials* **2006**, *27* (18), 3505.

(47) Muenster, B.; Welle, A.; Ridder, B.; Althuon, D.; Striffler, J.; Foertsch, T. C.; Hahn, L.; Thelen, R.; Stadler, V.; Nesterov-Mueller, A.; Breitling, F.; Loeffler, F. F. *Appl. Surf. Sci.* **2016**, *360*, 306.

(48) Schirwitz, C.; Loeffler, F. F.; Felgenhauer, T.; Stadler, V.; Breitling, F.; Bischoff, F. R. *Biointerphases* **2012**, *7* (1–4), 1.

(49) Stadler, V.; Kirmse, R.; Beyer, M.; Breitling, F.; Ludwig, T.; Bischoff, F. R. *Langmuir* **2008**, *24* (15), 8151.

(50) PEPperPRINT: Peptide Laser Printer http://www.pepperprint.com/technology/peptide-laser-printer/ (accessed Oct 3, 2016).

(51) Karlsruher Institut für Technologie, PEPperPRINT GmbH, **2015**, Verfahren zur kombinatorischen Partikelmanipulation zur Herstellung von hochdichten

Molekülarrays, insbesondere von Peptidarrays, und damit erhältliche Molekülarrays. Inventors: Maerkle, F.; Nesterov-Mueller, A.; Breitling, F.; Loeffler, F. F.; Schillo, S.; Bykovskaya, V.; Bojnicic-Kninski, C.; Leibe, K. 2015-02-05. DE, WO2014170031 (A3).

(52) Armstrong, R. W.; Combs, A. P.; Tempest, P. A.; Brown, S. D.; Keating, T. A. *Acc. Chem. Res.* **1996**, *29* (3), 123.

(53) Ugi, I.; Dömling, A.; Hörl, W. *Endeavour* **1994**, *18* (3), 115.

(54) Bienaymé, H.; Hulme, C.; Oddon, G.; Schmitt, P. *Chem. – Eur. J.* **2000**, *6* (18), 3321.

(55) Alvim, H. G. O.; da Silva Júnior, E. N.; Neto, B. A. D. *RSC Adv* **2014**, *4* (97), 54282.

(56) Ugi, I. *Isonitrile Chemistry*; Academic Press: New York, 1971.

(57) Ugi, I.; Werner, B.; Dömling, A. *Molecules* **2003**, *8* (1), 53.

(58) Tempest, P. A.; Brown, S. D.; Armstrong, R. W. *Angew. Chem. Int. Ed. Engl.* **1996**, *35* (6), 640.

(59) Blackwell, H. *Curr. Opin. Chem. Biol.* **2006**, *10* (3), 203.

(60) Lin, Q.; Blackwell, H. E. *Chem. Commun.* **2006**, No. 27, 2884.

(61) Lin, Q.; O'Neil, J. C.; Blackwell, H. E. *Org. Lett.* **2005**, *7* (20), 4455.

(62) Koltzenburg, S.; Maskos, M.; Nuyken, O.; Mülhaupt, R. *Polymere: Synthese, Eigenschaften und Anwendungen*; Lehrbuch; Springer Spektrum: Berlin, 2014.

(63) Walton, D. J.; Lorimer, J. P. *Polymers*; Oxford chemistry primers; Oxford University Press: Oxford ; New York, 2000.

(64) Matyjaszewski, K.; Spanswick, J. *Mater. Today* **2005**, *8* (3), 26.

(65) Moad, G.; Rizzardo, E. In *RSC Polymer Chemistry Series*; Gigmes, D., Ed.; Royal Society of Chemistry: Cambridge, 2015; pp 1–44.

(66) Anslyn, E. V.; Dougherty, D. A. *Modern physical organic chemistry*; University Science: Sausalito, CA, 2006.

(67) Goto, A.; Fukuda, T. *Prog. Polym. Sci.* **2004**, *29* (4), 329.

(68) Matyjaszewski, K. *Curr. Opin. Solid State Mater. Sci.* **1996**, *1* (6), 769.

(69) Boyer, C.; Bulmus, V.; Davis, T. P.; Ladmiral, V.; Liu, J.; Perrier, S. *Chem. Rev.* **2009**, *109* (11), 5402.

(70) Nicolas, J.; Guillaneuf, Y.; Lefay, C.; Bertin, D.; Gigmes, D.; Charleux, B. *Prog. Polym. Sci.* **2013**, *38* (1), 63.

(71) Moad, G.; Rizzardo, E.; Thang, S. H. *Chem. - Asian J.* **2013**, *8* (8), 1634.

(72) Matyjaszewski, K.; Xia, J. *Chem. Rev.* **2001**, *101* (9), 2921.

(73) Ehrenstein, G. W.; Riedel, G.; Trawiel, P. *Praxis der thermischen Analyse von Kunststoffen*; Hanser: München, 1998.

(74) Berek, D. *J. Sep. Sci.* **2010**, *33* (3), 315.

(75) Barth, H. G.; Boyes, B. E.; Jackson, C. *Anal. Chem.* **1996**, *68* (12), 445.

(76) Butt, H.-J.; Graf, K.; Kappl, M. *Physics and chemistry of interfaces*; Physics textbook; Wiley-VCH: Weinheim, 2003.

(77) Schulz, C.; Nowak, S.; Fröhlich, R.; Ravoo, B. J. *Small* **2012**, *8* (4), 569.

(78) Stevens, M. M. *Science* **2005**, *310* (5751), 1135.

(79) Feng, W.; Li, L.; Ueda, E.; Li, J.; Heißler, S.; Welle, A.; Trapp, O.; Levkin, P. A. *Adv. Mater. Interfaces* **2014**, *1* (7), 1400269.

(80) de los Santos Pereira, A.; Sheikh, S.; Blaszykowski, C.; Pop-Georgievski, O.; Fedorov, K.; Thompson, M.; Rodriguez-Emmenegger, C. *Biomacromolecules* **2016**, *17* (3), 1179.

(81) Bhat, R. R.; Tomlinson, M. R.; Wu, T.; Genzer, J. In *Surface-Initiated Polymerization II*; Jordan, R., Ed.; Springer-Verlag: Berlin/Heidelberg, 2006; Vol. 198, pp 51–124.

(82) Surfaces - Matyjaszewski Polymer Group - Carnegie Mellon University http://www.cmu.edu/maty/materials/Properties-of-well-defined/surfaces.html (accessed Aug 19, 2016).

(83) Mastan, E.; Xi, L.; Zhu, S. *Macromol. Theory Simul.* **2015**, *24* (2), 89.

(84) George, S. M.; Yoon, B.; Dameron, A. A. *Acc. Chem. Res.* **2009**, *42* (4), 498.

(85) Jiao, J.; Anariba, F.; Tiznado, H.; Schmidt, I.; Lindsey, J. S.; Zaera, F.; Bocian, D. F. *J. Am. Chem. Soc.* **2006**, *128* (21), 6965.

(86) Li, Y.; Wang, D.; Buriak, J. M. *Langmuir* **2010**, *26* (2), 1232.

(87) Campos, M. A. C.; Paulusse, J. M. J.; Zuilhof, H. *Chem. Commun.* **2010**, *46* (30), 5512.

(88) Belu, A. M.; Graham, D. J.; Castner, D. G. *Biomaterials* **2003**, *24* (21), 3635.

(89) Sodhi, R. N. S. *The Analyst* **2004**, *129* (6), 483.

(90) Mahoney, C. M. *Mass Spectrom. Rev.* **2010**, *29* (2), 247.

(91) Folder IONTOF_TOF-SIMS_5_Brochure.pdf https://www.iontof.com/download/IONTOF_TOF-SIMS_5_Brochure.pdf (accessed Sep 27, 2016).

(92) Taylor, A. J.; Graham, D. J.; Castner, D. G. *The Analyst* **2015**, *140* (17), 6005.

(93) Watts, J. F.; Wolstenholme, J. *An introduction to surface analysis by XPS and AES*; J. Wiley: Chichester, West Sussex, England ; New York, 2003.

(94) *Surface analysis by Auger and x-ray photoelectron spectroscopy*; Briggs, D., Grant, J. T., Eds.; IM Publications: Chichester, West Sussex, U.K, 2003.

(95) Brundle, C. R. *J. Vac. Sci. Technol.* **1974**, *11* (1), 212.

(96) Binnig, G.; Quate, C. F.; Gerber, C. *Phys. Rev. Lett.* **1986**, *56* (9), 930.

(97) Atkins, P. W.; De Paula, J. *Atkins' physical chemistry*, 8. ed.; Oxford Univ. Press: Oxford, 2006.

(98) Meyer, E. *Prog. Surf. Sci.* **1992**, *41* (1), 3.

(99) Lobo, R. F. M.; Pereira-da-Silva, M. A.; Raposo, M.; Faria, R. M.; Oliveira, O. N.; Pereira-da-Silva, M. A.; Faria, R. M. *Nanotechnology* **1999**, *10* (4), 389.

(100) Giessibl, F. J. *Rev. Mod. Phys.* **2003**, *75* (3), 949.

(101) Schüttler, A.; Meltzow, W.; Föhles, J.; Zahn, H. *Hoppe-Seylers Z. Für Physiol. Chem. 357* (1), 741.

(102) Neugebauer, D.; Matyjaszewski, K. *Macromolecules* **2003**, *36* (8), 2598.

(103) Teodorescu, M.; Matyjaszewski*, K. *Macromol. Rapid Commun.* **2000**, *21* (4), 190.

(104) Rademacher, J. T.; Baum, M.; Pallack, M. E.; Brittain, W. J.; Simonsick, W. J. *Macromolecules* **2000**, *33* (2), 284.

(105) Teodorescu, M.; Matyjaszewski, K. *Macromolecules* **1999**, *32* (15), 4826.

(106) Appel, E. A.; del Barrio, J.; Loh, X. J.; Dyson, J.; Scherman, O. A. *J. Polym. Sci. Part Polym. Chem.* **2012**, *50* (1), 181.

(107) Wycisk, A.; Döring, A.; Schneider, M.; Schönhoff, M.; Kuckling, D. *Polymers* **2015**, *7* (5), 921.

(108) Muenster, B. Dissertation: Entwicklung von Mikropartikeln für die kombinatorische Synthese hochdichter Peptidarrays durch laserbasierte Verfahren, Karlsruher Institut für Technologie, **2014**.

(109) Srila, W.; Yamabhai, M. *Appl. Biochem. Biotechnol.* **2013**, *171* (3), 583.

(110)   GenePix 4000B Microarray Scanner | Molecular Devices
        https://www.moleculardevices.com/systems/microarray-systems/genepix-4000b
        (accessed Sep 5, 2016).

(111)   Pentafluorophenol ReagentPlus®, ≥99% | Sigma-Aldrich
        http://www.sigmaaldrich.com/catalog/product/aldrich/103799?lang=de&region=DE
        (accessed Aug 27, 2016).

(112)   Bertozzi, C. R. *Science* **2001**, *291* (5512), 2357.

(113)   Stucchi, M.; Cairati, S.; Cetin-Atalay, R.; Christodoulou, M. S.; Grazioso, G.;
        Pescitelli, G.; Silvani, A.; Yildirim, D. C.; Lesma, G. *Org Biomol Chem* **2015**, *13*
        (17), 4993.

(114)   Jones, S.; Thornton, J. M. *Proc. Natl. Acad. Sci. U. S. A.* **1996**, *93* (1), 13.

(115)   Moreira, I. S.; Fernandes, P. A.; Ramos, M. J. *Proteins Struct. Funct. Bioinforma.*
        2007, *68* (4), 803.

(116)   Marcaccini, S.; Torroba, T. *Nat. Protoc.* **2007**, *2* (3), 632.

(117)   Oertel, K.; Zech, G.; Kunz, H. *Angew. Chem. Int. Ed.* **2000**, *39* (8), 1431.

(118)   Kim, S. W.; Bauer, S. M.; Armstrong, R. W. *Tetrahedron Lett.* **1998**, *39* (39),
        6993.

(119)   Constabel, F.; Ugi, I. *Tetrahedron* **2001**, *57* (27), 5785.

(120)   Waki, M.; Meienhofer, J. *J. Am. Chem. Soc.* **1977**, *99* (18), 6075.

(121)   Hoel, A. M. L.; Nielsen, J. *Tetrahedron Lett.* **1999**, *40* (20), 3941.

(122)   Blinco, J. P.; Trouillet, V.; Bruns, M.; Gerstel, P.; Gliemann, H.; Barner-Kowollik,
        C. *Adv. Mater.* **2011**, *23* (38), 4435.

(123)   Fryxell, G. E.; Rieke, P. C.; Wood, L. L.; Engelhard, M. H.; Williford, R. E.; Graff,
        G. L.; Campbell, A. A.; Wiacek, R. J.; Lee, L.; Halverson, A. *Langmuir* **1996**, *12*
        (21), 5064.

(124)   Xu, S.; Cruchon-Dupeyrat, S. J. N.; Garno, J. C.; Liu, G.-Y.; Kane Jennings, G.;
        Yong, T.-H.; Laibinis, P. E. *J. Chem. Phys.* **1998**, *108* (12), 5002.

(125)   Huang, C.; Moosmann, M.; Jin, J.; Heiler, T.; Walheim, S.; Schimmel, T. *Beilstein
        J. Nanotechnol.* **2012**, *3*, 620.

(126)   Halliwell, C. M.; Cass, A. E. G. *Anal. Chem.* **2001**, *73* (11), 2476.

(127)   Böhmler, J.; Ploux, L.; Ball, V.; Anselme, K.; Ponche, A. *J. Phys. Chem. C* **2011**,
        115 (22), 11102.

(128)   Barbot, C.; Bouloussa, O.; Szymczak, W.; Plaschke, M.; Buckau, G.; Durand, J.-P.; Pieri, J.; Kim, J. I.; Goudard, F. *Colloids Surf. Physicochem. Eng. Asp.* **2007**, *297* (1–3), 221.

(129)   Razgon, A.; Bergman, R. G.; Sukenik, C. N. *Langmuir* **2008**, *24* (6), 2545.

(130)   Sherman, R. J.; Hirt, D.; Vane, R. *Vac. Sci. Technol. A: Vac. Surf. Films* **1994**, 12 (4), 1876.

(131)   Parry, K. L.; Shard, A. G.; Short, R. D.; White, R. G.; Whittle, J. D.; Wright, A. *Surf. Interface Anal.* **2006**, *38* (11), 1497.

(132)   Scofield, J. H. *J. Electron Spectrosc. Relat. Phenom.* **1976**, *8* (2), 129.

8. Abbreviations

Ac-Gly	Acetylated glycine
Ac-Lys(Boc)	Acetylated lysine (*tert*-butyloxycarbonyl)
AFM	Atomic Force Microscopy
AOM	Acousto-Optic Modulator
APTES	(3-Aminopropyl) triethoxysilane
Asp	Aspartic acid
ATRP	Atom Transfer Radical Polymerization
a.u.	arbitrary unit
ß-Ala	beta-Alanine
Boc	*tert*-Butyloxycarbonyl
BOP	Benzotriazol-1-yloxy-tris(dimethylamino)phosphonium hexafluorophosphate
C	Celsius
CHCl$_3$	Chloroform
cm	centimeter
CRP	Controlled Radical Polymerization
Cu(I)Br	Copper(I)bromide
Cu(I)Cl	Copper(I)chloride
Cys	Cysteine
Đ	Dispersity
Da	Dalton
DCC	*N,N'*-Dicyclohexylcarbodiimide
DCM	Dichloromethane
DEAA	Diethylacrylamide
DIC	*N,N'*-Diisopropylcarbodiimide
DIPEA	*N,N*-Diisopropylethylamine
DMAA	Dimethylacrylamide
DMAc	*N,N*-Dimethylacetamide

DMF	*N,N*-Dimethylformamide
DMPA	2,2-Dimethoxy-2-phenylacetophenone
DNA	Deoxyribonucleic acid
DP	Degree of Polymerization
DSC	Differential Scanning Calorimetry
equiv.	equivalents
EtOH	Ethanol
eV	electronvolt
FDTS	1*H*, 1*H*, 2*H*, 2*H*-Perfluorodecyltrichlorosilane
Fmoc	Fluorenylmethyloxycarbonyl
Fmoc-Asp(OtBu)-OPfp	*N*-(9-Fluorenylmethyloxycarbonyl)-*tert*-butyl-aspartic acid pentafluorophenyl ester
Fmoc-β-Ala-OH	*N*-(9-Fluorenylmethyloxycarbonyl)-beta-alanine
Fmoc-Cys(Trt)-OPfp	*N*-(9-Fluorenylmethyloxycarbonyl)-trityl-cysteine pentafluorophenyl ester
Fmoc-Gln(Trt)-OPfp	*N*-(9-Fluorenylmethyloxycarbonyl)-trityl-glutamine pentafluorophenyl ester
Fmoc-Gly-OPfp	*N*-(9-Fluorenylmethyloxycarbonyl)-glycine pentafluorophenyl ester
Fmoc-Lys(Boc)-OPfp	*N*-(9-Fluorenylmethyloxycarbonyl)-*tert*-butyloxycarbonyl-lysine pentafluorophenyl ester
Fmoc-Phe-OPfp	*N*-(9-Fluorenylmethyloxycarbonyl)-phenylalanine pentafluorophenyl ester
Fmoc-Pro-OPfp	*N*-(9-Fluorenylmethyloxycarbonyl)-proline pentafluorophenyl ester
Fmoc-Tyr(tBu)-OPfp	*N*-(9-Fluorenylmethyloxycarbonyl)-*tert*-butyl-tyrosine pentafluorophenyl ester
g	gram
Gly	Glycine
h	hour
^{1}H-NMR	Proton Nuclear Magnetic Resonance Spectroscopy
HOBt	Hydroxybenzotriazole

K	Kelvin
kcts	kilo counts
keV	kilo electronvolt
kHZ	kilo Hertz
kV	kilo Volt
L	liter
LED	Light Emitting Diode
Lys	Lysine
MALDI-ToF	Matrix-Assisted Laser Desorption/Ionization Time of Flight
mbar	millibar
MCR	Multi Component Reaction
mHz	mega Hertz
Me$_6$TREN	Tris[2-(dimethylamino)ethyl]amine
MeOH	Methanol
µg	microgram
µm	micrometer
mg	milligram
mL	milliliters
mm	millimeter
ms	milliseconds
mW	milli Watt
min	minute
MLD	Molecular Layer Deposition
MMA	Methyl methacrylate
M$_n$	Number Average Molecular weight
N	Newton
NHS	*N*-Succinimidyl ester
nm	nanometer
NMI	1-Methylimidazole
NMP	Nitroxide Mediated Polymerization

ns	nanoseconds
NVOC	Nitroveratryloxycarbonyl
OPC	Organic photoconducting
OPfp	ortho Pentafluorophenyl ester
pA	picoAmpere
PBL	Polymer Blend Lithography
PBS	Phosphate Buffer Saline
PBS-T	Phosphate Buffer Saline with Tween 20
p(DEAA)	Poly(diethylacrylamide)
p(DMAA)	Poly(dimethylacrylamide)
PEGMA	Poly(ethylene glycol) methacrylate
PEGMA-co-MMA	Poly(ethylene glycol) methacrylate-co-methyl methacrylate
p(MMA)	Poly(methyl methacrylate)
ppb	parts per billion
ppm	parts per million
PS	Polystyrene
PyBOP	Benzotriazol-1-yl-oxytripyrrolidinophosphonium-hexafluorophosphat
RAFT	Reversible Addition Fragmentation Transfer
RNA	Ribonucleic acid
rps	revolutions per second
SAM	Self-Assembled Monolayer
SEC	Size Exclusion Chromatography
sec	second
SIMS	Secondary Ion Mass Spectrometry
SPPS	Solid Phase Peptide Synthesis
TAMRA	5-(6)-carboxytetramethylrhodamine
TAMRA-NHS	5-(6)-carboxytetramethylrhodamine *N*-succinimidyl ester
TEA	Triethylamine
TEMPO	2,2,6,6-Tetramethylpiperidin-1-oxyl
TFA	Trifluoroacetic acid

T_g	Glass transition temperature
TIBS	Triisobutyl silane
ToF	Time-of-Flight
ToF-SIMS	Time-of-Flight Secondary Ion Mass Spectrometry
t-RNA	Transfer Ribonucleic Acid
Trt	Trityl
Tween20	Polyoxyethylensorbitan monolaurate (surfactant)
Tyr	Tyrosine
U-4CR	Ugi four component reaction
UV	Ultraviolet
V	Volt
vol-%	volume percent
W	Watt
wt-%	weight percent
XPS	X-ray photoelectron spectroscopy

9. Appendix

9.1. Figures

9.2. Schemes

9.3. Tables

9.4. Equations

Danksagung

Zunächst möchte ich mich bei Prof. Dr. Frank Breitling und bei Prof. Dr. Michael Meier für die Möglichkeit meine Dissertation als Kooperationsprojekt in ihren Arbeitskreisen durchzuführen und für die Betreuung meiner Arbeit bedanken.

Bei meinen beiden Arbeitsgruppen, FuE2-PA (ehemals FuE5) am Campus Nord und AK Meier am Campus Süd, möchte ich mich für die gute Zusammenarbeit, die gute Arbeitsatmosphäre und ihre Unterstützung bedanken. Außerdem möchte ich mich bei allen Kollegen am IMT und am IOC bedanken, die mich unterstützt haben.

Besonders bedanken möchte ich mich bei Daniela Mattes für die vielen Gespräche, die tolle Zusammenarbeit und ihre Freundschaft.

Bedanken möchte ich mich auch bei allen, die mit mir in verschiedenen Projekten zusammengearbeitet haben, besonders bei Tobias Förtsch, Audrey Llevot, Dominique Moock und Benjamin Bitterer.

Bedanken möchte ich mich auch bei allen, die mich bei der Analytik meiner Proben unterstützt haben oder mir Chemikalien zur Verfügung gestellt haben. Besonders bedanken möchte ich mich bei Alexander Welle für ToF-SIMS Messungen, bei Vanessa Trouillet für XPS Messungen, bei Sven Ole Steinmüller für ToF-SIMS und XPS Messungen und bei Jonathan Berson für AFM-Messungen und für das Bereitstellen von PBL-Wafern. Auch möchte ich mich bei Rebecca Seim für die Zurverfügungstellung des Benzylisocyanids bedanken.

Vom DKFZ in Heidelberg, möchte ich bei Martina Schnölzer und Sabine Fiedler mich für MALDI-ToF Messungen und bei Ralf Bischoff für das Stellen der gelabelten Antikörper bedanken.

Auch bei meinen Freunden en vrienden möchte ich mich bedanken für ihre Freundschaft, dass sie immer ein offenes Ohr für mich haben und dass sie immer für mich da sind, auch wenn sie nicht in der Nähe sind.

Ein ganz großer Dank geht auch an meine Familie, meine Brüder, meine Großeltern und ganz besonders an meine Eltern für ihre Unterstützung und dafür, dass sie alle immer an mich geglaubt haben.

Maar mijn grootste dank geldt jou Jules, je bent er altijd voor mij geweest en hebt mij altijd gesteund van het begin tot het einde van mijn promotie. Jij hebt Nederland achtergelaten en bent met mij naar Duitsland verhuisd, zodat ik in Karlsruhe kon promoveren. Jij hebt succesvolle maar ook zware momenten met mij gedeeld en mij

aangemoedigd niet op te geven. En aan het eind, bij het schrijven van mijn proefschrift, heb jij, als mijn IT-guru, mij nog een crash cursus in opmaakstijlen van word en nuttige power point trucjes gegeven. Dankjewel dat jij in mijn leven bent en het compleet maakt.

Lebenslauf

Barbara Ridder

Geburtsort: Paderborn

2013 – 2016 Promotion

Karlsruher Institut für Technologie (KIT) (D)

Thema der Dissertation: 'Surface structuring in xy- and z-direction on the examples of peptide array synthesis and molecular layer deposition.' ausgeführt am Institut für Mikrostrukturtechnik (IMT) und am Institut für Organische Chemie (IOC) am Karlsruher Institut für Technologie (KIT) (D).

2010 – 2013 Master of Science im Fach Chemie

Radboud University Nijmegen (NL)

Thema der Masterarbeit: 'Difunctionalization of polymeric vesicles (stomatocytes)' ausgeführt in der Abteilung für Bioorganic Chemistry, Radboud University Nijmegen (NL).

2007 – 2010 Bachelor of Science im Fach Chemie

Radboud University Nijmegen (NL)

Thema der Bachelorarbeit: 'Tuning the temperature of thermoresponsive oligo (ethylene glycol) methacrylate-based polymers in solution.' ausgeführt in der Abteilung für Bioorganic Chemistry, Radboud University Nijmegen (NL).

2007: Abitur

Engelbert Kaempfer Gymnasium Lemgo (D)

1998 – 2007: Städtisches Gymnasium Bad Driburg (D), Staindrop Comprehensive School Staindrop (GB) und Engelbert Kaempfer Gymnasium Lemgo (D).

Publikationen

Ridder, B.; Foertsch, T. C.; Welle, A.; Mattes, D. S.; von Bojnicic-Kninski, C. M.; Loeffler, F. F.; Nesterov-Mueller, A.; Meier, M. A. R.; Breitling, F. *Appl. Surf. Sci.* 2016, *389*, 942-951. Development of a poly(dimethylacrylamide) based matrix material for solid phase high density peptide array synthesis employing a laser based material transfer.

Von Bojnicic-Kninski, C.; Bykovskaya, V.; Maerkle, F.; Popov, R.; Palermo, A.; Mattes, D. S.; Weber, L. K.; Ridder, B.; Foertsch, T. C.; Welle, A.; Loeffler, F. F.; Breitling, F.; Nesterov-Mueller, A. *Adv. Funct. Mater.* **2016**, *26*, 7067-7073. Selective Functionalization of Microstructured Surfaces by Laser-Assisted Particle Transfer.

Striffler, J.; Mattes, D. S.; Schillo, S.; Münster, B.; Palermo, A.; Ridder, B.; Welle, A.; Trouillet, V.; Stadler, V.; Markovic, G.; Proll, G.; Bräse, S.; Loeffler, F. F.; Nesterov-Müller, A.; Breitling, F. *ChemNanoMat* **2016**, 2, 897-903. Replication of Polymer-Based Microarrays by Multi-Step Transfer.

Loeffler, F. F.; Foertsch, T. C.; Popov, R.; Mattes, D. S.; Schlageter, M.; Sedlmayr, M.; Ridder, B.; Dang, F. X.; von Bojnicic-Kninski, C.; Weber, L. K.; Fischer, A.; Greifenstein, J.; Bykovskaya, V.; Buliev, I.; Bischoff, F. R.; Hahn, L.; Meier, M. A. R.; Bräse, S.; Powell, A. K.; Balaban, T. S.; Breitling, F.; Nesterov-Mueller, A. *Nat. Commun.* **2016**, *7,* 11844. High-flexibility combinatorial peptide synthesis with laser-based transfer of monomers in solid matrix material.

Muenster, B.; Welle, A.; Ridder, B; Althuon, D.; Striffler, J.; Foertsch, T. C.; Hahn, L.; Thelen, R.; Stadler, V.; Nesterov-Mueller, A.; Breitling, F.; Loeffler, F. F. *Appl. Surf. Sci.* **2016**, *360,* 306-314. *Solid-material-based coupling efficiency analyzed with time-of-flight secondary ion mass spectrometry.*

Nesterov-Mueller, A.; Maerkle, F.; Hahn, L.; Foertsch, T. C.; Schillo, S.; Bykovskaya, V.; Sedlmayr, M.; Weber, L. K.; Ridder, B.; Soehindrijo, M.; Muenster, B.; Striffler, J.; Bischoff, F. R.; Breitling, F.; Loeffler, F. F. *Microarrays* **2014**, *3,* 245-262. Particle-based microarrays of oligonucleotides and oligopeptides